"Rich Combustion And Partial Oxidation In Heat Recirculating Burners."

M. P. Gover

Ph.D. Thesis, September 1989, University Of London

List of Errata

Chapter 1:

P. 15, Para. 3, L. 3, For *richeat* read *richest*
P. 26, Para. 2, L. 16, For *he* read *the*
P. 49, Para. 2, L. 4, For *cylidrical* read *cylindrical*
P. 49, Para. 2, L. 6, For *visulisation* read *visualisation*

Chapter 3:

P. 95, Para. 2, L. 16, For *inhibted* read *inhibited*

Chapter 5:

P. 115, Para. 1, L. 8, For *lossses* read *losses*
P. 130, Para. 4, L. 3, For *reacants* read *reactants*

Chapter 6:

P. 148, Para. 2, L. 8 For *up* read *up to*
P. 152, Para. 2, L. 21 For *icreased* read *increased*

Department Of Chemical Engineering And Chemical Technology
Imperial College Of Science, Technology And Medicine
University Of London

Ph.D. Thesis
September 1989

"Rich Combustion And Partial Oxidation In Heat Recirculating Burners."

Author: Marcus Paul Gover, B.Eng.
Supervisor: Prof. F.J. Weinberg F.R.S.

A thesis submitted for the degree of Doctor of Philosophy and the Diploma of the Imperial College.

ABSTRACT

This thesis describes a study of very lean as well as very rich combustion and partial oxidation of methane and coal in heat recirculating burners. It includes a comprehensive literature survey of published work on heat recirculation and the use of coal in spouted beds, practical work and theoretical modelling.

A double spiral heat exchanger, incorporating a central combustion chamber, has been used to burn gaseous mixtures of up to 30% methane in air. Mixtures of 25% methane in air yielded up to 6% H_2 and 10% CO in the product stream.

Because of the complex geometry of the spiral burner and the unique relationships between composition, flow and temperature in heat recirculating burners generally, an electrically heated burner was commissioned to determine the effect of flow velocity and preheat temperature independently. This work showed that maximum yields of synthesis gases were obtained with methane-air mixtures in the region of 20% methane.

Combustion in the spouted bed burner has been studied extensively. Experiments have revealed the existence of an optimum bed depth for heat recirculation. A theoretical heat transfer model has been developed for the spouted bed which predicts, quite accurately, the lean stability limit for methane as well as particle and gas temperatures for different solids circulation rates.

Coal has been introduced into the spouted bed using a fluidised feeder. Pulverised Grimethorpe coal of size 425-600 μm has been burnt unsupported in the spouted bed with very few operational problems. The rich locus of stability for mixtures of coal, methane and air has been determined and the product gases analysed.

The spouted bed has been modified to burn coal more efficiently by the addition of a stainless steel gauze in the fountain region in order to produce a shallow secondary fluidised bed. With this development the fixed carbon burnout has been improved from approximately 27% to 67%.

ACKNOWLEDGEMENT

Various people have been very helpful during the course of this project and I would now like to thank them:

- Dr. N. Kermani and Dr. F.B. Carleton for much help and useful advice.
- Mr K. Gurney of the departmental student workshop for help in constructing and modifying the coal feeder.
- Mr. R. Wood of the departmental electronics workshop for his assistance with interfacing the electronic balance to the BBC computer.
- The technical staff in the departmental glassblowing shop for their assistance in making the quartz spouted bed vessel and sampling probe.
- Mr. I. Drummond and his staff for help with analytical work.
- The Underlying Research Programme of the U.K.A.E.A. for supporting the project.
- Most importantly, Prof. F.J. Weinberg F.R.S. for his overall guidance on the project.

CONTENTS

Page Number

Page Number

Page Number

LIST OF FIGURES

CHAPTER 6:

LIST OF SYMBOLS

Chapter 1

A = Arrhenius constant

Ar = Archimedes number = $g.d_p^3.\rho_f.(\rho_s-\rho_f)/\mu^2$

c = specific heat capacity at constant pressure

Co = initial oxygen concentration

Cv = volatile matter concentration

Dc = column diameter

Dg = gas phase molecular diffusivity of oxygen

Di = inlet nozzle diameter

d_o = initial coal particle diameter

d_p = particle diameter

Ds = spout diameter

Ea = activation energy

f = fraction of stoichiometric

[F] = fuel concentration

g = acceleration due to gravity

G = fluid mass flux

h = heat transfer coefficient

H = bed depth

Hm = maximum spoutable bed depth

k = chemical reaction rate constant

m = mass flowrate through heat exchanger

m = mass of carbon in bed

n = chemical reaction order

[O] = oxygen concentration

Δ P = pressure drop

q_c = specific heat of combustion

Qc = total heat of combustion

Q_L = heat loss

Qr = heat recirculated

r = rate of chemical reaction

R = gas constant

Re = Reynolds number = $\rho.u.d/\mu$

t = time

$\bar{t}$ = mean residence time
T = temperature
t_b = coal burnout time
u = velocity
Ua_H = superficial velocity at bed surface
Ums = minimum spouting velocity
x = volume fraction of fuel
ϵ = loose packed bed voidage
λ = particle shape factor
μ = fluid viscosity
ρ = density
ρ_c = carbon density
ρ_f = fluid density
ρ_s = solid density

Chapter 3

c_i = specific heat capacity of reactants
c_o = specific heat capacity of products
m_g = mass flowrate of gas
Qc = heat of combustion
T = temperature
X_{CH_4} = methane mole fraction
ρ = density
ϕ = methane equivalence ratio

Chapter 5

c_g = specific heat capacity of the gas
c_s = specific heat capacity of the solid
d_p = particle diameter
h = heat transfer coefficient
Hr = temperature rise due to combustion
m_g = mass flowrate of the gas
m_s = mass flowrate of the solid
Np = particle number density
q_c = specific heat of combustion
Qc = total heat of combustion
T_∞ = ambient temperature

Tu = gas preheat temperature
Tf = flame temperature
Te = product gas exit temperature
Tp_1 = bed particle temperature
Tp_2 = fountain particle temperature
X_{CH_4} = methane mole fraction
ρ = density
ϕ = methane equivalence ratio
$\rho_{mix,in}$ = initial density of reactant mixture

Chapter 6

C_{fixed} = fixed carbon
C_{total} = total carbon
$C_{volatiles}$ = carbon content of volatiles

Product Gas Compositions

All product gas compositions are given in volume % (dry), ie. excluding water vapour, unless otherwise stated.

Equivalence Ratio

Throughout this thesis the methane equivalence ratio, symbol ϕ, is defined in terms of mole fraction; ie.

$$\phi = \frac{[\text{actual } CH_4 \text{ mole fraction}]}{[\text{stoichiometric } CH_4 \text{ mole fraction}]}$$

CHAPTER 1

INTRODUCTION

1.1 Aims And Objectives

The main objectives of this project were to study rich combustion and partial oxidation in heat recirculating burners. Various burners were used, including one where the preheat was provided electrically, and both methane and coal were burned rich as well as lean.

The first burner to be tested was a double spiral heat exchanger encompassing a central combustion chamber, known as the "Swiss-roll" burner. This burner has been shown to be very efficient at burning lean mixtures of gaseous hydrocarbons in air (Lloyd and Weinberg, 1974). Hence the aim here was to investigate its potential for burning very rich methane-air mixtures to produce synthesis gases and higher hydrocarbons.

The electrically heated burner was commissioned to simulate heat recirculating burners with varying degrees of preheat. In this way the effect of preheat on the richeat burnable mixtures of methane and the yields of synthesis gas could be investigated. Also the catalytic effects of various metals on rich combustion could be studied.

The project set out to perform a very detailed study of spouted bed combustion. The spouted bed combustor consists of a moving particle heat exchanger which is also very suitable for the combustion of coal. For the purpose of optimising and understanding the parameters controlling the spouted bed it was intended to study lean methane combustion both theoretically and experimentally. Once the burner was optimised, the main objective would be to introduce coal into it both alone and together with methane for simultaneous gasification.

1.2 Theory And Previous Work

1.2.1 The Effect Of Preheat On Combustion

Before discussing this topic, the mechanism of flame propagation and the notion of flammability limits must be considered.

If an ignition source is applied to a long tube initially filled with a flammable mixture of fuel and air, a flame is seen to propagate along its length. The ignition energy causes the adjacent plug of gas to react and hence a flame front is initiated which propagates through the mixture. This flame front has a characteristic thickness and burning velocity dependent on both the physical and chemical properties of the particular fuel and oxidant mixture. The rate of propagation of the flame and hence the burning velocity will be proportional to the square root of the rate of reaction. Too small a reaction rate will yield insufficient heat for the flame to propagate and result in its extinction.

Although the rate of reaction involves over 100 reaction steps, it can be very approximately described by an Arrhenius type expression involving the concentrations of both the fuel and oxidant (Hardesty and Weinberg, 1974).

$$r = A.e^{-(E_a/RT)}.[F]^n.[O]^m$$

Thus, for a given temperature, there is a limiting value of fuel or oxidant concentration below which the flame will not propagate. These values are respectively termed the (fuel) lean and (fuel) rich flammability limits. For mixtures of methane in air at 293 K these limits are 5·3% and 15% methane (Lewis and Von Elbe, 1961). It should also be noted that this rate expression is extremely sensitive to temperature changes. A small rise in temperature will produce a large increase in reaction rate; see figure 1.

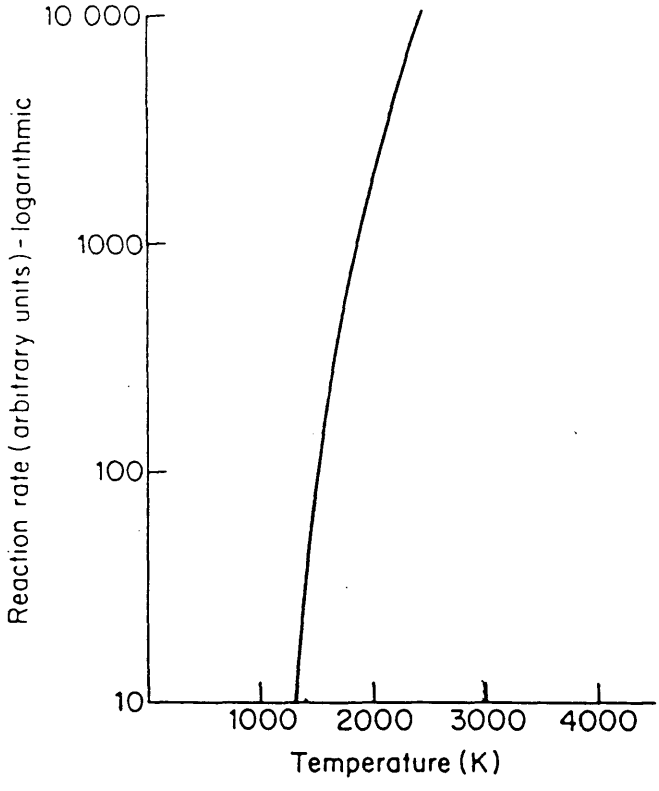

Figure 1 - The Variation Of Reaction Rate With Temperature
(From Weinberg, 1971)

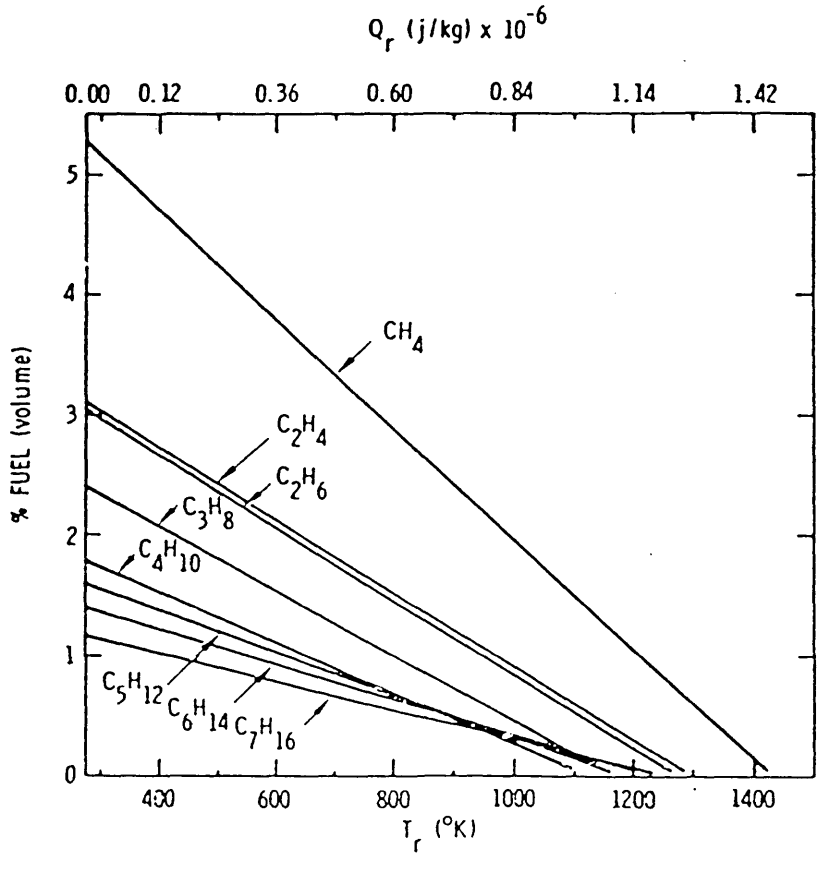

Figure 2 - Flammability Limits For Hydrocarbon - Air Mixtures As A Function Of Initial Mixture Temperature

(From Smith, 1955)

Accordingly, if the fuel-oxidant mixture is preheated the ensuing reaction rate is substantially increased and the minimum fuel/oxidant concentrations required for ignition are reduced. Hence one effect of preheat on a fuel-oxidant mixture is to extend its flammability limits.

This has been demonstrated firstly by Smith (1955) and also by Hustad and Sonju (1988). Both studies showed that the lean limit of flammability for hydrocarbons in air decreased linearly as a function of increasing temperature; see figure 2.

Alternatively if the initial fuel-oxidant mixture is held constant and preheated, the increased reaction rate results in a higher flame temperature.

1.2.2 Preheating With Recirculated Heat

Heat recirculation occurs where enthalpy is recycled from the products of a reaction, via a heat exchanger, and used to preheat the cold reactants. In combustion, as discussed earlier, this raises the flame temperature, increases the burning velocity and extends the flammability limits of the particular mixture. Thus the temperature profiles of combustion with and without heat recirculation are as shown below, for an adiabatic system with no dissociation where the heat of combustion is not a function of temperature.

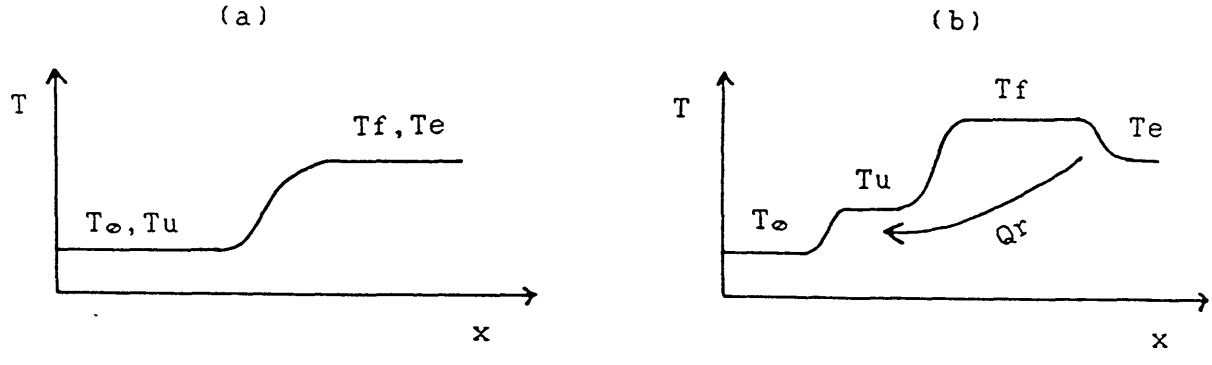

T = Temperature x = distance along flow

Figure 3

With a normal flame (a) the ambient temperature, T_∞, is also equal to the temperature of the unburnt premixed reactants, Tu. On combustion the temperature is raised by f.Qc/c to the flame or burnt temperature, Tf which is also equal to the final or exit temperature, Te. Qc is the heat of combustion, f the fraction of stoichiometric and c the mean specific heat capacity of the mixture at constant pressure (assumed equal for both reactants and products and also constant).

If some heat is recovered from the product gases and fed back to the reactants the temperature profile of the reaction is as shown in figure 3(b). The cold reactants are preheated from T_∞ to Tu by Qr/(m.c) - where Qr is the heat recirculation per unit time and m is the mass flowrate. The subsequent temperature rise, f.Qc/c, leads to a higher flame temperature, Tf, which is then cooled to the same final temperature, Te, as in the normal case by recycling excess heat, Qr. It should be evident that this is internal heat recirculation - the input and output temperatures of the system remaining unaffected (Weinberg, 1986).

A simple theory to describe how limiting conditions are affected by heat recirculation has been produced by Jones *et al.* (1978). It is based upon the experimental observation that for a particular fuel, at the lean limit of flammability, the final flame temperature is sensibly constant (Lloyd and Weinberg, 1975). Consider a heat exchanger with a hot limb, H, a cold limb, C, and a flame zone, F - see figure 4. Qt is the heat transferred in the exchanger, Qc the heat of combustion and the Q_L's represent heat losses from the respective parts of the system. Heat fluxes Q_∞, Qu, Qf and Qe correspond to local temperatures T_∞, Tu, Tf and Te respectively.

Heat balances on the zones C, H and F result in the following equations :

$$Qu - Q_\infty = m.c.(Tu - T_\infty) = Qt - Q_{L1}$$
$$Qf - Qe = m.c.(Tf - Te) = Qt + Q_{L2}$$
$$Qf - Qu = m.c.(Tf - Tu) = Qc - Q_{Lf}$$

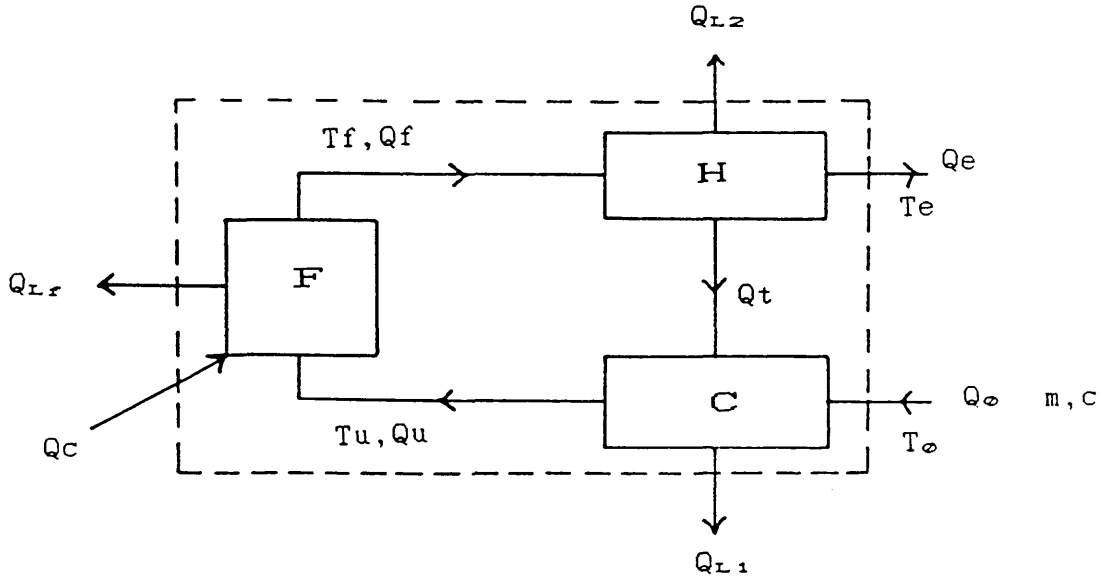

Figure 4 - Schematic Of Heat Flow In A Stationary Heat Exchanger / Combustor

An overall heat balance leads to :

$$m.c.(Te - T_e) = Qc - Q_{L1} - Q_{L2} - Q_{Lf}$$

and therefore,

$$m.c.(Tf - T_e) = Qc + Qt - (Q_{L1} + Q_{Lf})$$

Defining a mean heat transfer coefficient, h, and using an arithmetically averaged temperature difference results in :

$$\begin{aligned} Qt &= A.h.[\ \tfrac{1}{2}.(Tf + Te) - \tfrac{1}{2}.(Tu + T_e)] \\ &= \tfrac{1}{2}.h.A.(Tf - Tu + Te - T_e) \\ &= [A.h/(m.c)].[Qc - Q_{Lf} - \tfrac{1}{2}.(Q_{L1} + Q_{L2})] \end{aligned}$$

Assuming a thin flame zone such that $Q_{Lf} \rightarrow 0$, leads to :

$$Tf - T_e = \frac{Qc}{m.c} \cdot \left[1 + \frac{A.h}{m.c} \right] - \left[\frac{A.h.(Q_{L1} + Q_{L2})}{2.m^2.c^2} + \frac{Q_{L1}}{m.c} \right]$$

Substituting $Qc = x.m.q_c / \rho_a$ and rearranging gives :

$$Tf - T_{\infty} = \frac{x.q_c}{\rho_g.c} \cdot \left[1 + \frac{A.h}{m.c} \right] - \left[\frac{A.h.(Q_{L1} + Q_{L2})}{2.m^2.c^2} + \frac{Q_{L1}}{m.c} \right]$$

Where x = volume fraction of fuel, m = mass flowrate, ρ_g = fuel gas density, q_c = specific heat of combustion per unit volume and A = heat exchange area.

By the initial assumption of the theory, when the flame temperature, Tf, is constant 'x' will give the value of the lean limit of flammability. Thus a stability curve can be generated depending upon the mass flow, m, and the heat transfer represented by 'h' - see figure 5.

1.2.3 Heat Recirculating Devices

The most efficient heat recirculating burners recycle heat abstracted from the hot products rather than the hot products themselves. Recycling hot products dilutes the reaction mixture and beyond a certain amount will actually decrease the reaction rate. Furthermore heat recirculation is characterised by an excess of enthalpy over the initial and final states inbetween the points where recirculated heat is exchanged - see figure 3(b). This distinguishes true heat recirculation from other forms of heat feedback from the hot flame products, such as is involved in the mechanism of flame propagation itself. Hence heat recirculating burners are sometimes called 'excess enthalpy burners' (Hardesty and Weinberg, 1974 ; Kotani and Takeno, 1982).

A further distinction must be made between heat recirculating burners employing a cross flow heat exchanger and those which use a counter current one. With a single pass cross flow heat exchanger the temperature of the reactants entering the burner can never exceed that of the product gases leaving it. Accordingly the enthalpy of the system at the maximum flame temperature cannot exceed twice that in a system without heat recirculation - if the heat exchanger were given another pass this would increase to

three times that value. A countercurrent heat exchanger is equivalent to letting the number of passes in a cross flow exchanger tend to infinity. Here there is no theoretical limit to the enthalpy at the maximum flame temperature - it is only constrained by practical considerations such as the maximum working temperatures of construction materials, see figure 6.

Figure 7 shows a selection of heat recirculating burner designs. Examples e,f,g,j are cross flow and b,c,h are countercurrent heat exchangers. Heat is transferred by

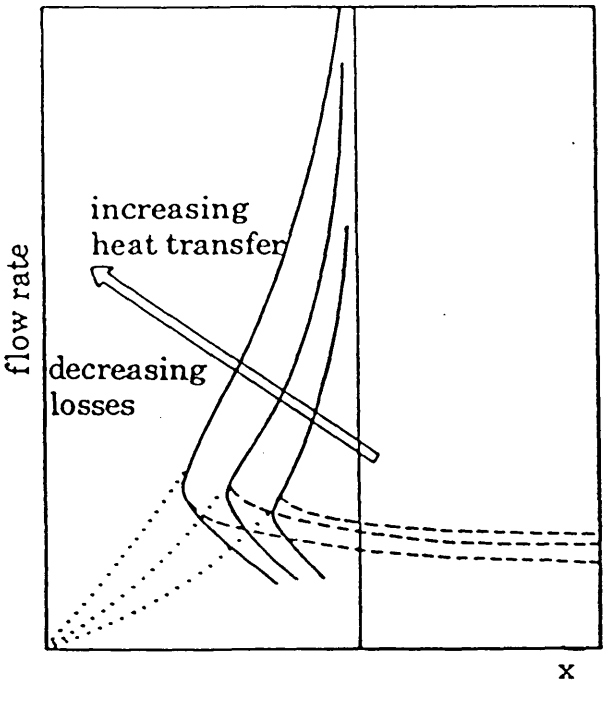

Figure 5 - Characteristic Stability Curves For Heat Recirculating Burners

(From Jones *et al.*, 1978)

---- Shows the effect as the mass flow → 0

.... Shows the effect as the heat losses → 0

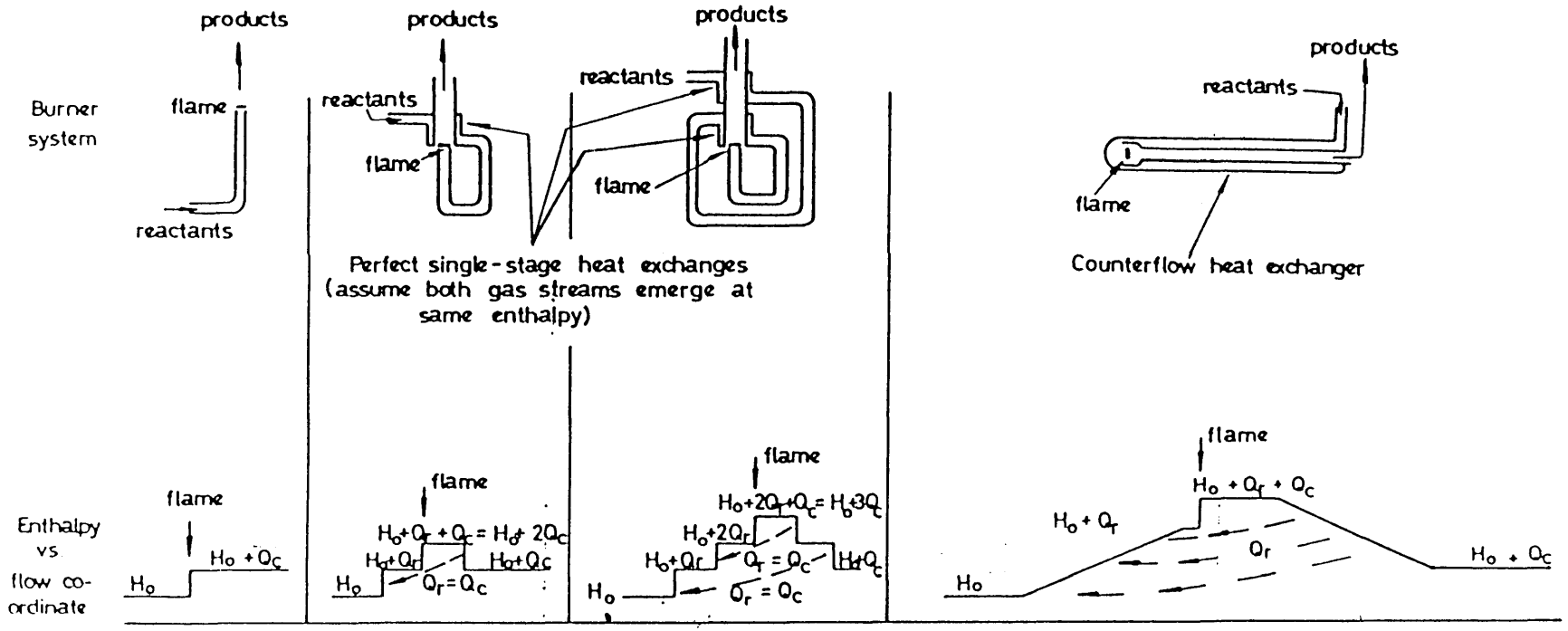

Figure 6 - Relation Between Enthalpy And Flow Coordinate For Various Burner Systems (From Weinberg, 1971)

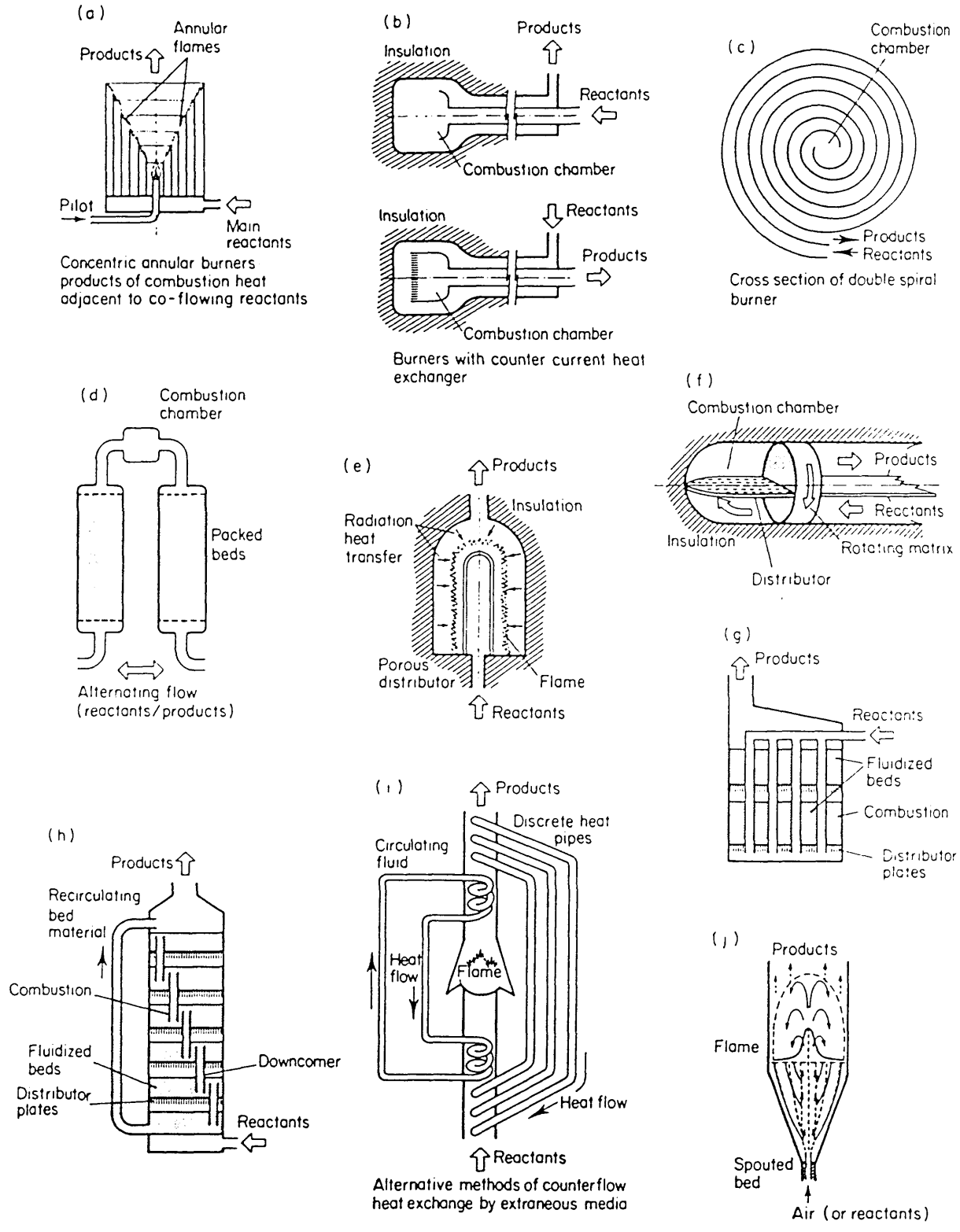

Figure 7 - Various Systems For Heat Recirculating Combustors. (From Weinberg, 1986)

radiation, through solid walls and via high heat capacity media which move between the hot products and cold reactants. These media can be circulating liquids / vapours (i), rotating matrices (f) or moving particles (j and h). The two burners studied in the present project are the "Swiss-roll" burner (c) and the spouted bed burner (j). These will be discussed in more detail later.

1.2.4 The Benefits Of Burning Lean

The ability to burn very lean fuel-air mixtures allows one to question the normal definition of a fuel. Any material capable of exothermic reaction can be regarded as a fuel if enough heat is recirculated to raise the reaction temperature it can produce unaided to a level where combustion can be sustained (Weinberg, 1975). Thus waste gases from many industrial processes, such as fermentation effluents or coal mine ventilation air, can be burned unsupported. Some low grade fuels actually have a negative cost as it is still common practice to add better fuels to them so that they can be burned. Together these fuels represent a large energy source, simply because there is so much of them. It was estimated (Roxbee-Cox, 1951) that the methane content of ventilation air from mines would be sufficient to satisfy the power requirements of all colliery machinery in he U.K.

Thus a prime reason for burning lean is to increase the efficiency by which we consume our limited national resources of fossil fuels. For instance it has been estimated (Weinberg, 1982) that by the year 2000, 80% of our energy will still be supplied by combustion. An improvement in combustion efficiency of just 5-10% would be equivalent to the combined contribution of nuclear, hydroelectric and all other non-combustion sources of power.

Another benefit of lean combustion is the reduction in pollutant emissions it affords. The combination of nitrogen and oxygen takes place at high temperatures and as lean combustion occurs at relatively low temperatures, low NOx emissions result. Lean combustion also has the advantage of

producing very little carbon monoxide.

1.2.5 The Benefits Of Burning Rich

For high temperature reactions, such as pyrolysis or partial oxidation, where the fuel is to be processed rather than burned, ultra-rich combustion employing heat recirculation allows the fraction of the fuel used for heat release to be minimised. The most prominent example of this is the production of synthesis gas, carbon monoxide and hydrogen, for conversion to chemicals. It will, however, be of advantage to any partial combustion reaction where inexpensive fuels are processed to more desirable products - eg. the production of carbon black.

Synthesis gas is usually used as a feedstock for the production of higher hydrocarbons (eg. by the Fischer - Tropsch process) and methanol synthesis. However the normal, non heat recirculation, methods for producing synthesis gas are often very expensive and the products require considerable refining prior to conversion - eg. steam reforming, autothermal reforming and non catalytic partial oxidation.

Burning rich can also be used as the first step in the reduction of pollutants, particularly NOx. It has been shown (Bartok and Song, 1982) that pollutant concentrations can be reduced by burning rich in a first stage, followed by the injection of air for a secondary lean combustion zone.

1.2.6 The "Swiss-roll" Burner

The "Swiss-roll" burner is a double spiral heat exchanger with a central combustion chamber - see figure 8. Hot exhaust gases from the combustion chamber exit through one channel of the spiral and preheat the reactant gases flowing through the other as they do so. Hence countercurrent heat recirculation takes place and, with the central combustion chamber shielded from heat loss, very high levels of preheat can be provided.

The first laboratory scale burner of this type was constructed from a single strip of inconel 600. The strip was folded in half and then wound spirally around this fold on spacers at the edge of the strip which were subsequently sealed with high temperature cement. Holes were made in the fold to allow reactant gases into the combustion chamber and thermocouples were distributed throughout in order to monitor the position of the flame and the amount of preheat (Lloyd and weinberg, 1974). Several burners were constructed with varying numbers of turns. Limiting stability curves for burners with 8 and 4½ turns are shown in figure 9. With methane (normal lean limit in air 5·3%) the richest mixture studied was 3·7% in air. As the number of turns was increased, for a given width of strip, progressively leaner mixtures could be burned. This trend continued until the side wall heat losses became controlling at large burner diameters. By using wider strips and adding insulation methane concentrations of less than 1% in air could be burned. An interesting result (Lloyd and Weinberg, 1975) was that the temperature in the reaction zone at the lean limit remained sensibly constant - at approximately 1400 K for methane. The explanation for this was thought to be that the limiting reaction rate was constant and, due to its high activation energy (268 kJ/mol. for methane - Burgoyne and Hirsh, 1954), far more dependent upon temperature than concentration. It was suggested that even sideways heat losses could be eliminated by using a torus shaped "Swiss-roll".

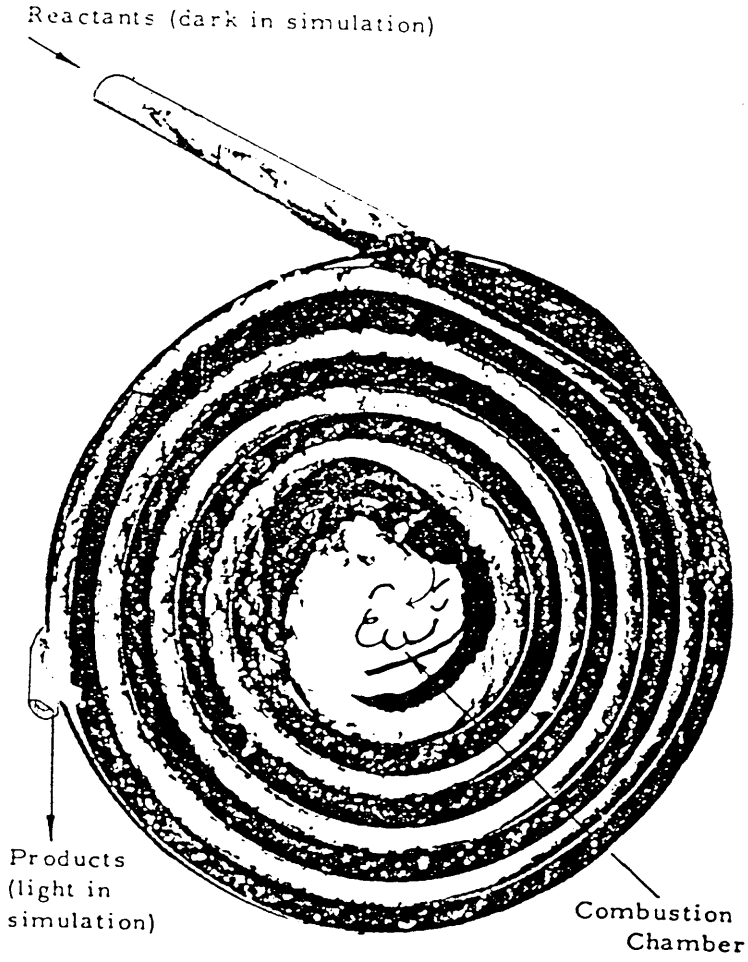

Figure 8 - The "Swiss-roll" Burner
(From Lloyd and Weinberg, 1974)

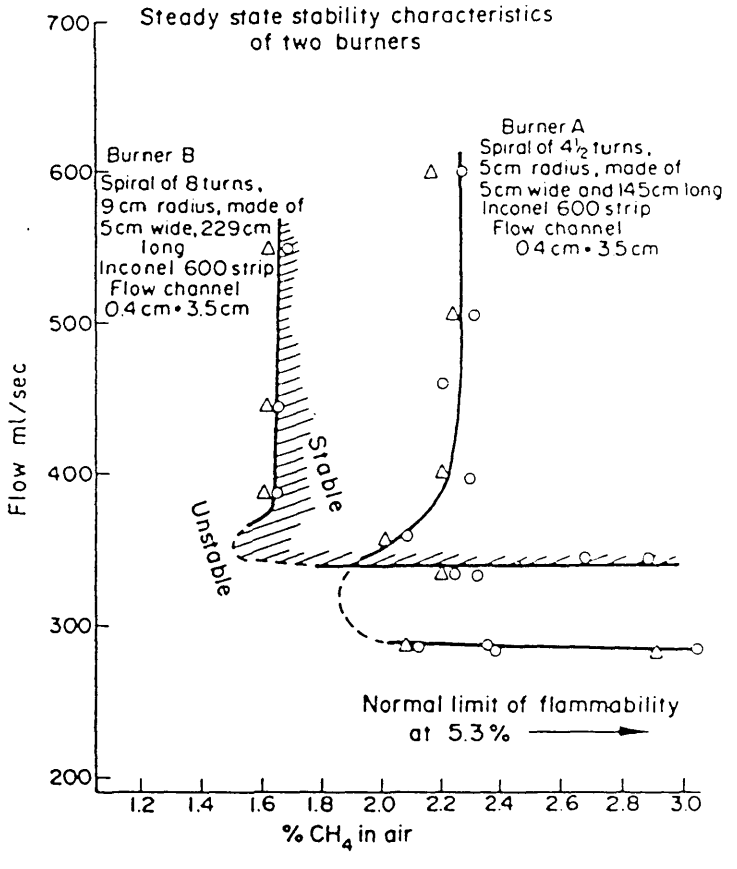

Figure 9 - Limiting Stability Curves For "Swiss-roll" Burners (From Lloyd and Weinberg, 1974)

An attempt to scale up the "Swiss-roll" burner was made at the Sunbury Research Centre of BP with the intention of recovering heat from solvent incineration (Murcar and Boden, 1984). The device was of a rigid metal construction and tended to strain and buckle due to differential expansion when subjected to the high temperatures of operation. Thus for industrial sized "Swiss-roll" burners some development in the design and materials of construction is still required.

By combining a mathematical description of a spiral with various heat transfer correlations Jones *et al.* (1978) developed a heat transfer model for the "Swiss-roll" burner. The first run of the model was for a large burner of eight turns, inside a thermos flask so that heat losses were effectively zero. A comparison between experimental and calculated results is shown in figure 10. To test a more realistic situation the model was then run for two burners of two turns and eight turns in conventional insulation. Figure 11 shows the experimental and calculated results for these cases; as can be seen the correlation is very good.

The geometry of the "Swiss-roll" is only suitable for gaseous or highly volatile liquid fuels; solid or viscous liquid fuels cannot easily be made to flow through the channels of the spiral (Weinberg, 1975). Also any pyrolysis products or soot formation would block the channels and coat the heat exchanger surfaces, thus decreasing its efficiency. In an attempt to overcome this, Lloyd and Weinberg (1976) constructed a "Swiss-roll" with a fluidised bed in the centre acting as the combustion chamber. Solid and liquid fuels could be injected into the central fluidised bed whilst the combustion air and gaseous products were conveyed through the surrounding spiral - see figure 12. However the fluidised bed, apart from making the burner very complicated, severely restricted the range of flow velocities over which a stable flame could be maintained at the lean limit of flammability.

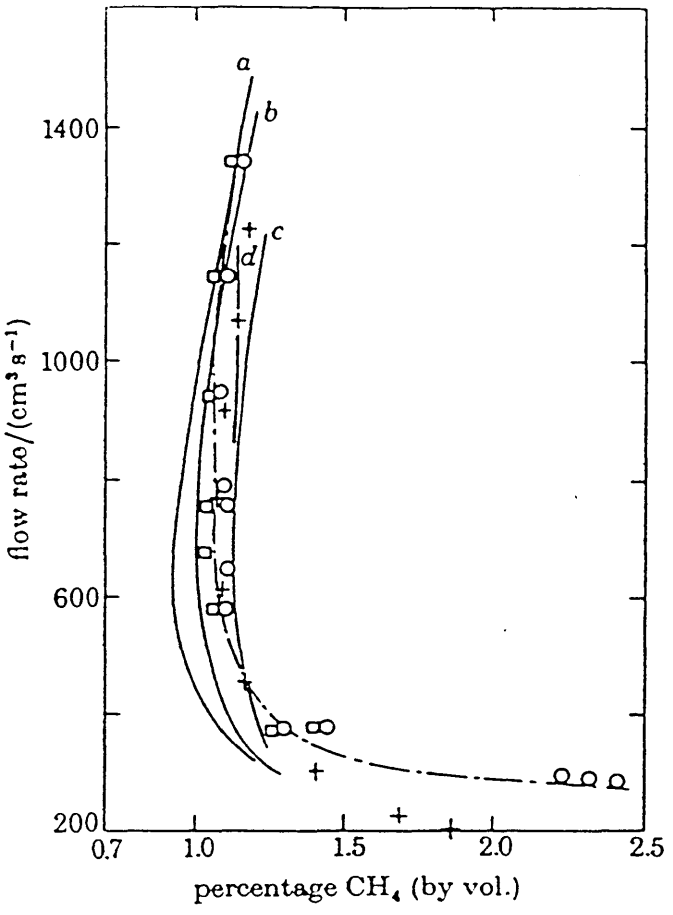

Figure 10 - Limiting Stability Curves For "Swiss-roll" Burners (From Jones *et al.*, 1978)

—·—·— = Experimental curve

o = Stable combustion

□ = Extinction

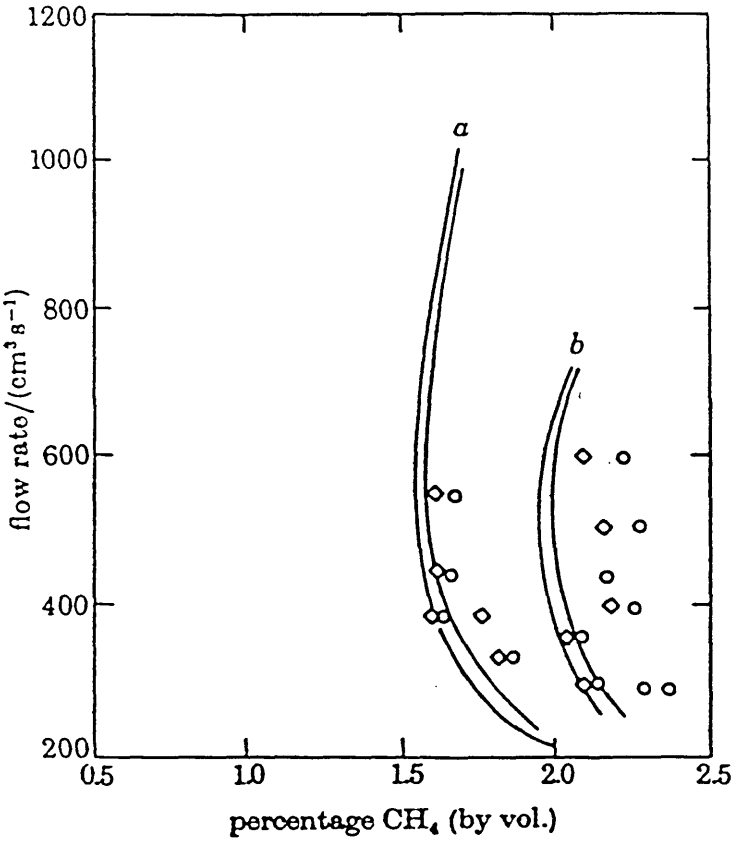

Figure 11 - Limiting Stability Curves For "Swiss-roll" Burners (From Jones *et al.*, 1978)

(a) = 8 turns , (b) = 5 turns

Experimental points : o = Stable combustion

◊ = Extinction

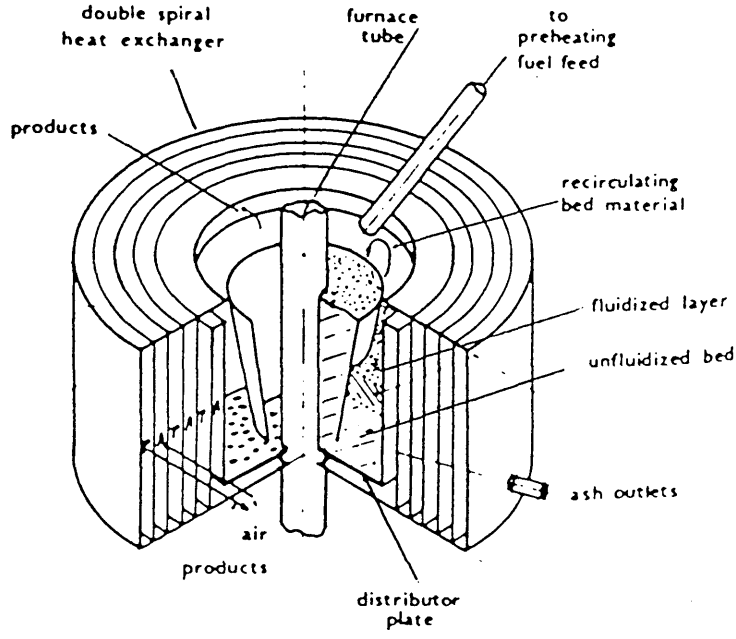

Figure 12 - "Swiss-roll" With Fluidised Bed Combustion Chamber (Fom Lloyd and Weinberg, 1976)

1.2.7 The Spouted Bed Burner

The ideal burner for solid or liquid fuels, as well as gaseous fuels which pyrolyse to solid or liquid products, would be a bed of moving particles. If the design of the bed geometry is such that the bed material moves in a cyclic pattern, passing through the flame zone, it can act as a mobile heat exchanger between hot products and cold reactants. Also any surface contamination of the bed material will be burnt clean in the flame. Small extensions to flammability limits can be attained by burning premixed gases in shallow fluidised beds, although the improvement over conventional burners is only slight (Cole and Essenhigh, 1973). To achieve the required degree of heat recirculation some form of forced cyclic particle motion is needed. The spouted bed provides the best example of this.

The spouted bed consists of a vessel, usually cylindrical, with an inverted conical base. A fluid can be injected at high velocity through a small inlet nozzle, located at the apex of the cone, into a bed of coarse particles. If the rate of injection is high enough a central void space, known as the spout, is formed by the resulting jet. Particles accelerate rapidly upwards in the spout and form a fountain above the bed which rains back onto the annulus, a downward moving bed of particles surrounding the spout forming a toroidal vortex - see figure 13. Hence a cyclic motion of solids is formed which, in the annulus, is countercurrent to the fluid flow. The concept was developed by Mathur and Gishler (1955) in Canada as a technique for drying wheat. Their investigations showed that there was a maximum spoutable bed depth and a minimum air inlet velocity for a given bed and inlet nozzle diameter. Increasing the bed diameter increased the maximum spoutable bed depth and decreased the minimum spouting velocity, whereas increasing the inlet nozzle diameter had the opposite effect. By using a semi-cylindrical vessel with a vertical flat glass plate, Mathur and Gishler were able to observe air steadily flaring out into the annulus as it travelled up the spout,

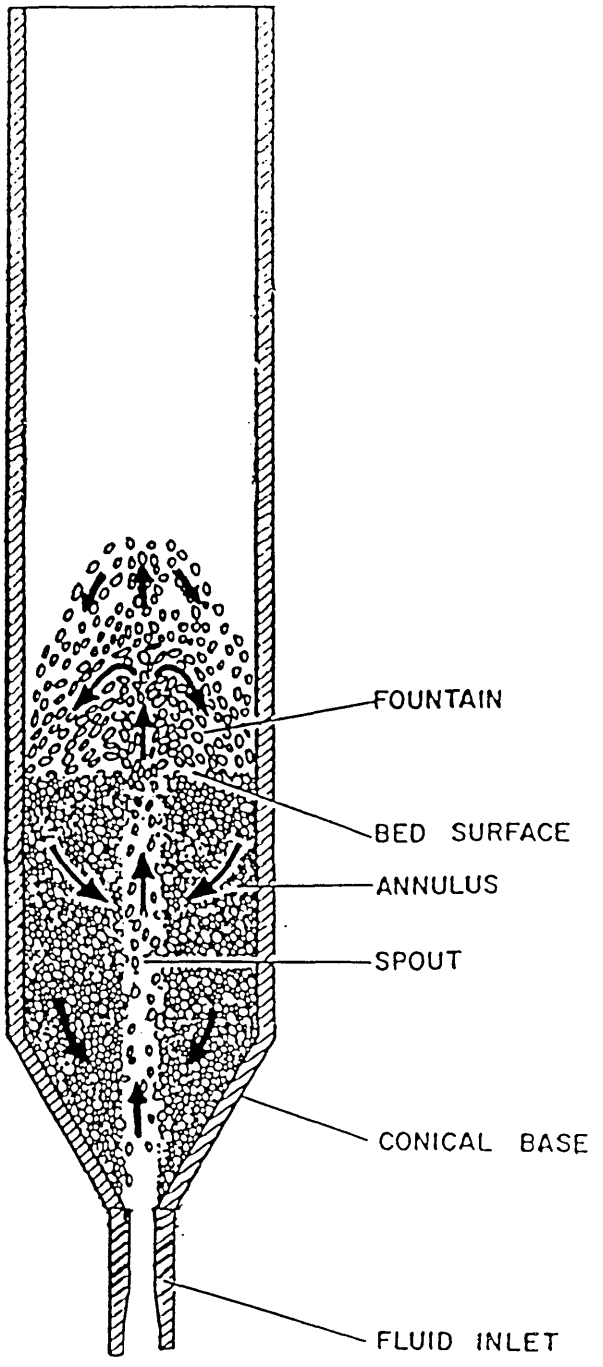

Figure 13 - The Spouted bed

(Adapted from Mathur and Epstein, 1974a)

estimating that 30% of the inlet air leaked from the spout in this way.

Many empirical and theoretical expressions have been developed to model the particle and fluid mechanics of cold (non-combusting) spouted beds. These have been comprehensively reviewed (Mathur and Epstein, 1974a) and include correlations for maximum spoutable bed depths, minimum spouting velocities, maximum pressure drops, spout diameters, particle size distributions, solid circulation rates and heat transfer coefficients among other bed parameters. Examples of some of these are shown below.

Maximum spoutable bed depth (Malek and Lu, 1965)

$$H_m/D_c = 0{\cdot}105.(D_c/d_p)^{0{\cdot}75}.(D_c/D_i)^{0{\cdot}4}.\ \lambda^2/(\rho_s)^{1{\cdot}2}$$

where : H_m = maximum spoutable bed depth, cm

ρ_s = particle density, 0·91–2·66 Mg/m^3

D_c = column diameter, range 10–23 cm

d_p = particle diameter, range 0·8–3·7 mm

λ = particle shape factor, range 1·0 for sand to 1·65 for gravel

$$\lambda = \frac{\text{surface area of a particle}}{\text{surface area of an equivolume sphere}}$$

Minimum spouting velocity (Mathur and Gishler, 1955)

$$U_{ms} = (d_p/D_c).(D_i/D_c)^{1/3}.[2.g.H.(\rho_s-\rho_f)/\rho_f]^{1/2}$$

where : U_{ms} = minimum spouting velocity, m/s

ρ_s = particle density, range 1·05–7·44 Mg/m^3

ρ_f = fluid density, Mg/m^3 based upon air

H = bed height, m

D_c = column diameter, m $\quad H/D_c = 1{\cdot}3–6{\cdot}7$

D_i = inlet diameter, m $\quad D_c/D_i = 3{\cdot}3–24{\cdot}0$

d_p = mean particle diameter, m ; $= 1/\Sigma(x_i/d_{pi})$

x_i = weight fraction of particles of size d_{pi}

Spouting pressure drop (Mukhlenov and Gorschtein, 1964)

$$\frac{-\Delta P_s}{H.\rho_b.g} = \frac{7{\cdot}68.(\tan\theta/2)^{0{\cdot}2}}{Re_i^{0{\cdot}2}.(H/D_i)^{0{\cdot}33}}$$

where : ΔP_s = spouting pressure drop, N/m^2
θ = internal cone angle, range 12-60°
D_i = inlet diameter, range 1·03-1·29 cm
H = bed depth, range 3-15 cm
d_p = particle size, range 0·5-2·5 mm
ρ_s = particle density, range 0·98-2·36 Mg/m^3
Re_i = Reynold's number based upon particle diameter and velocity through inlet orifice

Maximum pressure drop (Mukhlenov and Gorschtein, 1965)

$$(\Delta P_m)/(\Delta P_s) = 1 + 6{\cdot}65.(H/D_i)^{1{\cdot}2}.(\tan\theta/2)^{0{\cdot}5}(Ar)^{0{\cdot}2}$$

where : Ar = Archimedes number, $= g.d_p^3.\rho_f.(\rho_s-\rho_f)/\mu^2$
μ = fluid viscosity, kg/(ms)
ΔP_m = maximum pressure drop, N/m^2
other symbols and ranges are the same as the previous correlation

Mean spout diameter (McNab, 1972)

$$D_s = 0{\cdot}037.G^{0{\cdot}4}.D_c^{0{\cdot}68}/(\rho_b^{0{\cdot}41})$$

where : D_s = spout diameter, ft
D_c = column diameter, ft
ρ_b = solids bulk density, lb/ft^3
G = fluid mass flux, $lb/(hr.ft^2)$.
range : D_c = 10-61 cm
D_i = 0·6-10 cm
H = 15-183 cm
G = 0·35-1·8 $kg/(s.m^2)$
d_p = 1·3-7·3 mm
ρ_s = 0·92-1·4 Mg/m^3

Since its discovery, the spouted bed has found many applications including granulation, tablet coating, gas cleaning, comminution, iron ore reduction and cement clinker formation (Mathur and Epstein, 1974b). However this chapter will confine itself to combustion applications in spouted beds.

1.2.8 Combustion In Spouted Beds

The first reported use of a spouted bed for combustion was by Khoshnoodi and Weinberg (1978). The authors exploited the spouted bed's potential for recirculating heat by the hot particles, in order to burn low heating value fuels as well as ultra-lean hydrocarbon-air mixtures. With methane, the normal flammability limit could be reduced by a third and simulated low heating value fuels such as fuel-oil sand mixtures could be burned without difficulty. Temperature profiles were measured and a simple heat transfer model for the system developed. The system was subdivided into a gas flow and a circulating flow of solids, assuming that all the gas flowed through the spout and that combustion occurred therein. It was also assumed that particles attained thermal equilibrium with the gas in the hot and cold limbs of the heat exchanger, ie. the fountain and spout. By incorporating the concept of a constant final flame temperature at the lean limit of flammability, the lean limit itself could be calculated. This predicted that, in the absence of heat losses, the absolute minimum mixture strength burnable was half the normal lean limit of flammability. Additionally, by rearranging the equation produced by the model, the mass flow of solids for a given gas flow could be calculated. This is a very important parameter as it determines the effectiveness of the heat exchanger. Khoshnoodi and Weinberg also suggested certain refinements to the spouted bed such as the inclusion of a draft tube to prevent leakage from the spout into the annulus and a gauze above the bed on which a secondary fluidised bed could form, giving additional opportunities for heat recirculation and

pollutant reduction.

A study of spouted bed fluid mechanics (Arbib *et al.*, 1981) revealed some deviations from cold spouting behaviour. Compared to a cold spouted bed, the effect of combustion is to increase the pressure drop, decrease the minimum spouting velocity, increase the spout height and increase the solids circulation rate. This is due to the increased viscosity and linear velocity of the gas at high temperatures.

When lean mixtures of methane and air were burned at low flow velocities a flat flame stabilised above a packed bed. As the flow of gas was increased, first a pulsating-spouted combustion developed and then a steady combustion with the flame above the bed was stabilised. The flame consisted of a conical, bunsen type, flame above the spout surrounded by a flat flame above the annulus. Particles were seen to cascade up through the central flame and then re-enter the bed through the flat flame. The flat flame is caused by gas leaking from the spout into the annulus and percolating up through the packed bed. It is inherently more stable than the central flame due to the lower gas velocity and higher initial gas temperature there. However the flat flame could not survive long without the main conical flame as it relies upon this for a supply of hot particles. Similarly the flat flame stabilises the conical flame by replacing what would otherwise be a cold wall with a pilot flame of marginally higher flame temperature. At equivalence ratios nearer to stoichiometric, and at low flow velocities, the flame flashed back into the bed and stabilised in its upper layers. As the velocity was increased again, fluidised combustion occurred followed by spouting but with combustion still remaining submerged below the bed surface. All these combustion regimes were found to be sequence-dependent; see figure 14.

Measurements near the lean limit of flammability showed that temperature was uniform throughout the bed and hence that no reactions occurred therein. Based upon this experimental finding of isothermicity, an approximate

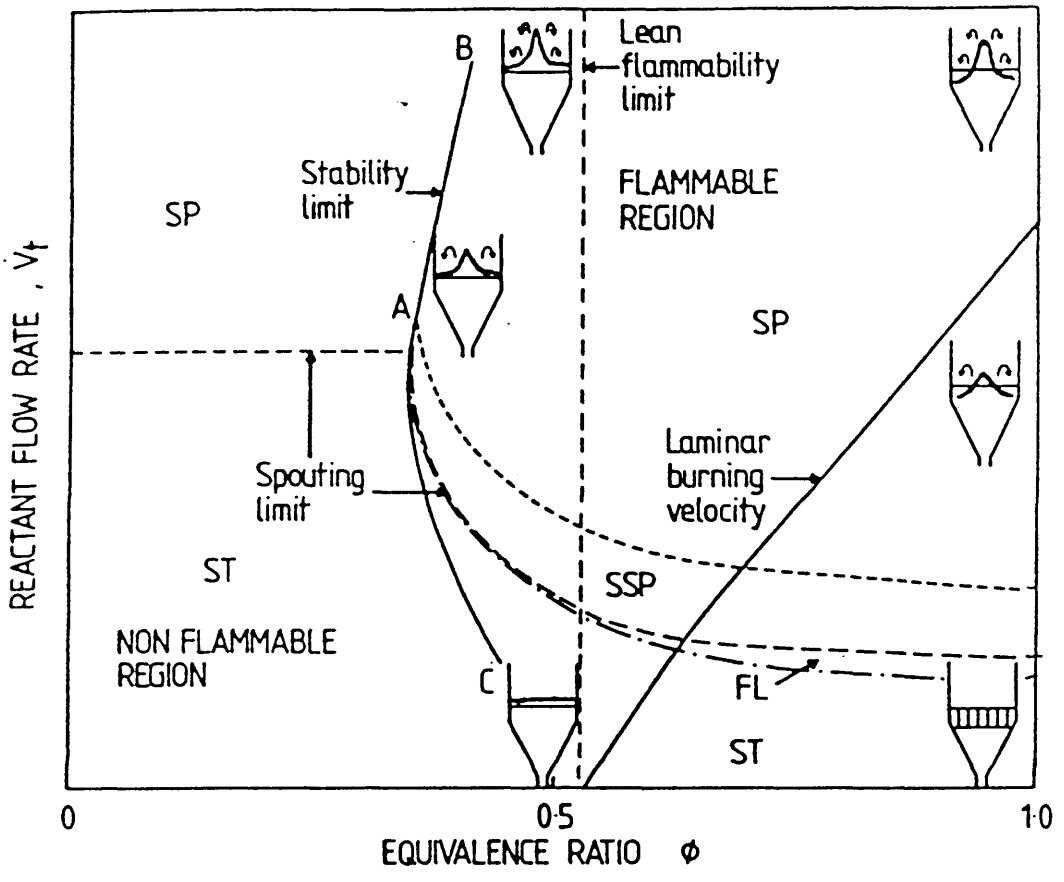

Combustion modes in the bed (ST-static; FL-fluidized; SSP-spouted, pulsating; SP-spouted).

Figure 14 (from Arbib *et al.*, 1981)

theoretical analysis of heat transfer within the bed was carried out. The analysis led to the conclusion that gas-particle contact times were insufficient for the two phases to attain thermal equilibrium. This offered an explanation for the experimental result that lean stability was restricted to 2/3 of the normal lean limit of flammability compared with a theoretical value of 1/2 the limit which could be achieved if the gas was preheated to the particle temperature.

Arbib and Levy (1982) used a spouted bed to burn low heating value fuels and waste fuels such as toluene, methanol-water mixtures and oil-water emulsions. Mixtures of 200-4000 ppm of toluene in air and methane were injected into the spouted bed. The methane flowrate could be reduced to give an equivalence ratio of 0·15 with 3430 ppm of toluene, which, when extrapolated, predicts that 6800 ppm of toluene could be burned unsupported in air. The normal lean flammability limit for toluene is 12700 ppm. Injecting methanol-water mixtures into the bed allowed a mixture of 1·6 volumes of water and 1 volume of methanol to be burned with 19% excess air. Also a 7 MJ/kg stable oil-water emulsion of 4·7 volumes of water and 1 volume of oil could be burned with 20% excess air. Liquid fuels of less than 10·5 MJ/kg cannot usually be burned without auxiliary fuel.

Ohtake *et al.* (1984) used a two dimensional rectangular spouted bed with a quartz side to allow visual observations of the combustion. During spouting four regimes were observed, a spout, a fountain, a moving bed and a packed bed region. Temperature profiles were measured which indicated that the particles were heated by convection in the spout and by conduction in the moving bed region. Heat transferred from the combustion gases to the particles was estimated as 8% of the total energy released. By photographing particle trajectories and using light scattering, particle velocities were calculated. In the moving bed region the particle path was almost parallel to the moving bed / packed bed boundary, however in the spout it was more complicated. Particles were seen to accelerate from the inlet nozzle until the spout diameter widened,

where their velocities decreased, and then accelerated again as they passed through the flame due to the gas expansion. Finally, in the fountain, the particle velocities fell to zero and they reversed direction.

With regard to extending the rich flammability limit, methane-air mixtures have been burned at up to 2·34 times their stoichiometric mixture composition (Weinberg *et al.*, 1988). The locus of stability limits for rich mixtures at different flowrates exhibits a reversed 'C' shape curve, approximately symmetrical with the corresponding lean limit curve. The shape is thought to be due to the decreased heat recirculation both at very low and very high flowrates. At low flows the particle circulation rate decreases and at high flows the contact time between gas and particles is diminished. It was also observed that no appreciable soot deposition occurred. On analysis the product gases were shown to contain about 15% H_2, 10-14% CO and 0·6% C_2 hydrocarbons - all volume % of dry products. Similarly rich methane-oxygen mixtures have been burned, in spouted beds, up to an equivalence ratio of 2·0. However this was accompanied by significant heat losses and higher equivalence ratios could have been attained with an adiabatic system. Product gases contained 42-55% H_2, 27-37% CO and up to 9% C_2 hydrocarbons - again all volume % of dry products.

Rich combustion in the spouted bed has also been studied using catalytically active bed material. This was first proposed in a third year undergraduate research report by Bartleet and Rimbotti who carried out much of the pioneering work on rich combustion in spouted beds whilst working with Professor Weinberg in 1982. Later Brophy and Telford (1985) used partial oxidation and steam reforming catalysts such as group viii metals on refractory supports at temperatures between 800 and 1200°C. With air, mixtures containing 25% methane were burned yielding synthesis gases containing up to 24% H_2 and 12% CO. Oxygen mixtures containing 60% methane (and 2·8% N_2 for tracing) yielded 60·4% H_2 and 30·1% CO in the product gases with 89·6% methane conversion.

1.2.9 Coal In Spouted Beds

The first reported use of coal in a spouted bed appeared in 1968 when this device was used for low temperature coal carbonisation (Barton *et al.*, 1968). Since then spouted beds have also been used for coal pyrolysis, combustion and gasification.

1.2.9.1 Coal Carbonisation

Low temperature coal carbonisation is a thermal process in the temperature range 450-750°C involving the evolution of volatile matter from the coal producing char, a complex liquid hydrocarbon tar, fixed gases and an aqueous liquor. The process is mainly used for the production of smokeless fuels and was developed in Britain and India during the 1950's. One problem with the process is the formation of char agglomerates due to the high rates of heating used. It was hoped that the violent agitation of relatively large particles in the spouted bed would overcome the agglomeration problem and so work was started on the subject, mainly in Australia.

Barton *et al.* (1968) carbonised various Australian coals in a six inch diameter spouted bed. They used -6 +10 mesh (1·68-3·36 mm) coal continuously fed from a vibratory feeder with electrically heated nitrogen and air as the spouting gases, giving bed temperatures from 450°C to 650°C. In all 31 carbonisation runs were carried out and only one showed any evidence of agglomeration. Careful control of the feedrate was shown to be important, if agglomeration was to be avoided.

For design purposes a model was proposed by Ratcliffe and Rigby (1969) to predict the concentration of the volatile matter in the exit char. The model was based upon particle exit age distributions and experimentally determined devolatilisation data from a simulated reactor. The authors considered the spouted bed to be a slowly moving packed bed, through which carbonising gas passed

thus contacting discrete particles. This was simulated by placing a single layer of particles in a stainless steel gauze bucket which was suspended over a 4" diameter packed bed through which preheated gases were passing in plug flow. However, to represent the spouted bed accurately, the authors also needed to know temperature profiles, gas compositions and gas velocities in the bed. Temperature and concentration profiles were measured directly in a spouted bed similar to that used by Barton *et al.* (1968). Velocity profiles were calculated from pressure drop measurements, using a previously derived relationship between pressure drop and velocity in a semi-cylindrical cold spouted bed. The model was tested with Liddel coal for which it predicted the exit char volatile matter content to within 7% of that found by experiment.

Nevertheless this model still required experimentally determined devolatilisation data for each temperature used and hence was of limited value from the point of view of predictive design. Quinlan and Ratcliffe (1971) set out to overcome this and produce a more general design equation. Using the results of Ratcliffe and Rigby (1969) the authors found that devolatilization could be represented by;

$$\frac{-dC_v}{dt} = k.(C_v)^n$$

where : n = reaction order,

k = rate constant.

C_v = volatile matter concentration

Hence from Levenspiel (1966) ;

$$\left[\frac{C_v}{C_{vo}}\right]_{Batch} = (1+At)^{1/(1-n)}$$

$$\approx (At)^{1/(1-n)} \qquad \text{For } At \gg 1$$

where : $A = (n-1).k.(C_{vo})^{n-1}$

By comparing the spouted bed with an ideal back mix reactor;

$$\left[\frac{\bar{C}_v}{C_{vo}}\right] = \int_o^\infty \left[\frac{C_v}{C_{vo}}\right]_{Batch} . \frac{1}{\bar{t}}.\exp\left[\frac{-t}{\bar{t}}\right] dt$$

$$= \int_o^\infty (A.t)^{1/(1-n)} . \frac{1}{\bar{t}}.\exp\left[\frac{-t}{\bar{t}}\right] dt$$

where : $\bar{t}$ = mean residence time

By also taking into account, $k = k_o.\exp(-Ea/(R.T)$, the model became a function of temperature rendering the experimental determination of devolatilisation rates for each temperature no longer necessary. Experiments with the six coals used by Barton *et al.* (1968) showed that the only parameter dependent upon coal type was the Arrhenius frequency factor which could be determined from one experiment with the coal.

1.2.9.2 Coal Pyrolysis

Coal pyrolysis is the thermal decomposition of coal in the absence of oxygen to yield volatile matter and liquid tars, leaving a solid char residue. Unlike in the case of coal carbonisation, the desired products are the tars which can be used as chemical feedstocks. Many good pyrolysis coals tend to cause agglomeration problems in conventional reactors, such as fluidised beds, and again it was thought that a spouted bed might overcome these problems.

Ray and Sarkar (1976) pyrolysed four Indian coals in an electrically heated 100 mm diameter spouted bed. Coal was fed in 1 kg batches of particle size 1·2-2·5 mm into the bed at temperatures of up to 540°C with preheated nitrogen as the spouting gas. Char samples were taken at fixed intervals after feeding the coal to the bed. The fractional change in volatile matter was taken as a kinetic parameter and used to study the process kinetics. Below 400°C the process showed a first order rate dependence, followed by a zeroth order rate equation. At higher temperatures it showed a second order rate dependence followed by a first order rate law, with a transition period between the two. The higher the temperature, the earlier the second order part terminated. The process had both a low activation energy and Arrhenius frequency factor which suggested that it was physical below 400°C and, at higher temperatures, chemical at the second order stage but physical at the first order stage. Thus the process may be considered as decomposition of the coal followed by the escape of the decomposition products by diffusion. The temperature determines whether the diffusion or decomposition is rate controlling.

Jarallah and Watkinson (1985) used a continuous process to pyrolyse four Canadian coals in a 128 mm diameter, electrically heated spouted bed. The bed comprised of inert particulate material (sand) and was fed with 1·19-3·36 mm coal particles from a vibratory feeder to the bottom of the vessel. Carbon dioxide and nitrogen formed the spouting

gases and the process was assessed by measuring the yields and compositions of the tars, chars and gases produced. Tar yields varied from 21% to 30·6% wt/wt MAF coal with CO, CO_2 and CH_4 being the main gases produced. Tar yields were also found to decrease if the char loading in the bed became too high or if the coal particle size was reduced below 0·65 mm.

Teo and Watkinson (1986) researched the rapid pyrolysis of lignite, bituminous and sub-bituminous coals in a spouted bed. A 25 mm diameter electrically heated spouted bed was used, with sand as the particulate material and coal of size less than 250 μm continuously fed from a vertical screw feeder. Maximum tar yields from the sub-bituminous coals were obtained at 500°C and were high in hexane soluble fractions. Gas yields contained mainly carbon oxides due to the coals' high oxygen contents, but there was also some methane, ethane and hydrogen. The bituminous coals gave maximum tar yields at about 700°C, the tars being aromatic and having 20 wt.% hexane soluble fractions with 50-79 wt.% benzene soluble fractions. The main constituent of the gases produced was methane, being 25-50 vol.%, with about 10-20 vol.% of hydrogen and carbon oxides. Water was the main constituent of the liquid produced from the lignite and, due to its high oxygen content, the gases consisted mostly of carbon oxides. Generally gas yields increased with tmperature as did the ratio of ethylene to acetylene produced.

1.2.9.3 Coal Combustion

Several studies have been undertaken purely on the combustion of coal in spouted beds.

Kumpinsky and Amundson (1984) assessed five different models simulating char combustion in the annulus of a spouted bed. A continuously stirred tank model (CST), a series of n CST's one on top of the other (CSTn), a CST model with transient single particle combustion (CSTt), a plug flow model (PF) and a model with radially and axially distributed concentration profiles in the annulus (RD). The

models also incorporated equations allowing for the distribution of temperature and reactant mole fraction in the boundary layer surrounding a single particle. Numerical solutions to the various models were compared by varying parameters such as the average oxygen mole fraction, the bed temperature, the inlet char particle size or the sand particle size in the spouted bed. The simplified CST, CSTt, CSTn and PF models gave reasonable estimates of the heat generation and the char intake but failed to predict the attainment of ignition or the char loadings in the bed. With the RD model, ignition could only be attained in regions near the spout but this was sufficient to predict much higher combustion rates than the other models. For a better representation of the spouted bed the authors suggested that a model consisting of several interconnected CST's for the base unit with a plug flow section for the annulus above it should be investigated. This would enhance the level of oxygen segregation in the bed and thus increase the probability of particles attaining ignition. This in turn would lead to reduced char loadings.

Zhao *et al.* (1987a) carried out two projects, one on flow regimes and combustion behaviour and the other (1987b) on coal burnout times in spouted and spouted-fluidised beds. In the first project a semi-cylidrical 0·152 m diameter spouted-fluidised bed of sand was used, to allow visulisation. Canadian Forestburg coal was pneumatically conveyed to the vessel from a rotary valve feeder. Different combinations of spouting and fluidising air flowrates produced four different combustion regimes, using coal particles of size 0·69–1·04 mm. A stable spouting, a pulsatory spouting, a jet submerged in a fluidised bed and a slugging regime. When finer coal particles were introduced, they were seen to burn in a secondary fluidised bed above the main spouted bed. Temperature profiles were found to be relatively uniform except for the case where fine coal particles were burned, here a temperature rise occurred above the bed. Oxygen concentration decreased slightly in the spout and then became constant above the bed. In the annulus it decreased gradually up to the bed

surface and then rapidly to a minimum in the fountain before increasing again. The subsequent rise in oxygen concentration was thought to be due to radial mixing of low oxygen gas from the annulus with the high oxygen gas from the spout. The main conclusion from all this was that substantial combustion was occurring in the fountain region.

In the second project (Zhao *et al.*, 1987b), burnout times were measured for coal particles of size 0·55-2·2 mm in the same spouted bed as used in the first project. The spouted bed was fed with coal until the desired temperature of 810°C was reached. The coal feed was then shut off and a 2g test batch of coal dropped into the top of the spouted bed. Coal particles were seen to ignite instantaneously and their burnout times were measured visually with a stop watch, to within ± 5% accuracy. The times recorded varied from 20s to 60s depending on the coal partcle size; see figure 15. This was considerably faster than burnout times measured in a similarly sized fluidised bed, suggesting that the spouted bed has a higher combustion efficiency for burning coal than the fluidised bed.

A simple model for the burnout time of the coal was formulated, involving a single film theory to describe combustion in the vicinity of burning particles. This gave the expression for the burnout time, t_b shown below.

$$t_b = \frac{m}{24.U_{mH}.A_m.C_o} + \frac{\rho_c.d_o^2.\lambda}{96.Sh_o.D_g.C_o} + \frac{\rho_c.d_o}{24.k_c.C_o}$$

Where λ is a factor which allows for changes in the Sherwood number, Sh, during combustion and is given in terms of the initial Sherwood number, Sh_o.

$$\lambda = \frac{4.Sh_o}{(Sh_o - 2.\epsilon)^4} \cdot \left[\frac{Sh_o^3}{3} - 3.\epsilon.Sh_o^2 + 12.\epsilon^2.Sh_o - 8.\epsilon^3.\ln\left[\frac{Sh_o}{2.\epsilon}\right] - \frac{44.\epsilon^3}{3} \right]$$

Where : U_{mH} = superficial velocity at bed surface
m = mass of carbon in bed
A_m = cross sectional area of annulus
C_o = initial oxygen concentration
ρ_c = carbon density
d_o = initial coal particle diameter
D_g = gas phase molecular diffusivity of oxygen
k_c = chemical reaction rate constant based upon surface area
ϵ = loose packed bed voidage

Figure 15 shows a comparison of predictions from the model with experimental burnout times. As can be seen the agreement is good.

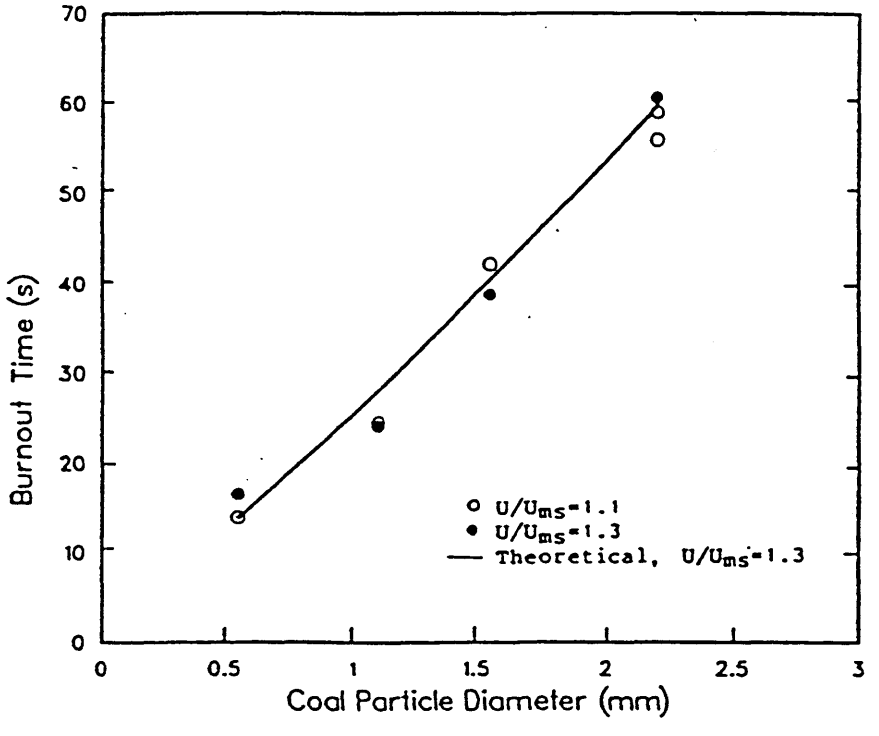

Figure 15 (from Zhao *et al.*, 1987b)

1.2.9.4 Coal Gasification

Coal gasification is the thermal decomposition of coal at high temperatures in a reactive atmosphere - with the emphasis on the production of useful gases or gases to drive turbines.

Ingle and Sarkar (1976) gasified a non caking Raniganj coal in a batch type, 10 cm diameter spouted bed. It was electrically heated and used air and steam as the spouting gases. The coal, of particle size 1·2-2·05 mm, was fed in batches of 1 kg with the bed at temperatures of 600°C, 700°C, 800°C, 900°C and 1000°C. The controlling reactions for this type of gasification are the reduction of CO_2 to CO and to a lesser extent the decomposition of steam by carbon. The CO/CO_2 ratio was measured at different temperatures and correlated as shown below.

$$[CO]/[CO_2] = - 0{\cdot}5833 + 2{\cdot}6 \times 10^{-3}.T$$

between 600°C and 800°C

and,

$$[CO]/[CO_2] = 3{\cdot}03 - 7{\cdot}565 \times 10^{-3}.T + 7{\cdot}05 \times 10^{-6}.T^2$$

above 800°C

where: T = temperature, °C

This showed that the CO/CO_2 ratio increased with temperature as expected, the reaction being highly endothermic.

Foong *et al.* (1980) tried to gasify caking coals in a spouted bed. This was an attempt to overcome the problems associated with gasifying caking coals in fluidised beds. On heating, caking coals tended to swell and become sticky, causing agglomeration which led to defluidisation. As mentioned before, the spouted bed can deal with agglomeration. A 0·15 m diameter spouted bed of silica particles was used with coal of size 0·8-3·6 mm

continuously fed to the top of the bed from a vibratory feeder. The spouting gases were air and steam; propane gas was used for start up. Three Western Canadian coals were gasified, Forestburg, Coleman and Sukunka, with the bed temperature being maintained between 1020 and 1220 K. The Forestburg coal produced gases containing 15% H_2, 8-11% CO, 1-3% CH_4 and 61% N_2 with a heating value of 3·7 MJ/m^3. The highest tolerable coal feedrate was 12 kg/hr. The Sukunka coal yielded gases with a heating value of 2·8 MJ/m^3 containing 7-11% H_2, 5-8% CO, and 69-75% N_2. The maximum tolerable coal feedrate was 6 kg/hr. The Coleman coal required higher temperatures and only produced a very weak gas. Caking problems were experienced in the feeding system with the Sukunka and Coleman coals. This could have been alleviated by feeding to the relatively cool base of the spouted bed. Nevertheless these caking coals could still be gasified despite the feeding problems, but at lower feedrates. The conclusions from this work were that the temperature should be kept as high as material and NOx considerations allow, with the gasification reactions being so endothermic. Also that the coal feedrate is critical in controlling caking problems, although generally an increased coal feedrate leads to an increased gas yield. Finally, that larger coal particles give higher gas yields due their longer residence times.

Foong *et al.* (1981) scaled up this work with a similar 0·31 m ID spouted bed. The bed material was gravel of size 1·0-3·4 mm and coal was continuously fed from a vibra screw feeder to either the top or bottom of the bed. Again Canadian Forestburg, Coleman and Sukunka coals were used. The gas yields are best shown in tabular form, as below.

Coal	Forestburg	Sukunka	Coleman
Feedrate	60 kg/hr	43 kg/hr	47 kg/hr
Gas yields			
% H_2	15·5	13·0	14·3
% CO	14·5-20·0	9·1-12·7	13·2
% CO_2	9·8-12·3	10·7-13·9	11·9
% CH_4	1·3-1·6	1·6-2·1	1·7
% N_2	54·5	59·0-66·0	60·4
Gas Heating value MJ/kg	4·4-4·7	3·3-3·6	3·7-3·8
Bed T , °C	805-850	920-965	985

Bottom feeding of the coal, apart from giving better mixing and longer residence times, was easier to control, allowing higher feedrates which gave increased gas yields. Scale-up also allowed the coal feedrate to be increased, by 20-30% per unit cross section of the bed. (The larger bed could tolerate 37% carbon whereas the smaller, 0·15 m, bed could only accept 10%). This gave rise to a 10-20% improvement in product gas heating value as well as a 6-16% increase in gas yield. Furthermore, the smaller relative heat losses and improved fluid mechanics of the larger bed led to smoother operation.

In order to compare coal gasification in a spouted bed with that in a fluidised bed; Watkinson *et al.* (1983) adapted the same 0·31 m diameter spouted bed so that a titanium distributor gauze could be inserted quickly into its conical section. In this way experiments could be carried out with coal from the same batch, operating in spouted and fluidised modes alternately. The bed material was gravel, size 1·2-3·4 mm, for spouting and sand, size 0·71-2·00 mm, for fluidising. Five Canadian coals of size 1·19-3·36 mm were used: Sukunka, Balmer rejects, Forestburg, Roselyn and Klimax coals. With the exception of the Klimax coal, which contains eutectic Na_2O in the ash -

a cause of agglomeration - all the coals could be gasified in both the spouted and fluidised modes. Caking and non-caking coals were readily gasified in both modes with similar gas yields and thermal efficiencies. However neither system was using an optimised coal size, there was no char recycle and further scale-up might have revealed differences between the two systems.

Still using the same 0·31 m diameter spouted bed, Haji-Sulaiman *et al.* (1986) measured gas compositions and temperature profiles during the gasification of two Canadian coals (Forestburg and Balmer coals of size 1·19-3·56 mm). Eighteen stainless steel probes were used, each with a 90 μm porous stainless steel filter at the end and a chromel-alumel thermocouple inside. The probes were mounted in six axial and three radial positions and were simultaneously sampled isokinetically to give concentration profiles. Measurements during the gasification of the Forestburg coal revealed that the oxygen concentration fell to zero very near the inlet to the bed. This showed that combustion only took place in the lower spout regions and that the CO_2 detected higher up the bed must have been the product of pyrolysis reactions. Also the presence of CH_4 in the upper annulus confirmed that pyrolysis reactions were taking place. The fact that CO and H_2 concentrations were only significant higher in the spout suggests that gasification reactions only occurred in the upper half of the bed. Temperature was found to increase rapidly in the lower spout, due to combustion, and then to decrease because of endothermic pyrolysis and gasification reactions. With the less reactive Balmer coal, containing less oxygen and volatiles, CO_2 concentration was found to decrease steadily up the bed and CH_4 concentration was low and constant. The conclusion from this was that pyrolysis occurred to a very limited extent with the Balmer coal.

The Coal Research Establishment of the British Coal Corporation (Butt *et al.*, 1987) has developed a spouted-fluidised bed coal gasifier. The aim was to provide clean hot gas at temperatures of up to 1600°C. The gasifier is based upon a submerged spout, spouted bed with two

laboratory scale versions (0·15 m and 0·3 m diameter) and a semi-commercial unit (0·5 t/hr) having been built. Three British coals have been tested - Daw Mill, Baddesley and Seamoor. However, as in many fluidised bed gasifiers, the fuel to gas conversion was low; on a mass basis about 60% in the 0·3 m diameter bed and 61% in the semi-commercial unit. This was mainly due to the elutriation of fines from the beds. In the U.K.,for economic reasons, a 90% conversion is required.

To minimise the effect of elutriation an experiment was carried out with the Baddesley coal whereby the carbon content of the bed was reduced and fines collected in the primary cyclone were recycled to the spout. In the 0·3 m diameter gasifier, using a sand bed, conversion was increased to 94%, producing 78 m^3/hr of 3·7 MJ/m^3 gross CV gas from 14·6 kg/hr of coal. With the 0·5 t/hr unit conversion was increased to only 69%, Due to the continued elutriation from the char bed. Nevertheless this still produced 1508 m^3/hr of 3·5 MJ/m^3 gross CV gas from 452 kg/hr of coal. The product gas also contained various pollutants - 350 vppm HCl, 200 vppm H_2S, 12 vppm CS_2, 100 vppm COS and 300 vppm NH_3.

To test the effect of enriching the gasifier contents with oxygen, the oxygen concentration in the fluidising gas was raised from 13·8% to 28·9% in the 0·3 m diameter unit. The calorific value of the gas so produced was increased from 3·1 MJ/m^3 to 4·7-6·4 MJ/m^3 with a conversion efficiency of 71-77% on a mass basis.

CHAPTER 2

THE "SWISS - ROLL" BURNER

2.1 Aims

As described in chapter 1, the "Swiss-roll" burner is a double spiral heat exchanger with a central combustion chamber. The geometry is such that it recirculates heat countercurrently between the hot products and cold reactants, with minimum heat loss as the combustion chamber is at the centre. Lloyd and Weinberg (1974) showed that a mixture of 1·6% methane in air could be burned in a "Swiss-roll" burner of eight turns, compared with a normal lean limit of 5·3% for methane. Thus the "Swiss-roll" burner is very efficient at recirculating heat and should also be able to burn very rich mixtures of gaseous hydrocarbons in air. It cannot however be used with liquid or solid fuels as these cannot easily be made to flow through the channels of the spiral.

A possible problem is that any soot formation, which is usually associated with rich combustion, would coat the surfaces of the heat exchanger and decrease its efficiency. However, no soot has been observed during a recent project studying the rich combustion of methane in a spouted bed (Jebrail, 1987). Accordingly this chapter describes attempts to investigate the potential of the "Swiss-roll" burner for the partial oxidation of methane to synthesis gases and higher hydrocarbons, it being initially thought that the richer the mixture burned the larger the yield of synthesis gases. A small laboratory scale burner was fabricated for this purpose.

2.2 Construction Of The Experimental "Swiss-roll" Burner

The "Swiss-roll" burner used for the laboratory experiments was fabricated from inconel (600) strip annealed to a thickness of 0·2 mm and cut to a width of 40 mm. Two 1 m length pieces of this strip were rolled together into a spiral leaving a 40 mm diameter combustion chamber in the centre and a 3 mm spacing between strips. This was achieved by sellotaping two lengths of thick string to each strip before rolling them together around a 40 mm diameter section of brass tube. One face of the spiral was then sealed with low grade alumina cement, leaving a tiny hole in the centre for the insertion of a thermocouple probe. After the cement had been left to dry for about 24 hours, the string was removed and the sellotape burnt away from the channels with a blow torch. The top of the spiral was then also sealed with alumina cement, leaving a central 20 mm diameter hole for access to the combustion chamber and ignition. A 0·125 mm R-type thermocouple, encased in a 20 mm length of 3 mm diameter twin bore recrystallised alumina rod, was inserted through the tiny hole to the centre of the combustion chamber and cemented in place. Finally, a short length of ¼" copper tube was cemented into the outer turn of each channel for the attachment of supply and exhaust pipes. The newly constructed burner, having 5½ turns and a channel cross sectional area of 0·9 cm^2, was then fired in a high temperature oven to cure the cement.

To support the "Swiss-roll" burner when in use, a 'quick release' type clamp was designed - see figure 16. This served two functions: firstly to hold the burner in place and secondly to seal the combustion chamber after ignition. To perform the latter function a stainless steel plate was screwed down from the top of the clamp onto a piece of 'Kaowool' insulation which acted as a gasket. The clamp also allowed the "Swiss-roll" burner to be rotated to any angle between a horizontal and a vertical position.

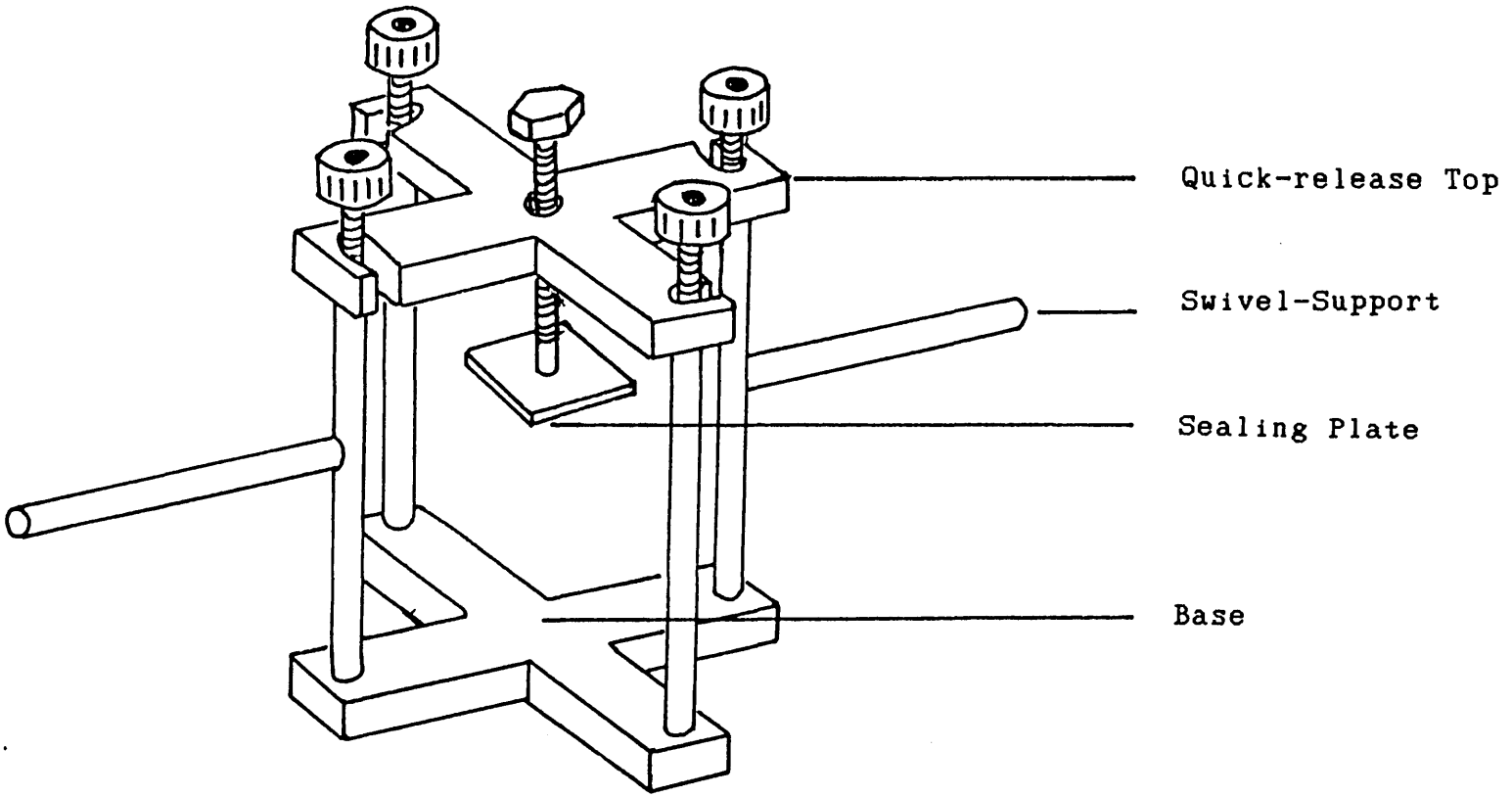

Figure 16 - "Swiss-roll" Burner Support Clamp

2.3 Gas Feeding System

A schematic diagram of the gaseous fuel supply system is shown in figure 17. It consisted of a number of rotameters and mercury manometers measuring a supply of methane and air at a pressure of two bar (abs.) to a copper mixing vessel and then into the "Swiss-roll" burner. Air was obtained from a compressor, having first been filtered and dried, and methane from a cylinder of 'Technical Grade' (96% pure) methane supplied by BOC plc.

In order to span the whole flammability range of methane, three rotamters were used, operating in the flow ranges of 4-26 cc/s, 25-85 cc/s and 60-300 cc/s of methane. The air rotameter covered a range of 150-950 cc/s. All the rotameters were calibrated at two bar (abs.) pressure using a bubble flowmeter, after the entire system had first been pressurised to test for leaks. The excess mixture burner was provided so that the total mixture flow rate could be varied without altering the methane equivalence ratio. Reinforced PVC tubing and needle valves were used throughout the system and a number of flame traps was also included to prevent flash back.

2.4 Analytical System

2.4.1 Analytical Equipment

The products from the "Swiss-roll" burner were entirely gaseous (including steam) and so gas chromatography was an obvious choice of analytical technique. The particular instrument used was a PYE UNICAM GCD gas chromatograph upgraded to include a thermal conductivity detector in addition to its original flame ionization detector. The thermal conductivity detector was operated in a thermostatic oven set at 120°C and controlled by a Taylor Servex Katharometer Control Unit. The built in flame ionization detector was operated at 150°C.

Two 1/8" diameter stainless steel columns were used,

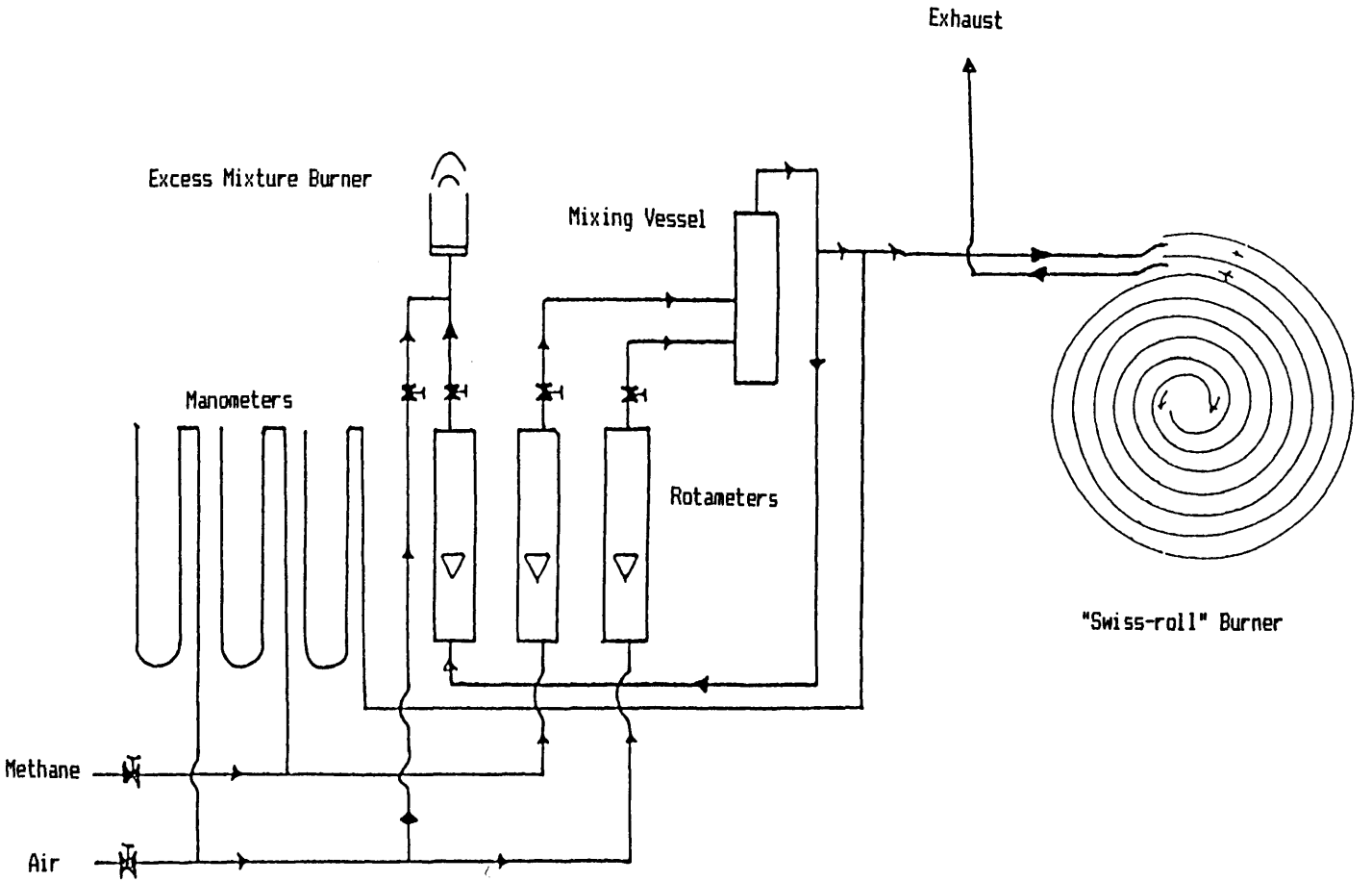

Figure 17 - "Swiss-roll" Gas Feeding System

one of 3 m length, packed with poropak-N, and the other of 2 m length, packed with molecular sieve. Both columns were arranged in series and maintained at a temperature of 30°C in the chromatograph's oven. An empty column of equal resistance (ie. pressure drop) to the molecular sieve column was also included, in parallel with it. This enabled the carrier gas to be diverted around the molecular sieve column in order to analyse the C_2 hydrocarbons that would be absorbed by this column, if allowed to pass through it. The carrier gas used was a mixture of 8% hydrogen in helium which allowed product gases containing hydrogen to be analysed accurately. Pure helium cannot be used as a carrier gas with samples whose hydrogen content is less than 8% since the thermal conductivity of hydrogen - helium mixtures is nonlinear below this critical concentration. Other gases that could be analysed were oxygen, nitrogen, carbon monoxide, methane, carbon dioxide, ethylene, ethane and acetylene. The outputs from the two detectors were fed to a Linseis two channel chart recorder and the system was calibrated with a calibration mixture of known composition. This mixture consisted of 8·80% H_2, 5·14% O_2, 8·73% CO, 5·6% CH_4, 4·86% CO_2, 2·45% C_2H_4, 2·50% C_2H_6 and 2·60% C_2H_2 with the remainder being N_2. Both the calibration mixture and the carrier gas mixture were obtained from Cryoservices, Leicester.

2.4.2 Sampling System

Samples were aspirated from a 'T' piece fitted in the exhaust pipe leading from the "Swiss-roll" burner. A schematic diagram of the sampling system is shown in figure 18. The samples were sucked with a small 2·5 cc/s pump into a 250 ml pyrex sample tube, having first passed through a water trap and a glass wool filter. To collect a sample both valves of the sample tube were opened and the pump was switched on, pumping at a constant rate in accordance with BS1756, for four minutes in order to obtain an average sample of the product gases during the period. After four minutes, the exit valve from the sample tube was closed,

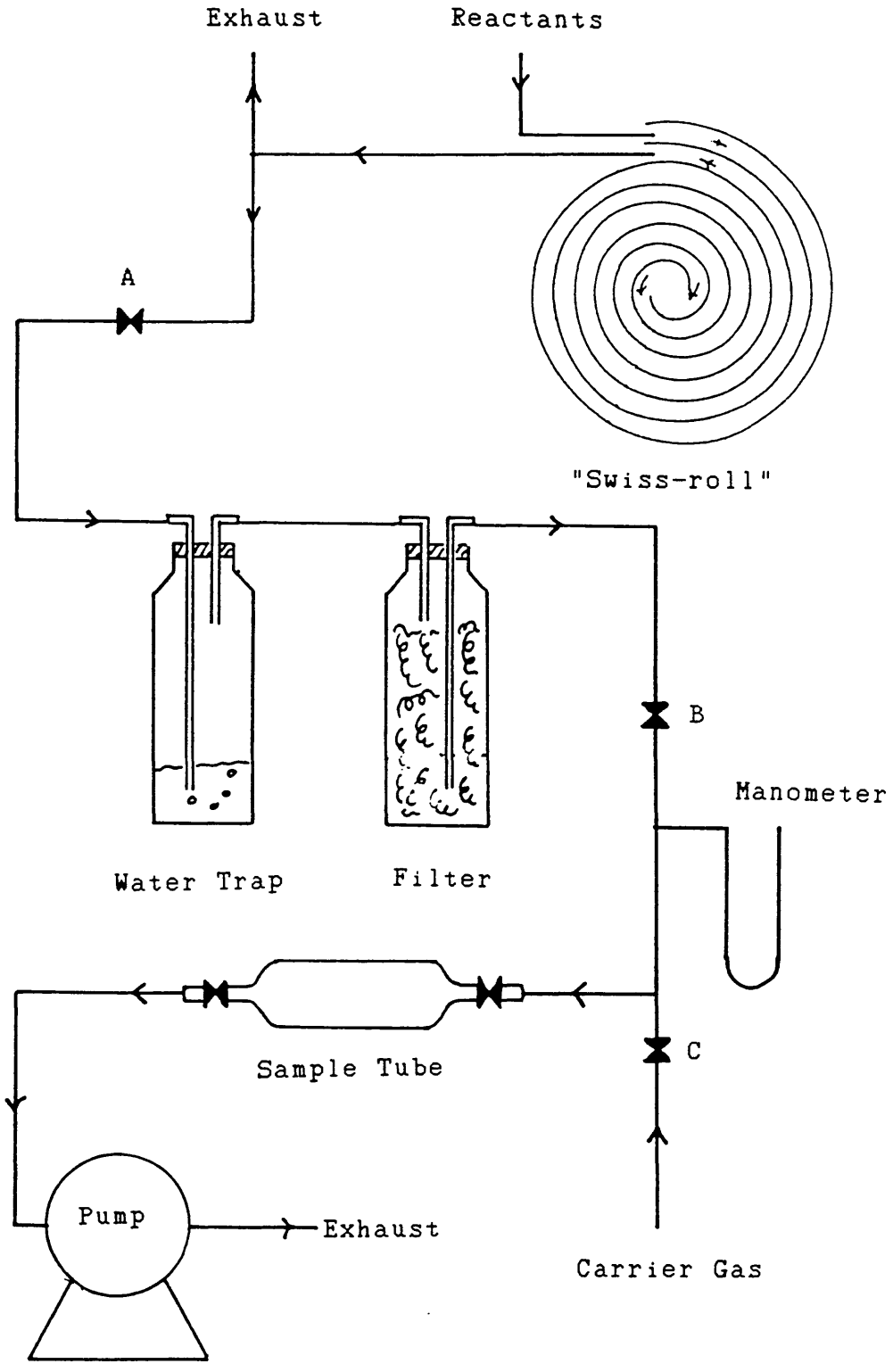

Figure 18 - Gas Sampling System

the sampling system isolated with valves A and B and the sample tube pressurised to 1·5 bar (abs.), with the 8% H_2 in He carrier gas, by opening valve C. The sample tube inlet valve was then also closed and, after removal from the system, the sample could be released under its own pressure through the injection loop of the chromatograph prior to injection.

2.5 Experimental Procedure

2.5.1 Ignition

The burner was initially sandwiched between two thick layers of 'Kaowool' insulation. During ignition, the access port to the combustion chamber was left uncovered and a mixture of 7% methane in air fed to the inlet pipe. A flame could then be stabilised outside the burner on the access port. The total mixture flow rate was then reduced, using the bleed to the excess mixture burner, until the flame flashed back into the combustion chamber. Having waited a minute or so for the flame to establish itself, a square of 'Kaowool' was placed over the access port and the stainless steel lid screwed down from the top of the clamp to seal the combustion chamber - see plate 1 (a). The state of the flame could then be monitored using the *in situ* thermocouple located at the centre of the spiral. As the temperature started to rise the bleed valve to the excess mixture burner was gradually closed and the full flow diverted through to the "Swiss-roll" burner. If the temperature dropped, indicating that the sealing process had extinguished the flame, the whole process had to be repeated.

2.5.2 Operation

Once the "Swiss-roll" burner had been successfully ignited, it took up to 20 minutes for the system to achieve a steady state. This was due to the relatively high heat

capacity of the metal and alumina cement used in the construction of the burner. The predominant mechanism of heat transfer during the warming up period was convection which was consequently limited by the film coefficients of the inconel strips. Conduction played a small part as the walls of the combustion chamber were of negligible thickness compared to their length. This resulted in considerable heat transfer across the walls of the channels but very little along their length. Also, as the burner warmed up, so the gas temperature and viscosity increased, both of which affect the pressure drop across the spiral. Thus steady state was characterised by a relatively constant temperature reading and pressure drop.

With the "Swiss-roll" burner fully warmed up, the methane equivalence ratio and total mixture flow rate could be adjusted to the required settings. On the burner's first run it was operated in the lean mode to check its efficiency against the results of previous workers. If a lean stability limit of 2% methane in air could be achieved the burner was considered satisfactory. Failure of this test indicated that the flow was bypassing some of the channel and that the burner had not been correctly fabricated. In this project, however, the first burner constructed passed this test. All subsequent work was performed with the "Swiss-roll" burner operating in the rich mode. Here the operating temperature was of the order of 1200°C, resulting in the whole burner becoming very hot, see plate 1 (b), and being subjected to high thermal stresses. The effect of this is discussed later.

2.5.3 Shutdown

When operating rich, the procedure for closing down the burner was first to shut off the air supply, extinguishing the flame, and then to reduce the methane flow slowly to zero. In this way stoichiometric mixtures were avoided whilst the burner was hot.

Plate 1 - The "Swiss-roll" Burner

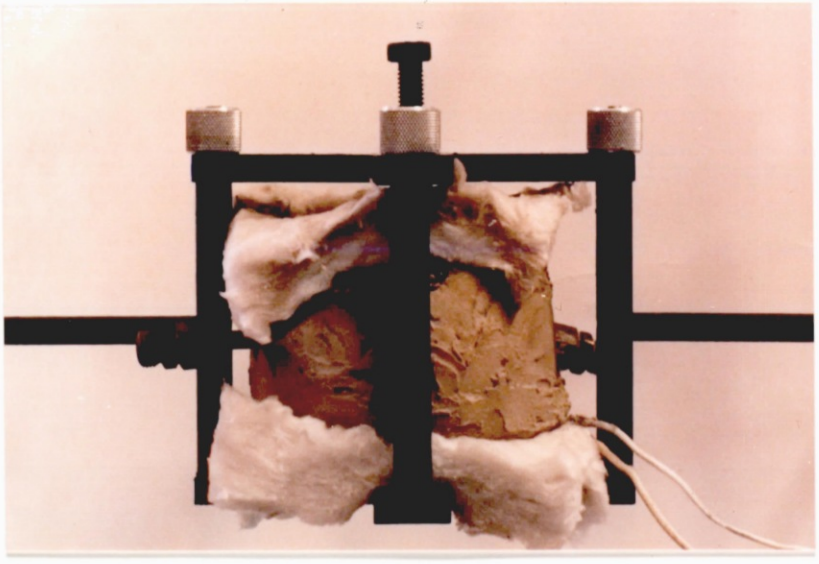

(a) Prior To Ignition

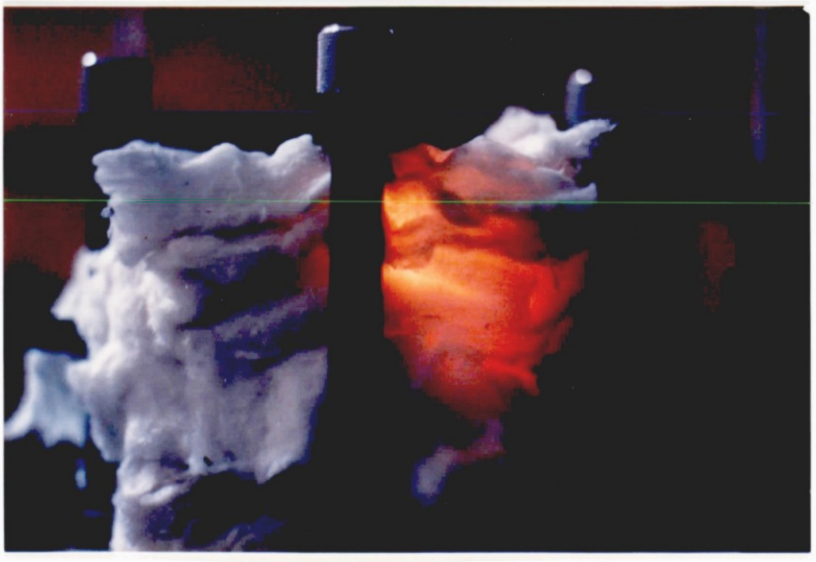

(b) During Operation

2.6 Results

The initial results with the "Swiss-roll" burner appeared to be very promising. With the burner in a horizontal attitude it appeared to be burning mixtures of up to 30% methane in air quite stably. Temperatures recorded by the central thermocouple were in the range of 900 - 950°C and the pressure drop across the burner was approximately 30 cm Hg. To investigate the state of combustion a sample was taken from the exhaust line whilst burning a mixture of 20% methane in air. The results are given below, with the remainder being N_2

Species :	H_2	O_2	CO	CH_4	CO_2	C_2H_4
Vol.% :	1·96	11·00	0·30	16·96	0·46	0·10

A mass balance revealed that the level of methane conversion was only 23%. It was thought that this could be due to the high air flow rate used, 680 cc/s, or to the horizontal attitude of the burner. With the burner in a horizontal position, the flow entered the combustion chamber tangentially at a velocity of 9·44 m/s. This would probably have created a cyclone effect and separated some of the methane and air - air being approximately twice as dense as methane.

The next step was to arrange the "Swiss-roll" burner so that the reactant mixture was injected vertically, rather than horizontally, into the combustion chamber. This was achieved by carefully positioning the "Swiss-roll" burner in the clamp and then rotating it through 90° once it had been ignited and sealed. The air flow rate to the burner was also reduced to 434 cc/s. It was hoped that, with a lower gas velocity and gravitational forces acting to counter the centrifugal forces of the gas circulating in the combustion chamber, the "Swiss-roll" burner would give a higher methane conversion. The results from an analysis of the exhaust gas from 18% methane in air are shown below. The

recorded temperature at the centre of the spiral was 923°C and the preesure drop was 19 cm Hg.

Species :	H_2	O_2	CO	CH_4	CO_2
Vol.% :	1·64	15·83	0·28	15·47	0·10

Again a mass balance revealed that the methane conversion was only 16% and that most of the fuel was still bypassing the flame.

Having operated the "Swiss-roll" burner in both the horizontal and vertical position without achieving complete combustion the next logical progression was to test the effect of packing the combustion chamber. The main design criterion was to find an inert packing material capable of withstanding high temperatures and of a sufficient particle size to minimise the pressure drop. Accordingly the "Swiss-roll" burner was returned to the horizontal position and 75g of coarse alumina particles, of size 1·68-2·00 mm , were poured into the combustion chamber - settling to form a loosely packed bed. The concept was that the packing would eliminate the cyclone effect and prevent the methane from bypassing the flame.

The "Swiss-roll" burner was now much more difficult to light with the flow rate having to be greatly reduced before the flame would flash back into the packing. Also, because of the extra thermal capacity of the packing, the spiral took much longer to warm up and reach a steady state - up to 40 minutes. The air feed to the burner was further reduced to 255 cc/s giving a pressure drop of 10 cm Hg and a temperature of 1151°C with a 25% methane mixture. An analysis of the products from this is shown below.

Species:	H_2	O_2	CO	CH_4	CO_2	C_2H_4	C_2H_6	C_2H_2
Vol % :	5·66	1·01	9·42	11·55	4·45	0·45	0·12	0·41

A mass balance showed that the methane conversion had now

increased to 59%. This was a great improvement on the previous performances, but still far from ideal.

A final attempt to improve the methane conversion was made by introducing catalytically active material into the "Swiss-roll" burner. The combustion chamber was repacked with a mixture of 30g of tin / antimony oxide, in pellets of diameter 3 mm and length 5 mm, and 45g of the coarse alumina as before. The burner was fed with a 21% methane in 340 cc/s air mixture, resulting in a temperature of 1250°C and a pressure drop of 12 cm Hg. An analysis of the exhaust gas so produced is shown below.

Species:	H_2	O_2	CO	CH_4	CO_2	C_2H_4	C_2H_6	C_2H_2
Vol % :	4·25	2·64	6·58	11·20	4·37	0·32	0·12	0·26

This produced a methane conversion of 53%.

2.7 Discussion

Despite having a methane conversion of only 59% the packed "Swiss-roll" burner did manage to produce moderate amounts of synthesis gas. Also there was no evidence of soot formation, even whilst burning mixtures of up to 25% methane in air. On examining the burner after combustion neither the white alumina particles used for packing nor the surfaces of the inconel spiral were discoloured by any carbonaceous residues. This demonstrates that a stationary heat exchanger, keeping both process and utility streams separate, can be used effectively as a combustor for ultra rich mixtures of methane in air. The main reason for the low methane conversion was that the flame did not fill the combustion zone. This is common with flames deficient in the component of higher diffusion coefficient which tend to burn in a filamentary way. Lean hydrogen flames exhibit this behaviour, burning as small filaments separated by a

large quantity of holes. Equally, rich hydrocarbon flames tend to be cellular although this is not normally associated with methane, however methane flames this rich have not been studied before.

Due to the high temperatures involved and the different relative coefficients of expansion of the construction materials, the burner was subjected to very high thermal stresses, especially during the warming up and cooling down periods. As a direct consequence of this the "Swiss-roll" burner developed many cracks in its cement casing during each operation. These cracks could be patched with more cement as a temporary measure but after four or five runs of up to an hour each the burner was rendered unserviceable and a new one had to be built. Photographs (a) and (b) in plate 2 show the extent of the damage to one particular "Swiss-roll" after such problems. In these photographs the top of the burner has been cut off to show the damage to the combustion chamber. Thus the laboratory scale "Swiss-roll" burner described here is not a practical combustion device, as each one built has a maximum operating life of about five hours. Having discovered this, any further work would have to be carried out with the "Swiss-roll" completely redesigned in such a way that it could withstand the high thermal stresses. This would probably involve a total ceramic construction, perhaps with two ceramic spirals attached to separate lids which would then slot together.

Plate 2 - Damage To The "Swiss-roll" Burner

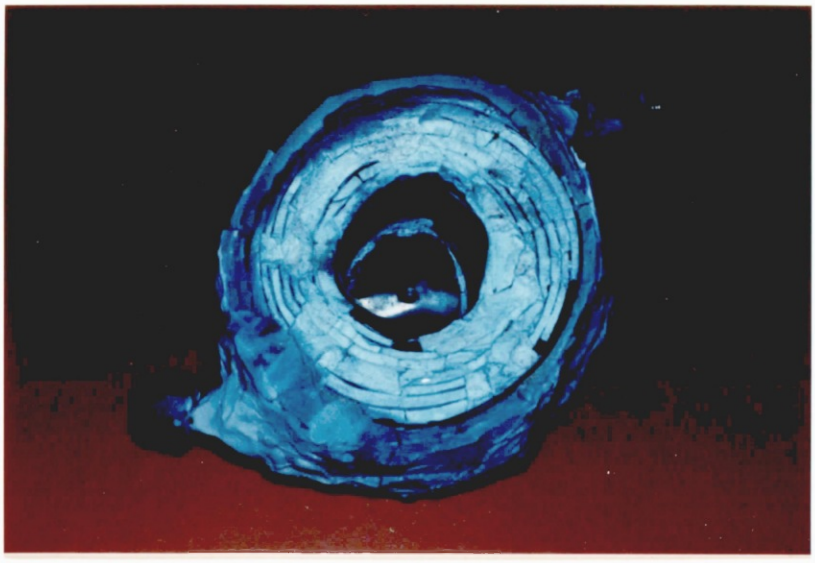

(a) General View

(b) Combustion Chamber

CHAPTER 3

THE ELECTRICALLY HEATED BURNER

3.1 Aims

Because of the complex geometry of the spiral burner and the high thermal stresses involved it suffered from many constructional and operational problems. From this view point, a much simpler heat recirculating burner would be more desirable. However a simpler burner would recirculate less heat and thus have a smaller degree of preheat. A simpler burner would not, therefore, be able to burn such rich mixtures as the "Swiss-roll" burner. Consequently more information was required with regard to the effect of preheat on the richest burnable mixtures and hence the yields of synthesis gases and higher hydrocarbons. Also, a knowledge of the unique relationships between composition, flow and temperature in heat recirculating burners generally would be of considerable value for design purposes. Accordingly an electrically heated burner was designed and commissioned to determine the effect of flow velocity and preheat temperature independently.

Additionally, other ancillary topics could be investigated. Various metals, such as the inconel used for the "Swiss-roll" construction for example, could be lowered into the flame of the electrically heated burner to test for any potential catalytic effect. Also an investigation of the variation of flame temperature at the rich stability limit could be carried out. However, the main aim of the work described in this chapter was to simulate, and so test, heat recirculating burners with varying degrees of preheat.

3.2 Construction Of The Electrically Heated Burner

A schematic diagram of the burner is shown in figure 19. It was constructed from a length of 41·5 mm OD, 2 mm wall thickness, quartz tube. This was drawn into a cone at one end, of internal angle 30°, and fitted with a 3 mm diameter inlet nozzle at the apex. The vessel was loosely packed with coarse alumina particles, of size 1·68–2·00 mm, to a depth of 35 cm. This served to distribute the flow and give a uniform temperature profile across the vessel. Also an R-type thermocouple (0·125 mm diameter) was set in the centre of the vessel, just below the surface of the packing to register the preheat temperature.

The external heating was provided by means of an electrical heating element wound around the first 30 cm of the cylindrical part of the burner tube. This was achieved by first winding quartz tape around the heating section, then 5 m of 8 Ω/m nichrome wire at a pitch of 1 turn/cm and finally another layer of quartz tape for electrical insulation. The two ends of the heating element were held in place by twisting 40 cm lengths of thick nickel wire around the burner tube at each end of the heating section. The loose ends of these were twisted together into two single strands, inserted into ceramic beads for electrical insulation, and then used for connection to the power supply. The heating section was finally enveloped in a 4 cm thick blanket of 'Kaowool' for thermal insulation. The power to the heater was supplied from an 8A variac. With the total resistance of the element being 40 Ω, this gave a maximum power input of 1·44 kW. However the variac was never set above 200 V (1 kW) as a precaution against burning out the element.

Figure 19 - The Electrically Heated Burner

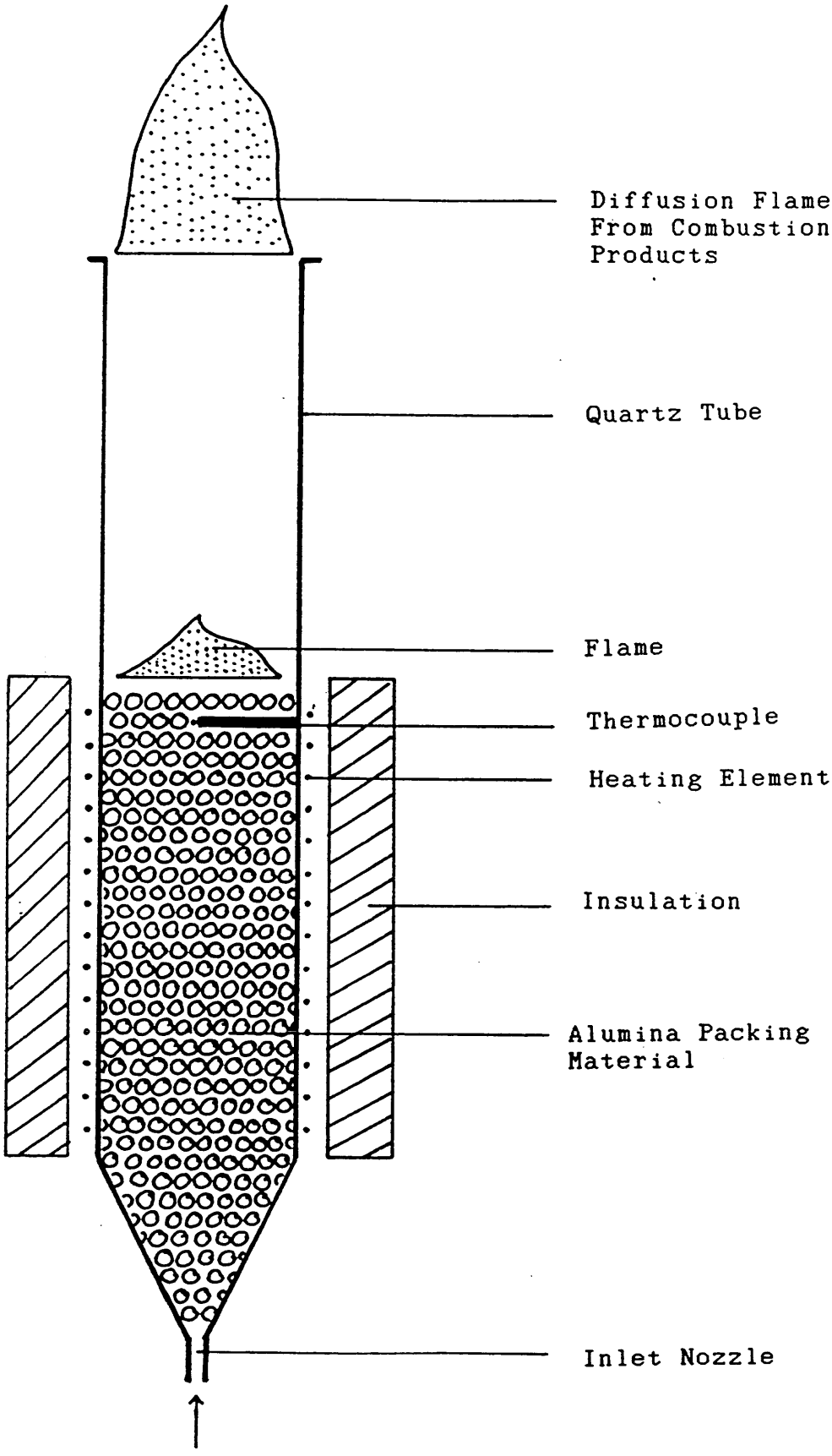

3.3 Gas Feeding System

The equipment supplying gaseous fuel (methane) and air was identical to that used for the "Swiss-roll" burner and is shown in figure 17. It simply consisted of a number of rotameters and mercury manometers measuring a supply of methane and air, at 2 bar (abs.) pressure, to the inlet of the electrically heated burner.

3.4 Analytical System

3.4.1 Analytical Equipment

All the products from the electrically heated burner were gaseous and so a gas chromatograph was used for their analysis. The instrument used has already been described in the "Swiss-roll" chapter (2) and will not, therefore, be discussed again here.

3.4.2 Sampling System

Samples of the combustion products were taken using a quartz sampling probe. The average composition of the total flue gas mixture was obtained by maintaining a constant rate of flow during the sampling period, in accordance with BS1756 : Part 1 : 1971. The probe consisted of a 3 mm OD quartz tube bent into an 'L' shape. It was held in an adjustable clamp so that it could be located accurately in different positions above the flame in the burner vessel. Experiments showed that the composition profile across the burner tube was relatively uniform. Accordingly the probe position was fixed centrally about 5 cm below the burner outlet and samples from this location were accepted as being representative. For additional security, two samples of each mixture were taken and always analysed within 24 hours of collection.

3.5 Experimental Procedure

3.5.1 Ignition

A mixture of 7% methane in air was initially ignited at the top of the burner with the electrical preheat set to zero. The mixture strength was then increased to approximately 14% methane, quite close to the normal rich limit. After this the required power input to the heating element was set using the variac and the system was left to reach a steady state preheat temperature. In this way preheat was only applied to very rich mixtures, for safety reasons, to avoid preheating explosive mixtures. A pilot light was also left burning near the exit from the burner to ignite any flammable combustion products.

3.5.2 Operation

The electrical heater did not have a temperature controller and so particular temperatures had to be set by trial and error, waiting for thermal equilibrium between each adjustment. This process was slow but could be accelerated by calibrating the system at various air flow rates. With a power input of 1 kW and an airflow of 400 cc/s a maximum preheat temperature of 1000°C could be achieved. This was considered sufficient, as higher temperatures would probably lead to early pyrolysis of the reaction mixture as well as the burn out of the heating element. Heating mixtures of up to 25% methane in air to temperatures as high as 1000°C yielded no evidence of premature pyrolysis. This was determined by examining the packed bed region of the burner after operation and discovering the alumina particles to be still white with no deposits of tar, soot or any other pyrolysis products.

3.5.3 Shutdown

When burning rich, the first shutdown operation was to isolate the power supply from the electrical heater. Having done this, the air supply was slowly decreased and finally shut off - thus extinguishing the flame. The methane flow could then also be reduced to zero. In this way introducing stoichiometric methane-air mixtures was avoided whilst the burner was hot.

3.6 The Effect Of Preheat On Rich Combustion

The electrically heated burner was used to determine the richest burnable mixtures and the corresponding product compositions for methane combustion at two different air flow rates with varying degrees of preheat.

3.6.1 Experimental Procedure

The operations, described below, were first carried out using an air flow rate of 285 cc/s and then repeated with 410 cc/s air. The rich limit was defined as the condition where the flame lifted from the bed surface and did not return. Each limit point was repeated three times to guard against error.

Having ignited the burner with a 7% methane in air mixture and zero preheat, the methane flow was gradually increased to first find the rich limit without preheat. After each small increase in methane feedrate the system was left for several minutes for the flame to stabilise before continuing. In this way it was hoped to avoid an artificially high rich limit. Once the limit had been determined, the mixture strength was slightly reduced to allow stable combustion and two samples were taken for product analysis. Each sample was aspirated for four minutes into a 250 ml sample tube, thus obtaining a representative average sample. The temperature registered by the thermocouple was also recorded.

With the first point completed, the power to the

heating element was switched on and the variac set to 40 V. The system was then left for about an hour for the preheat temperature to stabilise. This temperature was recorded and the methane feedrate increased to determine the new rich stability limit, as before. Similarly, once the limit had been found, the mixture strength was slightly reduced and two samples were taken for analysis. This procedure was repeated another eight times, increasing the voltage, and thus the power, to the system by 20 V each time up to a maximum of 200 V or 1000 W. The samples, so taken, were analysed whilst waiting for the system to reach thermal equilibrium, after the preheat had been increased.

3.6.2 Results And Discussion

With 285 cc/s air flow the highest preheat temperature obtained was 836°C at which the richest burnable mixture had a methane equivalence ratio of 2·53. With 410 cc/s air the corresponding values were 921°C and an equivalence ratio of 2·61. The complete loci of rich limit points for both air flow rates are shown in figure 20. It is interesting to note that the points for both 285 cc/s air and 410 cc/s air lie on the same curve. Thus the rich stability limit is strongly dependent upon temperature but not upon flow rate. Although the points lie on a curve, a straightline can be fitted to them; see figure 21. This gives an approximate empirical correlation between preheat temperature and the richest burnable mixture.

$$\phi = 1{\cdot}2.10^{-3}.(T) + 1.3835$$

where : ϕ = methane equivalence ratio
T = preheat temperature, °C

When extrapolated to room temperature, 25°C, this suggests a rich stability limit of $\phi = 1{\cdot}414$ as compared with the normal rich limit of flammability for methane of $\phi = 1.578$. The lean stability limit has been shown to behave in a similar manner to the lean flammability limit when the

GRAPH OF THE RICHEST BURNABLE MIXTURE VS PREHEAT TEMPERATURE FOR MIXTURES OF METHANE AND THE FLOWRATES OF AIR SHOWN.

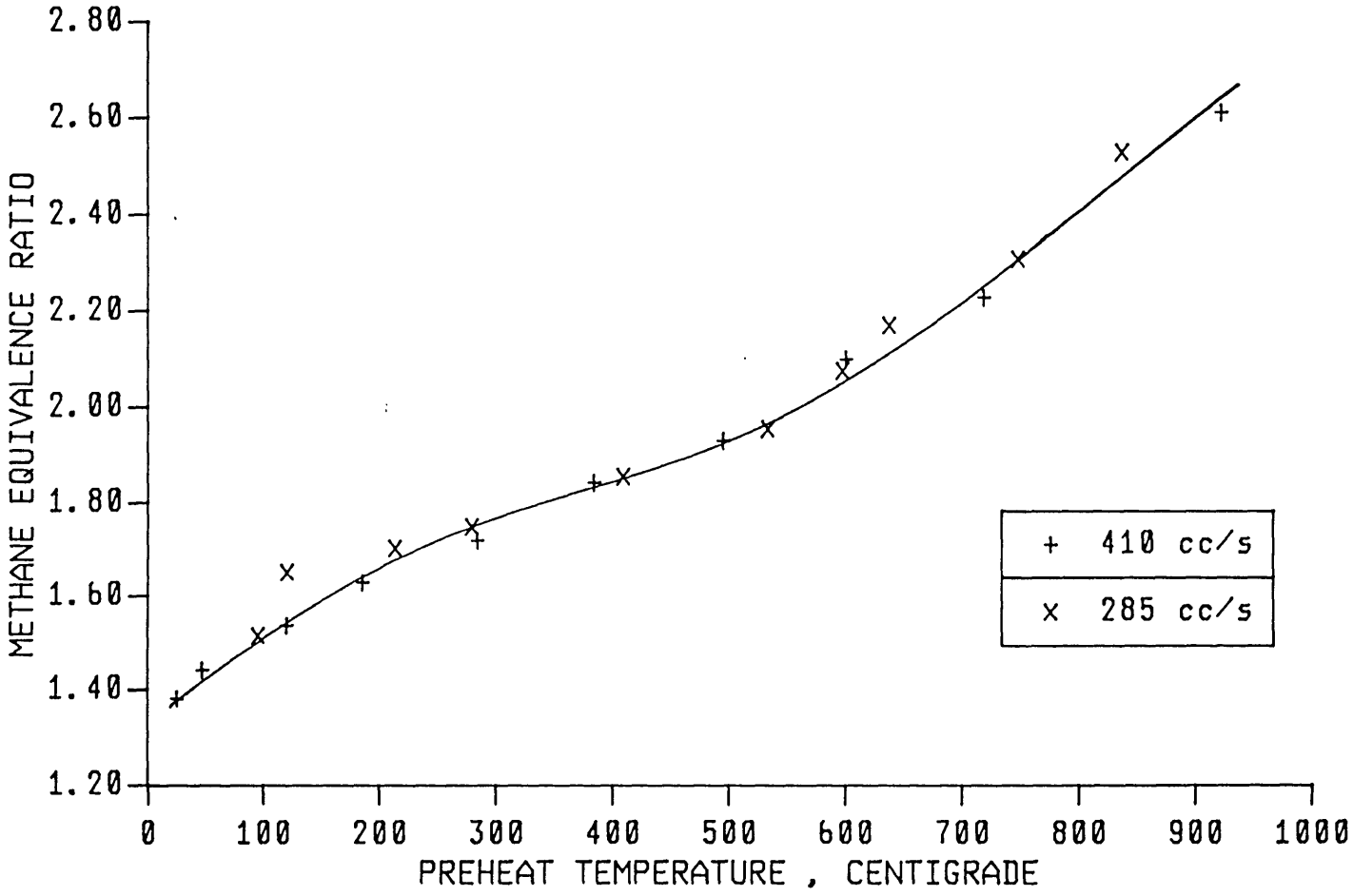

Figure 20

GRAPH OF THE RICHEST BURNABLE MIXTURE VS PREHEAT TEMPERATURE FOR MIXTURES OF METHANE AND THE FLOWRATES OF AIR SHOWN.

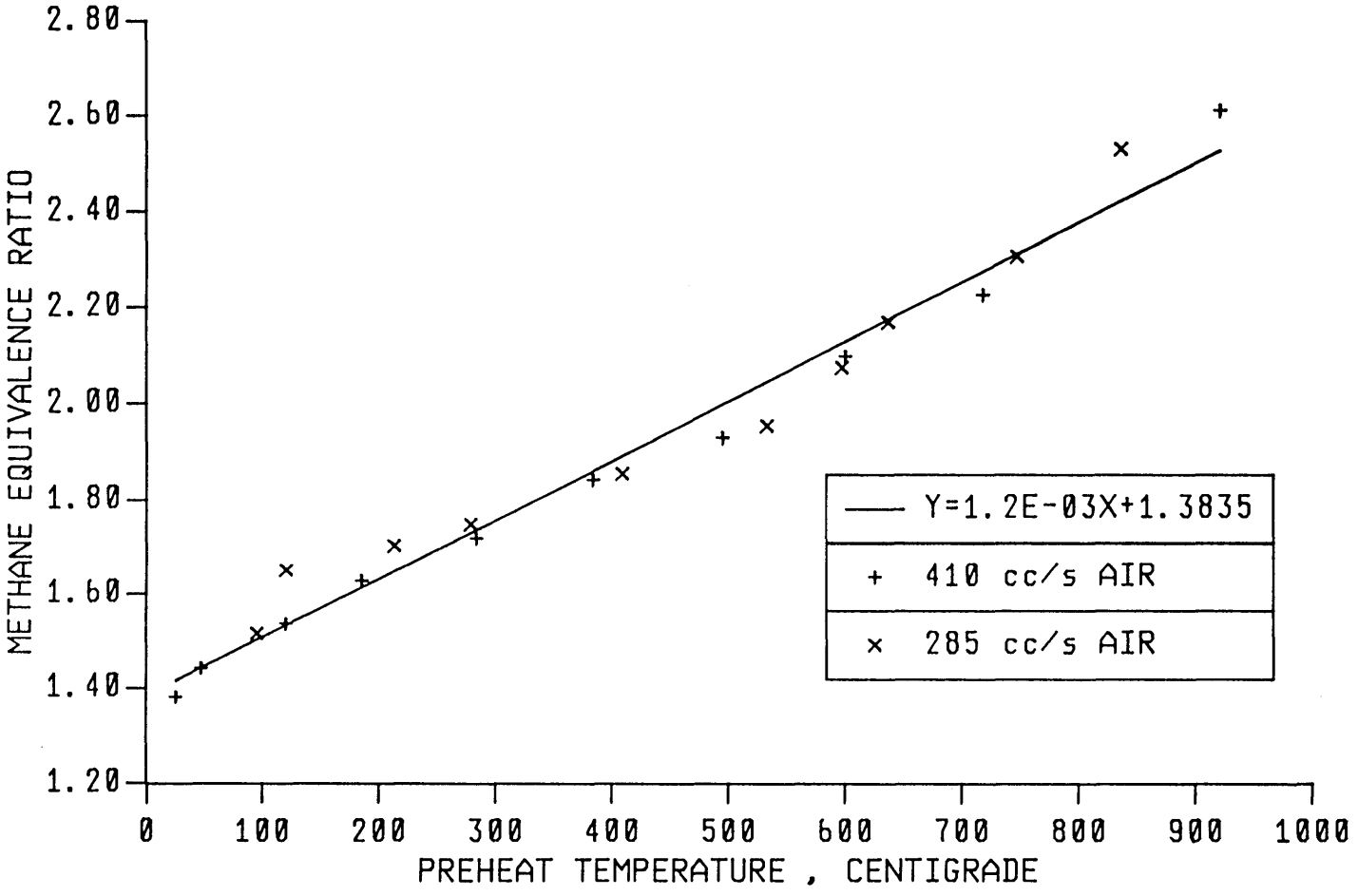

Figure 21

reactant gases are preheated, (Lloyd and Weinberg 1974, 1975). Furthermore, it has been known for a long time that the lean limit of flammability is a linear function of the preheat temperature, for example Smith (1955) confirmed this for mixtures of methane in air. This suggests that the mechanisms of flame stabilisation at the lean and rich limits may be similar and that the flow in this burner is laminar and slow enough for a stability limit to behave as a flammability limit in a stationary gas.

The analyses of the samples taken at the two air flow rates are shown in figures 22 and 23. Both graphs show maxima in CO and H_2 production. These occur at equivalence ratios of 2·0 with 285 cc/s air and 2·1 with 410 cc/s air. At lower equivalence ratios CO production exceeds that of H_2 but at an equivalence ratio of about 1·95, for both flows, they cross over and H_2 yields become higher than those of CO. With 285 cc/s air the maximum yields of CO and H_2 are approximately 13·0% and 13·5% respectively and with 410 cc/s air the corresponding yields are 13·5% and 15·0%. In both cases, although more dramatically with 410 cc/s air, as the mixture becomes richer so the methane conversion drops. This is accompanied by an increase in the yield of acetylene, which approximately mirrors the yield of methane up to an equivalence ratio of 2·2. After this the acetylene yield levels out at about 3% in both cases. As would be expected from a mixture becoming steadily richer, CO_2 production decreases with increasing equivalence ratio. Trace yields of ethylene are also shown which slightly increase with increasing mixture strength.

Clearly the previous assumption that the richest mixtures gave the highest synthesis gas yields was incorrect. This was based upon a calculation from the overall stoichiometric equation for the case where all the available oxygen is converted to carbon monoxide. This suggested that the optimum mixture strength for producing synthesis gas was 29·6% methane in air, ie.:

$$CH_4 + 2{\cdot}38\ [0{\cdot}21\ O_2 + 0{\cdot}79\ N_2] \longrightarrow CO + 2\ H_2 + 1{\cdot}88\ N_2$$

Figure 22

GRAPH OF EXHAUST GAS COMPOSITION VS EQUIVALENCE RATIO
FOR THE ELECTRICALLY HEATED BURNER WITH 285 cc/s AIR.

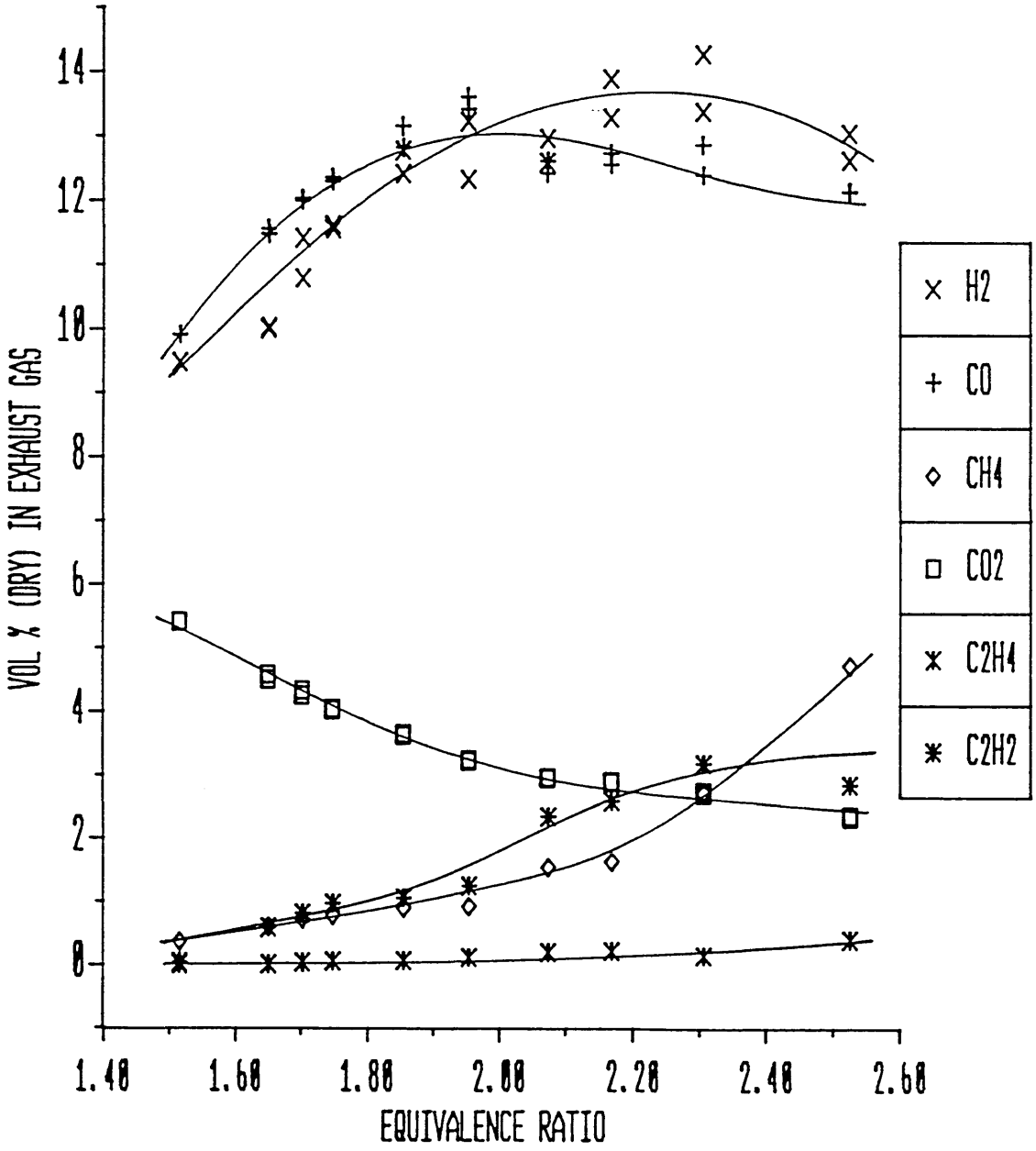

Figure 23

GRAPH OF EXHAUST GAS COMPOSITION VS EQUIVALENCE RATIO
FOR THE ELECTRICALLY HEATED BURNER WITH 410 cc/s AIR.

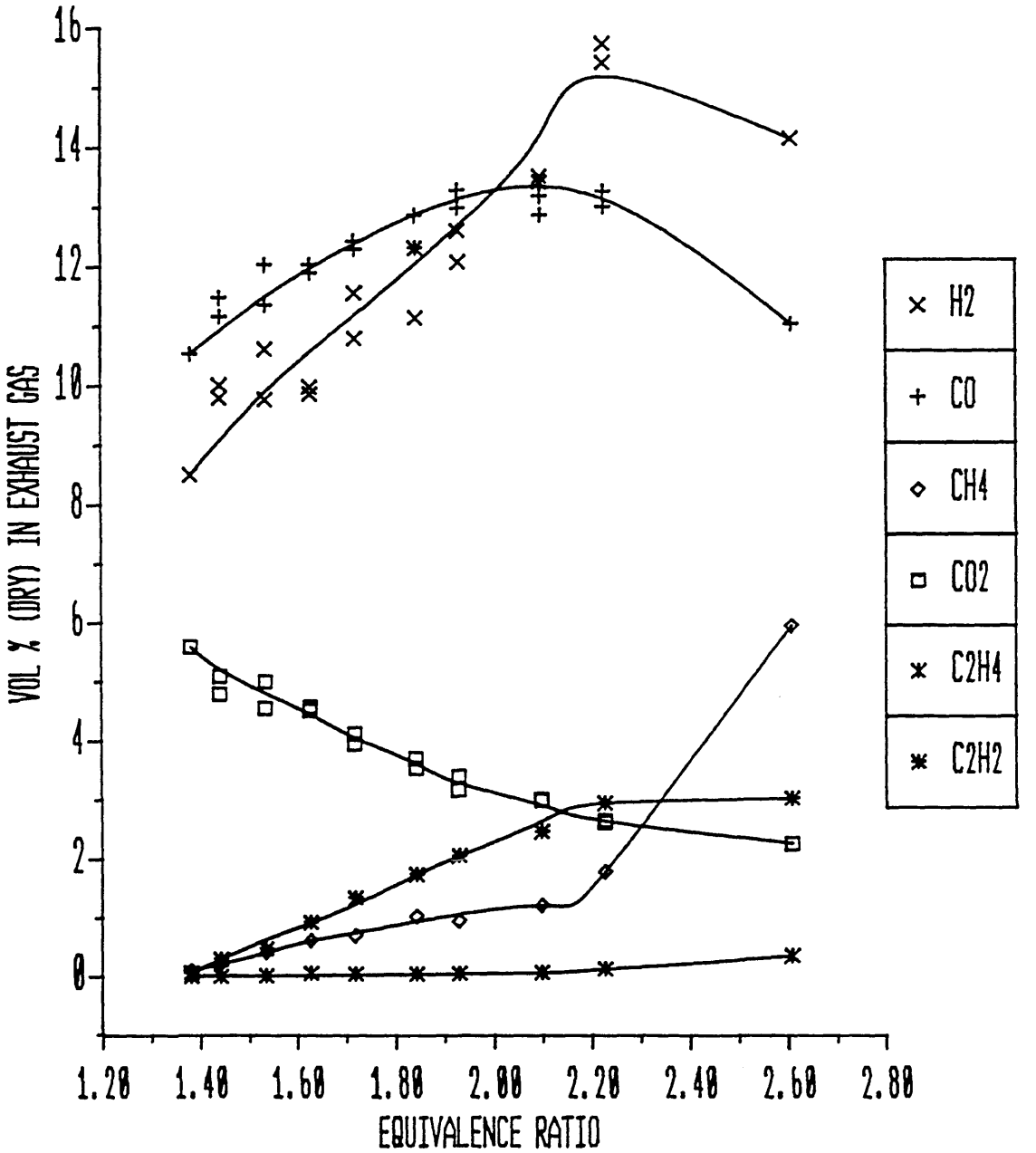

Consequently a burner, such as the "Swiss-roll", achieving very high levels of preheat and enabling very rich mixtures to be burned is not necessary for maximum synthesis gas production. A much simpler heat recirculating burner, perhaps based upon a simple annular heat exchanger, could work very well as a synthesis gas producer.

3.7 Calculation Of The Final Flame Temperature

Having measured the preheat temperatures and determined the product gas analyses corresponding to the various equivalence ratios in the electrically heated burner it was relatively straight forward to calculate the respective flame temperatures. This is an interesting parameter and the aim was to investigate its variation with preheat at the rich limit.

3.7.1 Method Of Calculation

The flame temperature was calculated from a heat balance across the flame zone.

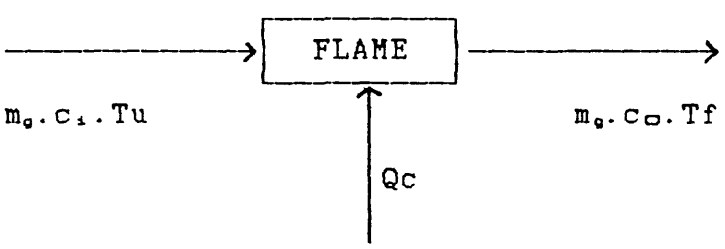

ie. – $m_g.c_i.Tu + Qc = m_g.c_o.Tf$

as, $Qc = q_c.m_g X_{CH4}.\rho_{CH4}/\rho_{mix}$

so, $Tf = Tu.c_i/c_o + q_c.X_{CH4}.\rho_{CH4}/(c_o.\rho_{mix})$

where : Tf = flame temperature, K
Tu = preheat temperature, K
m_g = gas mass flow rate, kg/s
$c_{i/o}$ = specific heat capacity in/out, J/kg/K
q_c = specific heat of combustion for methane, J/kg
Qc = total heat of combustion for methane, W
x_{CH_4} = methane mole fraction
ρ = density, kg/m^3

For each rich limit point experimentally determined in the electrically heated burner the preheat temperature, Tu, was known. However the mean heat capacities of the reactants/products and the heat of combustion had to be calculated from the product gas analyses. Using the gas chromatograph results, a mass balance was performed for each point and the corresponding overall reaction equation determined. From this the heat of combustion was calculated by subtracting the heats of formation of the reactants from those of the products. For each point, the mean specific heat capacity of the reactants was calculated at 298 K using the mole fractions of the respective reactant species. In order to calculate the same parameter for the products, it was first assumed that they were at a temperature of 1600 K. Then, using component heat capacities at 1600 K, the overall heat capacity was again calculated using the mole fractions of the respective product species. All data was taken from the JANAF tables (1971). A temperature of 1600 K was chosen as a first estimate of the flame temperature and would have been revised if necessary - although 1600 K proved to be a satisfactory approximation. Mean molecular masses for the products and reactants were also calculated to convert the heat capacities from a molar to a mass basis. As there were 20 such calculations to perform, ten for each air flow rate, the calculation procedure was coded into a spreadsheet and carried out with the aid of an IBM type personal computer. An example of the output, giving calculation details is shown in table 1.

Air cc/s	CH4 Mol F	TU , K
285	0.206	910

$$CH4 + aO2 + bN2 = cH2 + dO2 + eN2 + fCO + gCH4 + hCO2 + iC2H4 + jC2H2 + kH2O$$

Species	GC Vol%	mols i/o	Mol Frac	Rho Kg/m3	Rho Mix	RMM Kg	RMM Mix	HF J/mol	(+/-) nHF	Cp 298K J/mol/K	Cp 298K xi.Cpi	Cp 1600K J/mol/K	Cp 1600K xi.Cpi
CH4		1	0.206	0.679	} (298 K)	0.016		-74800	74800	35.605	7.33463		
O2		0.8094175	0.16674	1.353	1.1087763	0.032	0.026195	0	0	36.784	6.1333642		
N2		3.0449515	0.62726	1.185	}	0.028		0	0	29.097	18.251384		
	TOT MOL =	4.8543689											
H2	13.6	0.6301178	0.1183435			2E-3		0	0			32.7	3.869831
O2	0.8	0.0370658	6.9614E-3			0.032		0	0			29.344	0.2042747
N2	65.72	3.0449515	0.5718773			0.028		0	0			35.104	20.075182
CO	12.64	0.5856389	0.1099898			0.028		-110420	-64666.24			35.446	3.8986985
CH4	1.57	0.0727415	0.0136617			0.016	0.0238462	-74800	-5441.067			88.453	1.208419
CO2	2.89	0.1339	0.025148			0.044		-393146	-52642.26			58.829	1.4794308
C2H4	0.2	0.0092664	1.7403E-3			0.028		52208	483.78218			111.999	0.1949169
C2H2	2.58	0.119537	0.0224504			0.026		226531	27078.847			77.673	1.7437938
H2O		0.6912645	0.1298275			0.018		-241590	-167002.6			47.911	6.2201668
	TOT MOL =	5.3244834											
								HC J/mol=	-187389.5	Cpi J/mol =	31.719378	Cpo J/mol =	38.894714
								HC J/Kg =	1.17118E7	Cpi J/Kg =	1210.8962	Cpo J/Kg =	1631.0678

$$Tf = (Cpi/Cpo).Tu + HC.XCH4.RhoCH4/(Cpo.RhoMixin) = 1581.4087\ K$$

Table 1 - Example Flame Temperature Calculation

3.7.2 Results And Discussion

For each methane equivalence ratio found to be a rich limit in the electrically heated burner both the preheat temperature and the calculated flame temperature are plotted in figure 24. As can be seen, for both 285 cc/s and 410 cc/s air, the flame temperature remains approximately constant at a value of 1600 K with a maximum variation of ±50 K. This is quite an interesting result as the same phenomenon was found at the lean limit by Lloyd and Weinberg (1975), except that the constant flame temperature there was 1400 K. To explain this finding at the lean limit Jones *et al.* (1978) put forward the hypothesis that the limiting reaction rate was constant and due to its high activation energy (268 kJ/mol. for methane - Burgoyne and Hirsh, 1954) far more dependent on temperature than concentration. Accordingly, as the fuel concentration decreases with the lean limit, the corresponding reduction in the heat of combustion is exactly balanced by the increase in the thermal enthalpy due to preheat (Weinberg, 1986). As the calculations showed, the heat of combustion at the rich limit falls quite dramatically with increasing methane equivalence ratio. A graph of this is shown in figure 25. This is primarily due to the increasing quantities of C_2H_4 and C_2H_2 formed in progressively richer mixtures as well as the diminishing amounts of CO_2. CO_2 has a high negative heat of formation (-393 kJ/mol. at 298 K) and thus the higher the CO_2 level the higher the heat of combustion. Both C_2H_4 and C_2H_2 have positive heats of formation (52 kJ/mol. and 226 kJ/mol. at 298 K respectively) and so increases in the levels of these, particularly C_2H_2, will substantially decrease the heat of combustion. From figure 24 it is clear that as the mixture becomes richer the decrease in enthalpy due to the drop in the heat of combustion is balanced by the rise in enthalpy due to preheat. Thus, here again, the rich limit is shown to behave in a similar manner to the lean limit.

GAS TEMPERATURES VS EQUIVALENCE RATIOS FOR METHANE COMBUSTION IN THE ELECTRICALLY HEATED BURNER. TU = MEASURED , TF = CALCULATED.

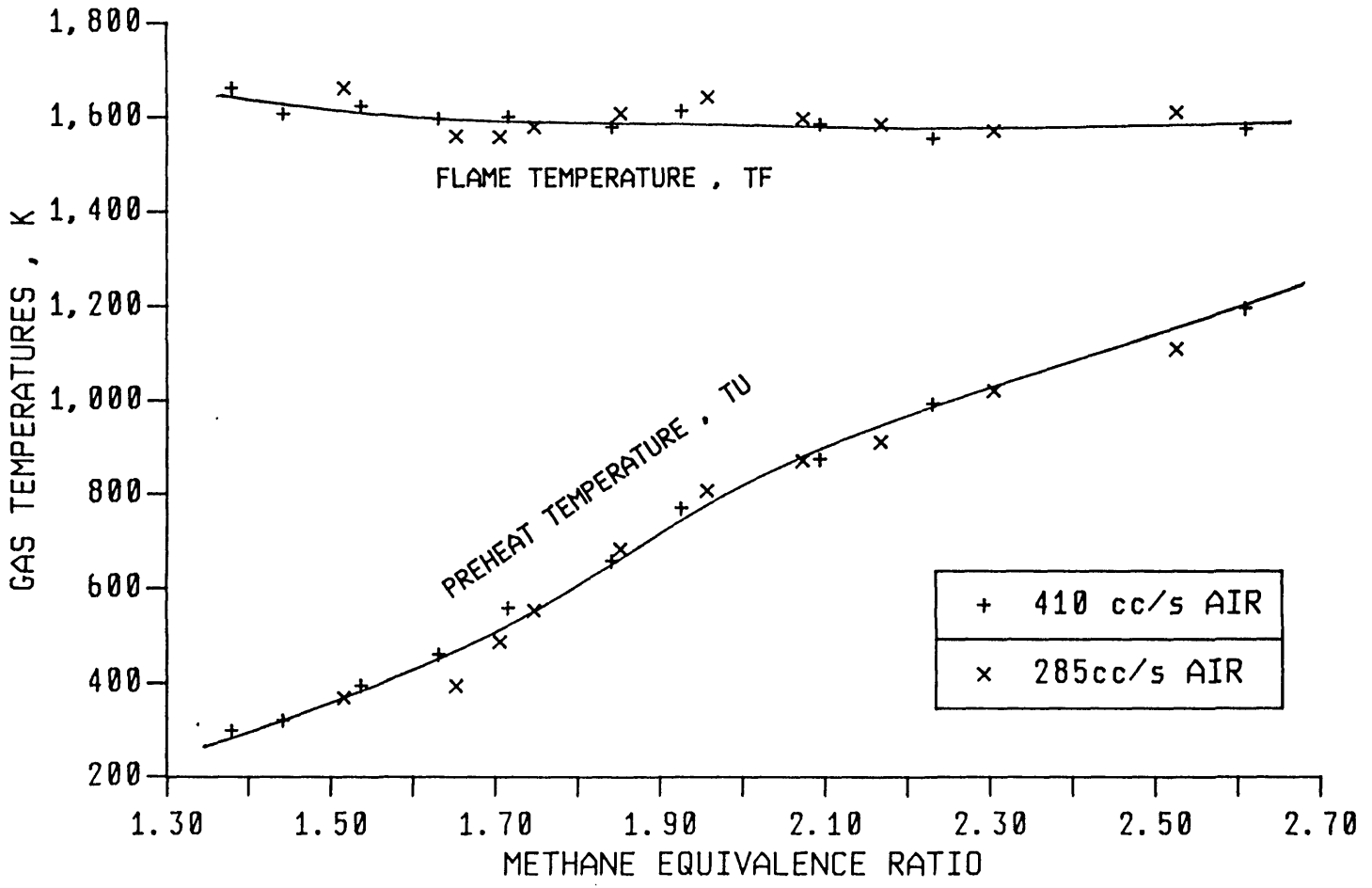

Figure 24

CALCULATED HEAT OF COMBUSTION VS METHANE MOLE FRACTION AS CALCULATED FROM THE ELECTRICALLY HEATED BURNER.

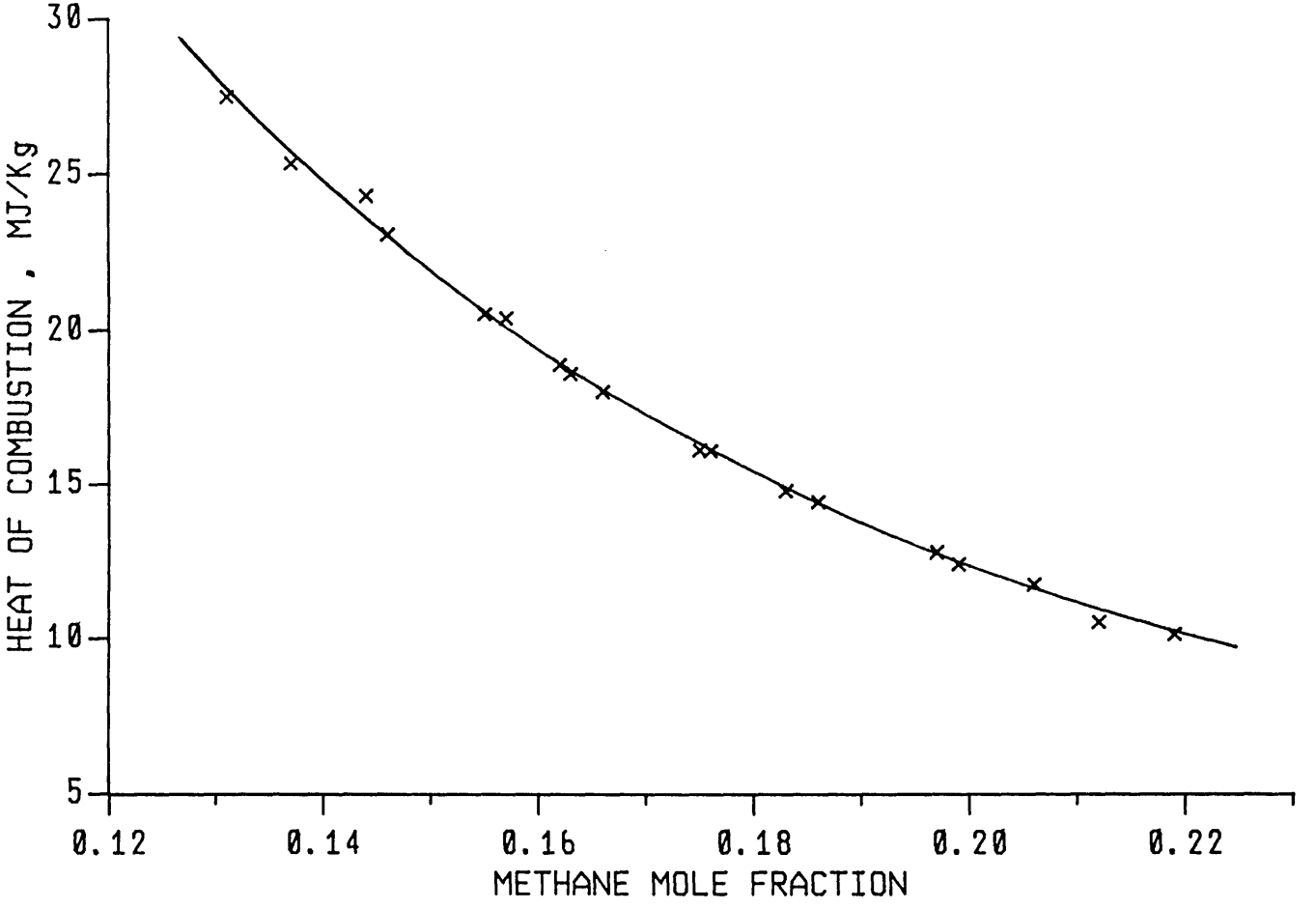

Figure 25

3.8 Catalysts In The Electrically Heated Burner

Another use of the electrically heated burner was for the testing of various metals for catalytic effects. This could easily be achieved by lowering samples of the metal into the combustion products above the bed surface.

3.8.1 Experimental Procedure

Four different metals were tested for catalytic effects in rich methane flames. These are shown in plate 3 and were (a) 0·9g of coiled platinum wire, (b) 2g of bunched nichrome wire (80% Ni, 20% Cr), (c) a 2x10 cm piece of inconel strip wound into a spiral weighing 5·2g and (d) a 2x10 cm piece of 8 mesh steel gauze wound into a coil weighing 4·5g. The burner was ignited as usual with a 7% methane in air mixture - the air flow rate being 295 cc/s. The methane flow was then increased to give a 14% mixture and the variac set to 128 V, giving a power input of 410 W. As the burner warmed up, so the methane equivalence ratio was gradually increased to 2·0. Two samples were then taken for analysis and the preheat temperature recorded. After this the platinum wire was lowered from the burner outlet down onto the bed surface so that it was in the flame. It was left there for ten minutes to achieve thermal and chemical equilibrium before two samples were taken for analysis. This procedure was then repeated with the nichrome wire. When this was tried with the inconel strip and steel gauze, the flame became unstable and was eventually extinguished. To overcome this the methane equivalence ratio was reduced to 1·9. At this mixture strength the flame remained stable with the coils resting on the bed surface. As before, duplicate samples were taken for product gas analysis before and after introducing the metals. In all cases samples were taken with the sampling probe located immediately above the metal being tested in the burner. This was an attempt to monitor any changes caused by the metals in the knowledge that the available surface areas of potential catalysts were very small.

Plate 3 - Metals Tested In The Electrically Heated Burner

(a) Platinum Wire

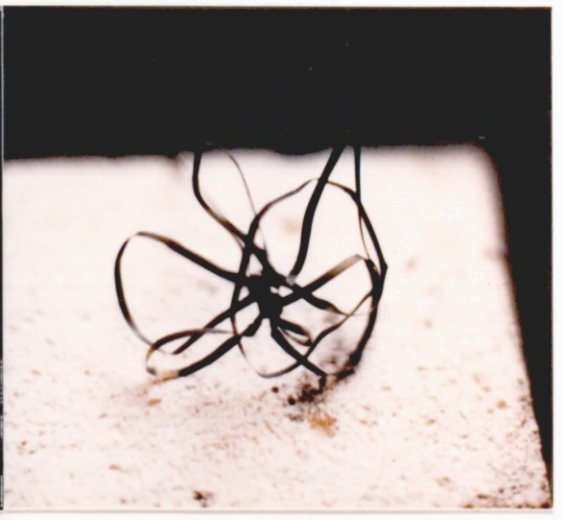

(b) Nichrome Wire

(c) Inconel Strip

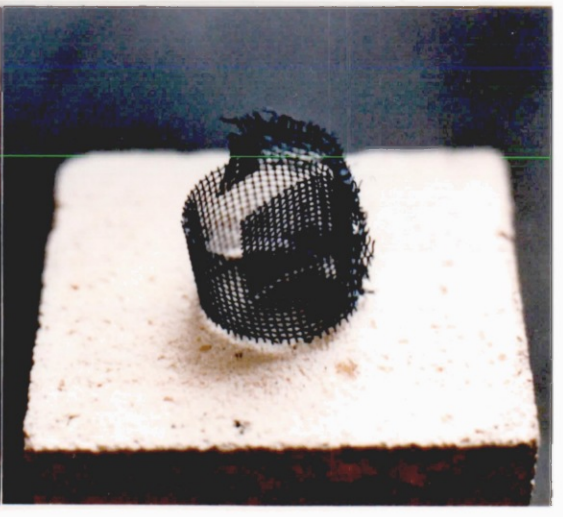

(d) Steel Gauze

3.8.2 Results And Discussion

The results from these tests are shown in figure 26. With a methane equivalence ratio of 2·0 and 295 cc/s air the preheat temperature was 569°C, with an equivalence ratio of 1·9 it was 572°C. As can be seen from the graph, the platinum wire had a small effect, increasing H_2 and CO yields by about 0·75%, whilst simultaneously reducing CO_2, C_2H_2 and CH_4 levels in the product stream. The inference from this is that the platinum wire has increased the CH_4 conversion and also converted some CO_2 and C_2H_2 to CO and H_2. Plate 4(a) shows a photograph of the platinum wire in the burner, resting on the bed surface. The platinum wire is glowing almost white hot which suggests that some catalytic effect is taking place. This effect would probably have been more pronounced if the available surface area of catalyst had been higher. The nichrome wire also has a small effect with CO increasing by about 0·75% and H_2 decreasing by less than 0·5%. There was a corresponding reduction in the C_2H_2 level with tiny increases in CO_2 and C_2H_4 yields. Thus the nichrome wire was probably converting C_2H_2 to CO and C_2H_4. Plate 4(b) shows a photograph of the wire resting on the bed surface in the flame. It is glowing very brightly but not as hot as the platinum wire, suggesting perhaps a smaller catalytic effect. Again the available surface area was relatively small, which may account for the small magnitude of the effects.

The inconel strip had very little effect, only decreasing the H_2 yield very slightly. Despite the negative result, the outcome is of some use as this was the material used to construct the "Swiss-roll" burner. Thus the conclusion is that the inconel channels in the "Swiss-roll" had little or no catalytic effect on the combustion products. A photograph of the inconel strip in the electrically heated burner is shown in plate 4(c). Finally, the steel gauze appeared to have the greatest effect although still relatively small. This reduced the CO yield by about 0·5% and the H_2 by about 1%. There was also

Figure 26

GRAPH OF THE EFFECT ON EXHAUST GAS COMPOSITION OF SUSPENDING VARIOUS POTENTIAL CATALYSTS ABOVE THE BED , WITH 295 cc/s AIR.
(a) = WITHOUT CATALYST , (b) = WITH CATALYST
CH4 EQUIVALENCE RATIO :- (i) = 2.0 , (ii) = 1.9

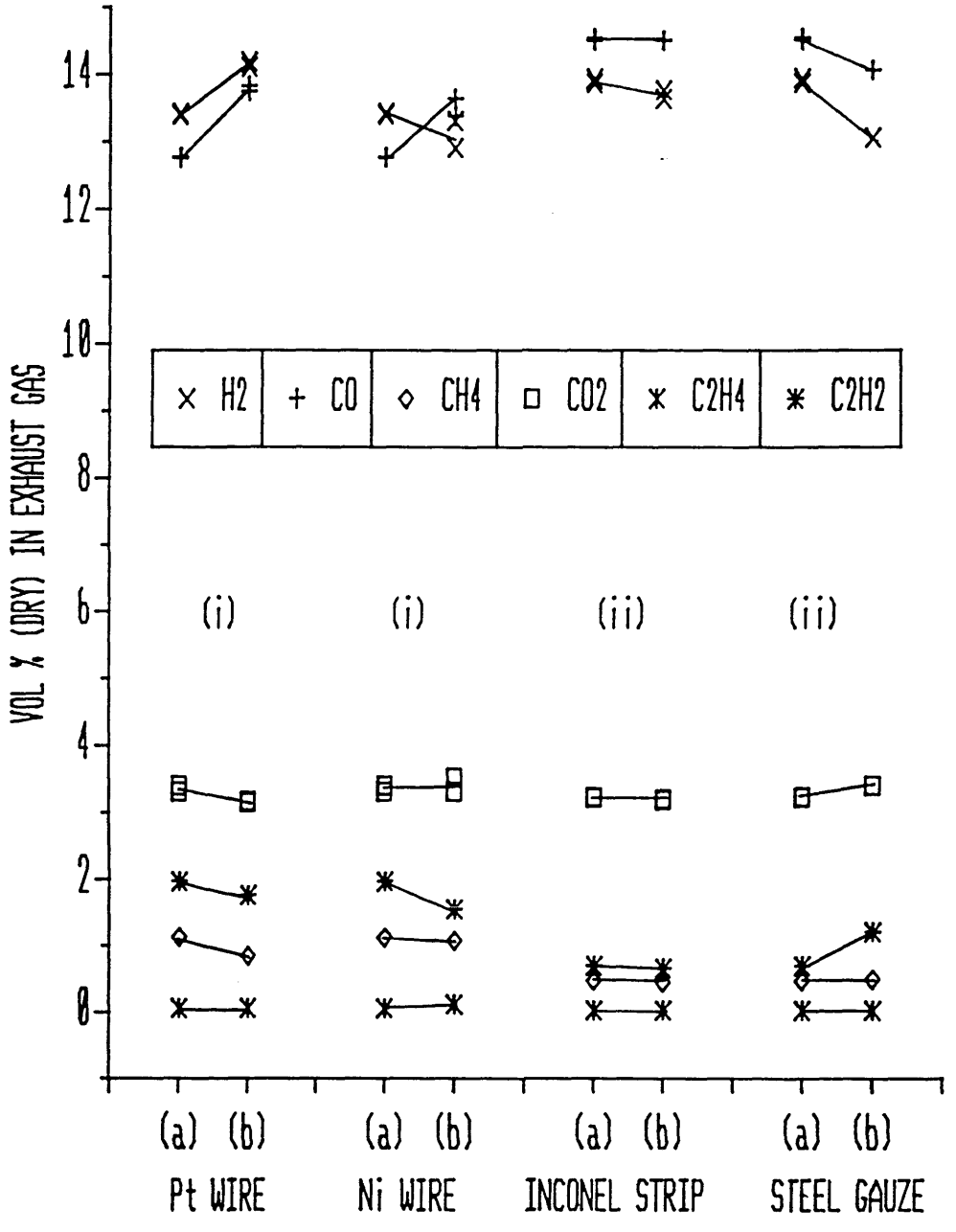

Plate 4 - Metals Tested In The Electrically Heated Burner

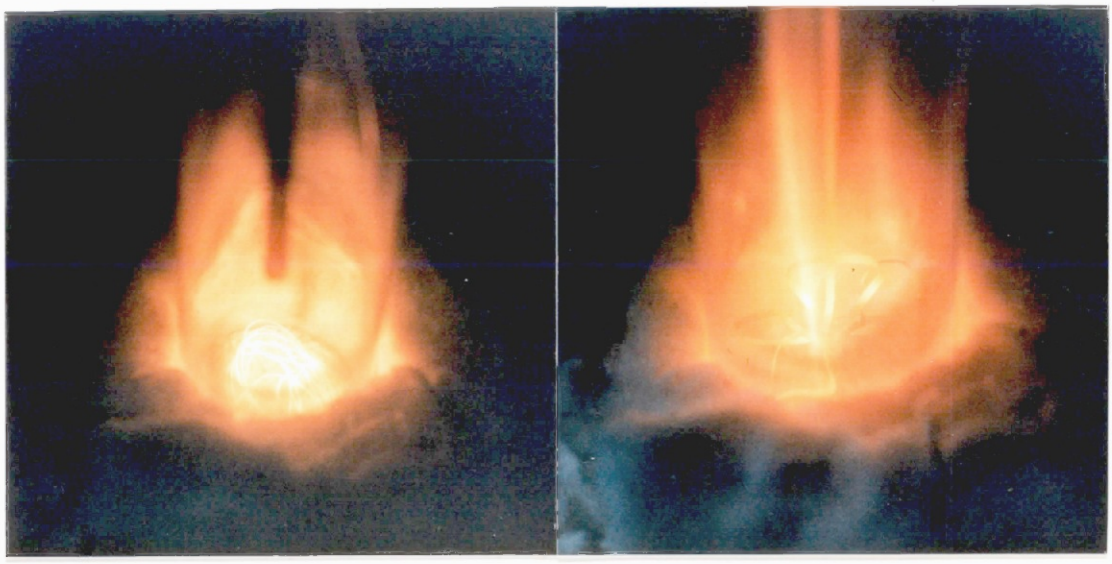

(a) Platinum Wire (b) Nichrome Wire

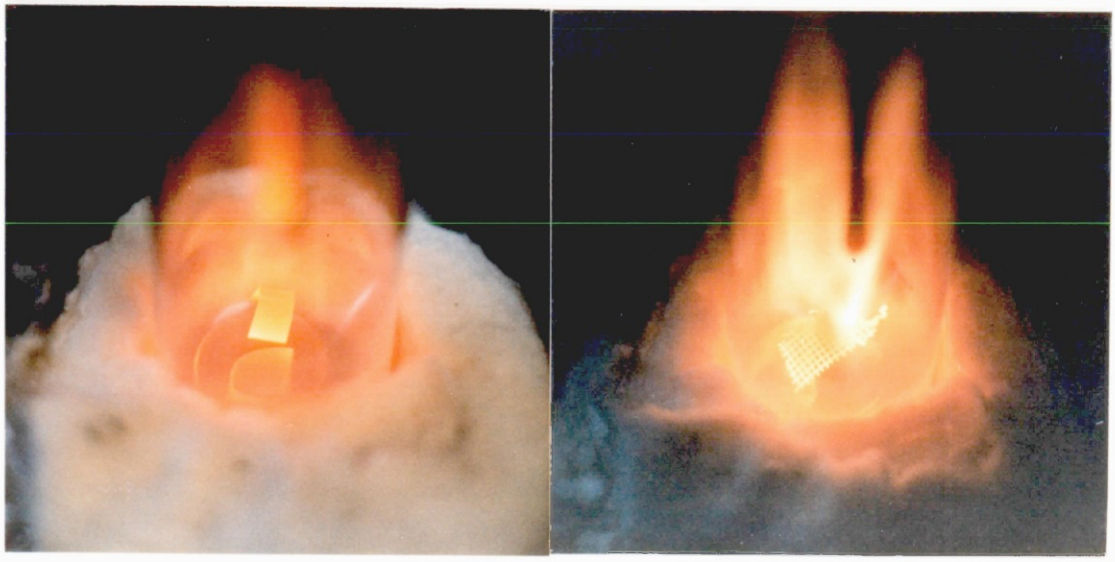

(c) Inconel Strip (d) Steel Gauze

a corresponding increase in C_2H_2 production of about 0·7% with a tiny rise in the CO_2 level. Thus the the steel gauze converted CO and H_2 to C_2H_2 and CO_2. Plate 4(d) shows a photograph of the steel gauze on the bed surface in the burner. It is also glowing very brightly, suggesting a catalytic effect. The gauze had the highest surface area of all the metals tested which perhaps explains why it had the greatest effect.

Reaction mechanisms to explain these effects have been proposed by Warnatz (1984). With the platinum wire where CO_2, CH_4 and C_2H_2 decreased whilst CO and H_2 increased,

$$CO_2 + H \longrightarrow CO + OH \qquad (I)$$
$$C_2H_2 + O \longrightarrow CH_2 + CO \qquad (II)$$
$$CH_2 + H \longrightarrow CH + H_2 \qquad (III)$$
$$CH + O \longrightarrow CO + H \qquad (IV)$$
$$CH + O_2 \longrightarrow CO + OH \qquad (V)$$
$$CH_4 + H \longrightarrow CH_3 + H_2 \qquad (VI)$$

With the nichrome wire, where C_2H_2 and H_2 decreased whilst CO and C_2H_4 increased, the above equations apply but additionally,

$$CH_2 + CH_3 \longrightarrow C_2H_4 + H \qquad (VII)$$

In the case of the steel gauze, where CO and H_2 were reduced whilst C_2H_2 and CO_2 were increased the above rections are inhibted. Clearly if reaction (II) is inhibited then reaction (III) is consequently stopped and H_2 and CO production is decreased. At the same time, less C_2H_2 is oxidised and this yield is increased. Also if reaction (I) is inhibited, less CO is produced resulting in less CO_2 being consumed, thus raising the CO_2 levels.

CHAPTER 4

COMBUSTION OF GASES IN THE SPOUTED BED BURNER

4.1 Aims

As described in chapter 1 the spouted bed is a recirculating particulate bed consisting of a high velocity spout, a fountain of particles above the bed and a slow downward moving annulus. The recirculating hot particles recycle heat from the hot products and thereby preheat the cold reactants. Thus it can burn very lean or very rich mixtures of hydrocarbons in air.

The work reported in this chapter was carried out as a precursor to introducing coal into the bed. The main objective was to find the optimum operating conditions for combustion in the spouted bed. Details of the most suitable particle types and sizes are readily available in the literature. There is, however, little information relating to the optimum bed depth for combustion - this being defined as the depth of particles allowing maximum heat recirculation. Accordingly the work discussed here sets out to find this optimum bed depth for the particular bed geometry used. The concept of the experiment was that the bed depth producing the highest level of heat recirculation would also afford the greatest extension to the lean flame stability limit. Thus the aim was to find the depth of particles which allowed the leanest mixture of methane in air to be burned in the spouted bed.

4.2 Design And Construction Of The Spouted Bed

The main constraint on the design of the spouted bed vessel was the laboratory air supply with a maximum flow of about 1000 cc/s. On the basis of this a vessel size of about 4 cm diameter and 50 cm height was selected. Quartz was chosen as the construction material because of its high temperature tolerance and transparency - it has a melting point of approximately 1700°C. A diagram of the reactor vessel is shown in figure 27. It consisted of a 41·5 mm OD, 2 mm wall thickness quartz tube drawn into a cone at one end, with an internal angle of 30°, to maximise the solids circulation rate. Attached to the end of the cone was a ground quartz socket into which the inlet nozzle was inserted. The inlet nozzle was also manufactured from quartz with a tip diameter of 3 mm. In order to facilitate stable spouting with high particle bulk densities the nozzle protruded by about 10 mm into the cone - see figure 28. This also prevented the inlet gas jet from being deflected by the walls of the cone.

Arbib *et al.* (1981) reported that inert alumina particles suffered less from attrition, due to the thermal stresses, than sand or crushed fire brick in combusting spouted beds. The authors also found that the smallest particles gave the best heat transfer but, if made too small, led to pulsating combustion and unsteady spouting. Alumina particles of size 0·85-1·00 mm were found to be the smallest particles giving satisfactory spouting as well as making ignition easy and giving rise to very little elutriation. The same principles were adopted in this study and alumina particles of size 0·8-1·0 mm and loose bulk density 1·8-2·1 g/cc were employed.

A lagging jacket for the spouted bed was made from 'Kaowool' blanket. This was done by wrapping the insulating material around the quartz vessel to a depth of 4 cm and then fixing it in place with wire ties. A small hole and a slit were cut in the insulation for visual observation of the flame and the fixing of a thermocouple junction. In this way the vessel could easily be inserted into the

Figure 27 - The Spouted Bed Vessel

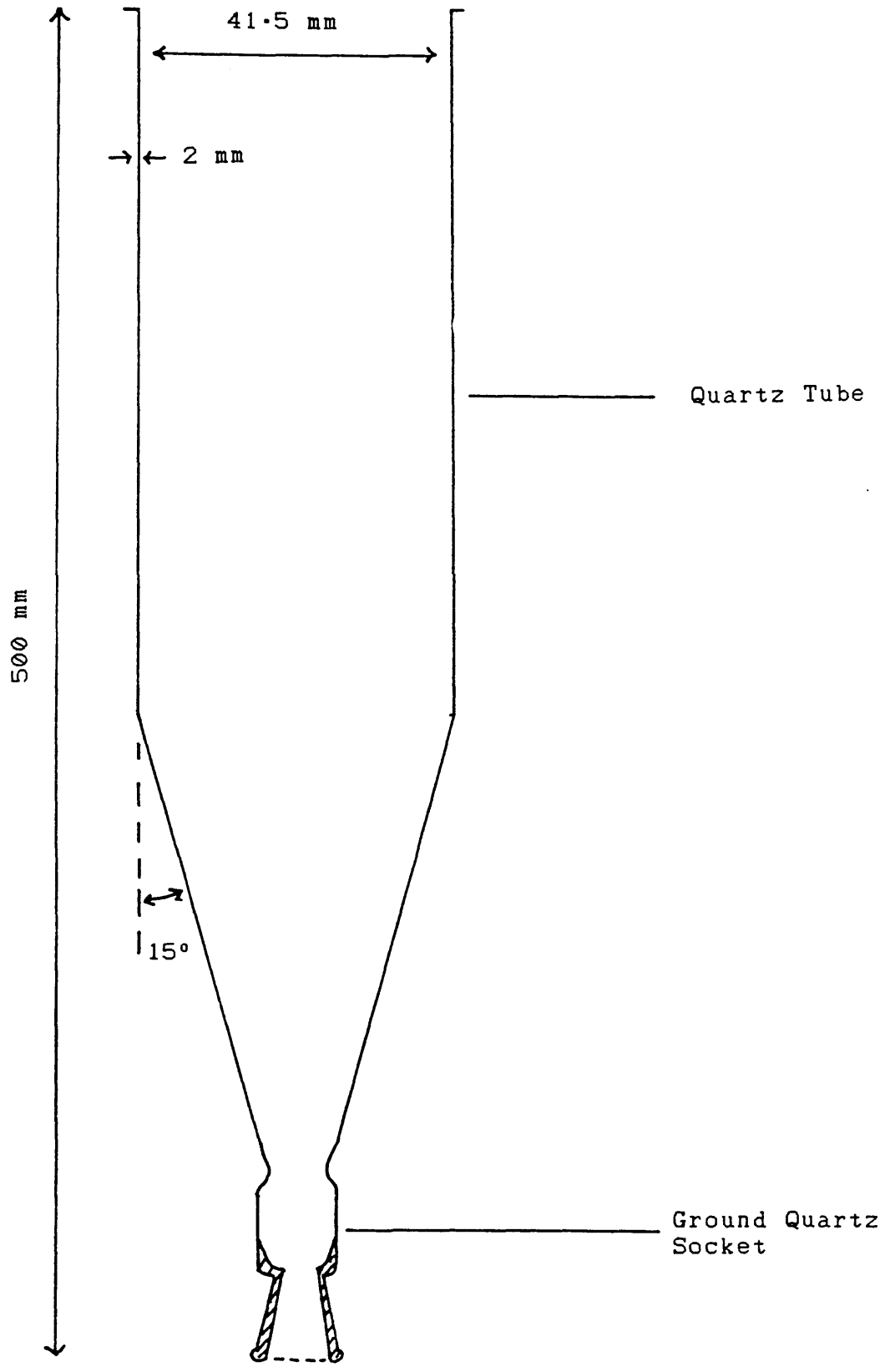

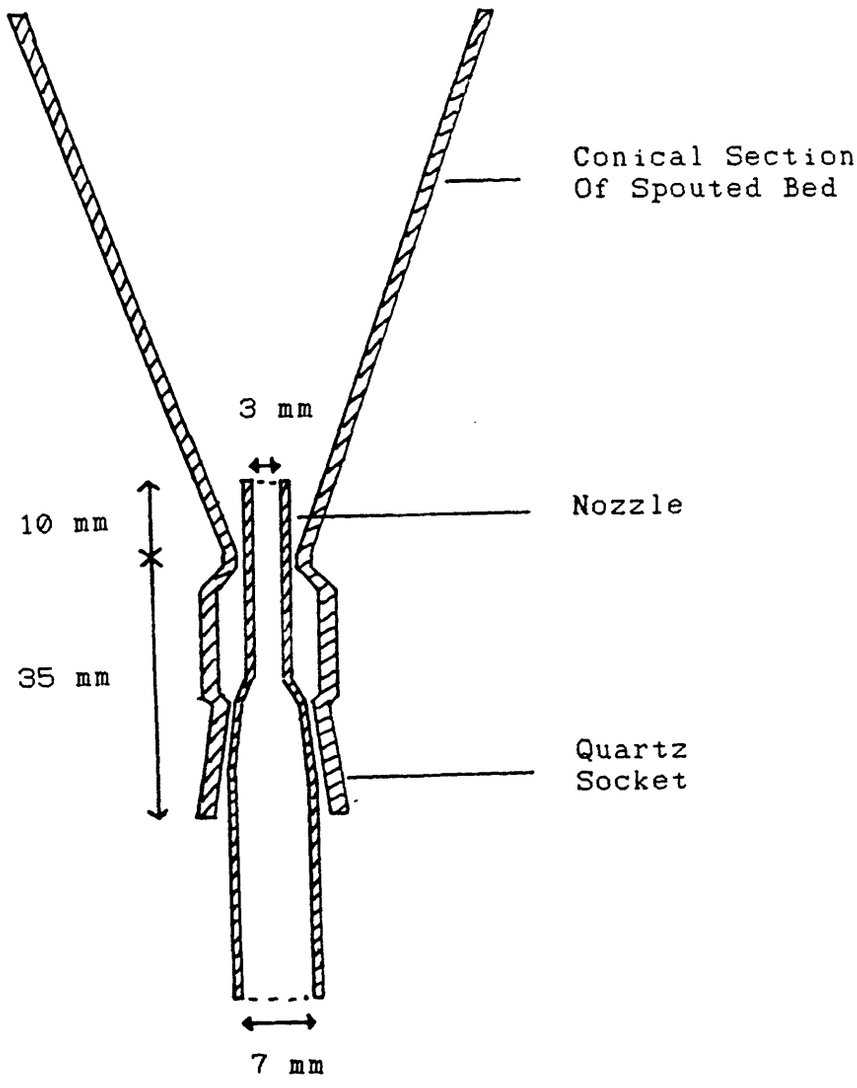

Figure 28 - Quartz Inlet Nozzle

insulating jacket before use, if desired.

4.3 Ancillary Experimental Equipment

The gas feeding system is identical to that used in the previous chapters and is described in chapter 2. All the products from the spouted bed in these experiments were gaseous and so the same analytical system was used as for the "Swiss-roll" burner. This is also described in chapter 2. Product sampling was carried out in the same way as described for the electrically heated burner, chapter 3.

The bed temperature was monitored by means of an 'R' type thermocouple attached to the outside of the spouted bed vessel with high temperature alumina cement. The output from the thermocouple was monitored with a digital volt meter accurate to 0·01 mV. When the burner was insulated with 'Kaowool' the thermocouple junction was assumed to approach thermal equilibrium with the bed inside the burner tube and thus to give a fairly accurate representation of the bed temperature at that point. This assumption was confirmed previously by Arbib *et al.* (1981) who also found that, for steady state combustion in insulated spouted beds, the temperature was quite uniform throughout the bed - the mean temperature difference between the top and bottom was of the order of 40 K. This indicates that no significant part of the exothermal chemical reaction occurs in the bed and that it may be treated as isothermal. On the basis of this experimental finding of isothermicity, the reading from the one thermocouple was taken to be a true indication of the average bed temperature.

4.4 Experimental Procedure

4.4.1 Ignition

The quartz spouted bed vessel was first fixed vertically in place below the exhaust duct by means of steel clamps. These clamps were positioned so that they gripped the vessel above and below the lagging jacket if this was fitted. The inlet nozzle was then inserted and a high air flow rate fed through it - about 900 cc/s. After this the desired weight of particles was poured in from the top of the vessel so that spouting could be instigated without the usual high pressure drop, encountered prior to the spout breaking through an initially quiescent bed. Once stable spouting had been established, the air flow rate was reduced to about 700 cc/s and a flow of methane fed to the nozzle such that the mixture strength was 7% methane. The mixture was ignited at the exit from the spouted bed and, initially, a flame stabilised here. The methane flow was then slowly increased, bringing the mixture closer to stoichiometric, which caused the flame to flash back into the spouted bed and eventually stabilise on the bed surface. However the flame first passed through a pulsatory mode, accompanied by a great deal of noise, before achieving steady combustion.

4.4.2 Operation

Once the bed had been ignited satisfactorily, it was left for between five and ten minutes to establish itself. The desired flow rate and mixture strength could then be set. This was always done by first setting the air flow rate and then adjusting the methane flow to give the required composition. If it was necessary to pass through a stoichiometric composition, 9·5% methane in air, this was always done so as to minimise the time spent there and so avoid the associated high temperatures. With the desired flows set, the system was left for up to 30 minutes to reach a steady state. This was determined by a constant

pressure drop across the bed and, if the insulating jacket was in place, a relatively constant bed temperature. Once the steady state had been attained, the desired measurements were made. A pilot flame was always left burning at the exit from the burner vessel to ignite any flammable combustion products.

4.4.3 Shutdown

Two different procedures were used for closing down the burner, depending upon the equivalence ratio being operated at. If the mixture to be extinguished was lean, the methane flow was simply cut off and the air flow left to cool down the bed before also being shut off. If a rich mixture was being burned, the air flow was first slowly decreased to zero. Once the mixture had exceeded the rich stability limit and the flame had extinguished, the methane flow was shut off. Hence stoichiometric methane-air mixtures were avoided whilst extinguishing both lean and rich flames.

4.5 Bed Depth Optimisation

Using various weights of bed material, the lean locus of stability was determined as a function of total mixture flow rate. The weight of particles allowing the leanest mixtures to be burnt was taken as the optimum weight for heat recirculation.

4.5.1 Experimental Procedure

The operations described below were carried out four times, with 28g, 63g, 114g and 164g of alumina particles, in an unlagged spouted bed vessel. These weights of particles gave bed depths of approximately 5 cm, 7 cm, 9 cm and 11 cm. An unlagged bed was used so that the lean limit could be identified with greater ease and more accuracy. The lean stability limit was defined as the point where the flame lifted from the bed surface up above the fountain and

did not return. Each point was also repeated three times to guard against error.

The spouted bed was ignited, as described earlier, with a 7% methane in air mixture. After the bed had warmed up, the air flow rate was set at 325 cc/s and the methane flow gradually reduced to find the lean limit of stability. After each small decrease in the methane feedrate, the system was left for several minutes to allow the flame to stabilise before continuing. By doing this it was hoped to avoid recording an artificially low lean limit - the bed, having a high thermal capacity, retained heat for some time after the methane flow was reduced. This procedure was then repeated using air flow rates of 365, 410, 452, 495, 540, 580, 625 and 665 cc/s. The bed was additionally left for an extra 20 minutes after the air flow had been changed for the steady state to be recovered.

4.5.2 Results And Discussion

Figure 29 shows a graph of the loci of lean stability limits for the weights of particles tested as a function of total mixture flow rate. With a 5 cm deep bed containing 28g particles, the lean limit ranged from an equivalence ratio of 0·59 at a high air flow rate to 0·52 at a low flow rate. The 7 cm deep bed, containing 63g alumina particles, gave corresponding values of 0·52 at a high flow rate and 0·47 at a low flow rate. Using 114g alumina particles, forming a 9 cm deep bed, gave a lean limit of equivalence ratio 0·51 at a high flow rate and 0·43 at a low flow rate. So far, the results suggested that the deeper the bed the leaner the leanest burnable methane-air mixture. This would agree with the work of Arbib *et al.* (1981) who suggested that using a deeper bed would increase the particle-gas contact times thus moving the system closer to thermal equilibrium and recirculating more heat. However with the lean stability curve for 164g alumina particles, bed depth 11 cm, the lean limit at a high flow rate had an equivalence ratio of 0·50 and at a low flow rate 0·44. Thus the deeper, 11cm, bed cannot burn as lean as the 9 cm bed

Figure 29

GRAPH OF TOTAL METHANE / AIR MIXTURE FLOWRATE VS EQUIVALENCE RATIO FOR THE WEIGHTS OF PARTICLES SHOWN.

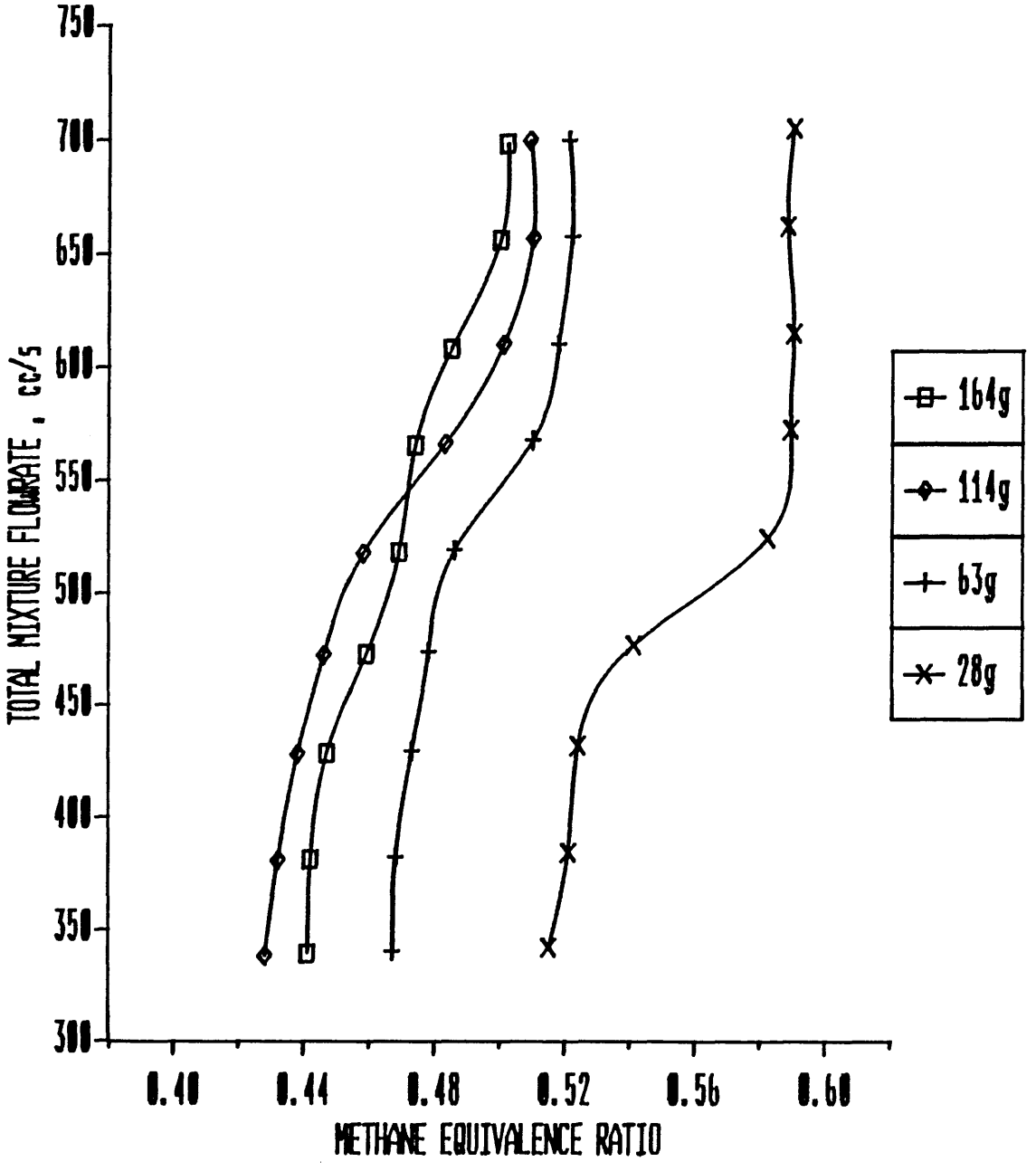

and therefore recirculates less heat.

In a heat exchanger such as the spouted bed, heat is transferred by moving particles. The degree of heat recirculation must depend upon the surface area of particles available per unit time which in turn depends upon the particle mass circulation rate. The higher the particle mass flow rate, the more effective the heat exchanger and the higher the heat recycle. For a given gas flow rate, increasing the bed depth increases the mass of particles entrained by the gas and, therefore, the particle mass flow rate. For the system described here this argument applies up to a bed depth of 9 cm. However there is a maximum concentration of particles that a given gas flow can hold in suspension - this maximum particle load is achieved with the 9 cm deep bed. With the deeper bed the weight of particles becomes too heavy for the gas to lift and the particle mass circulation rate actually decreases. This reduction in particle mass flow rate decreases the efficiency of the heat exchanger and thus also the degree of heat recirculation. In conclusion, then, for the system under investigation the optimum bed depth for heat recirculation is 9 cm or 114g particles.

4.6 Lean And Rich Combustion At The Optimum Bed Depth

Using the optimum bed depth of 9 cm, or 114g particles, the lean stability curve for the spouted bed with insulation was determined. The rich loci of stability were also determined for the system with and without insulation. The product gases were analysed from the insulated spouted bed whilst burning mixtures rich of the normal rich limit of flammability for methane.

4.6.1 Experimental Procedure

The first experiment was to determine the lean limit for an insulated bed containing the optimum weight of 114g particles. The insulated bed was first clamped in position with the thermocouple cemented in place and connected to

the digital voltmeter. The spouted bed was then ignited as before but with 114g alumina particles. For each of the air flow rates used in the previous experiment, the mixture was made progressively leaner, by reducing the methane flow, until the lean limit was found. This time the system was left for five to ten minutes after each methane flow reduction for the flame to stabilise, as the insulated bed held its heat for much longer. In the lagged bed, the lean limit was identified by observing, through the small window in the lagging, the flame lifting and from the sharp drop in bed temperature, recorded by the thermocouple, as the flame lifted from the bed. This procedure was repeated in the second experiment to find the rich stability limits, at the same air flow rates with 114g particles, for the spouted bed with and without insulation - except that the methane flow was increased rather than reduced. The rich limit was similarly defined as the point where the flame lifted from the fountain and was detected visually in the unlagged bed and with the aid of the thermocouple in the insulated bed.

In the final experiment the bed was insulated, the air flow rate fixed at 405 cc/s and the product gases from various rich methane-air mixtures analysed. This was achieved by first igniting the lagged spouted bed in the usual way with 114g alumina particles and setting the desired air and methane flow rates. The system was then left for about 30 minutes to reach a steady state. Once the bed temperature and pressure drop indicated that a steady state had been achieved, two samples were taken, as described in chapter 3, for later analysis. This procedure was carried out with methane equivalence ratios of 1·6, 1·7, 1·8, 1·9 and 2·0.

4.6.2 Results And Discussion

Using the optimised bed depth of 9 cm or 114g particles, the leanest burnable mixture was 2·78% methane in air with an equivalence ratio of 0·292. This occurred in the lagged spouted bed with a total mixture flow rate of 422 cc/s. the richest burnable mixture was 19.8% methane in air

with an equivalence ratio of 2·083 occurring at a total mixture flow rate of 505 cc/s. The complete set of lean and rich stability curves for combustion both with and without insulation are shown in figure 30. The addition of insulation to the bed extended the lean and rich limits by 1·4% and 4·2% methane in air respectively, at an air flow rate of 405 cc/s. All the curves, particularly at the rich limit, exhibit the characteristic 'C' shape first observed by Khoshnoodi and Weinberg (1978). Their shape is thought to be due to decreased heat recirculation both at very low and very high flow rates; the former as a consequence of reduced particle mass circulation rates and the latter of decreased particle-gas contact times at high flow velocities. Plate 5 shows photographs of (a) lean and (b) rich gaseous combustion in the unlagged spouted bed. As can be seen, the bed becomes much hotter during rich combustion and the conical flame is less distinguishable.

The fact that the loci of stability, with and without, insulation had separations of approximately 0·15 ø, for the lean limit, and 0·44 ø, for the rich limit, can be used to calculate the heat losses from the unlagged spouted bed. Lloyd and Weinberg (1974) demonstrated the existence of a constant final flame temperature at the lean stability limit and in chapter 3 it was shown that, at the rich limit of stability, this phenomenon also exists. Therefore the extra heat input required by the unlagged bed, at the stability limits, must represent its heat loss. At the lean limit, with an air flow rate of 405 cc/s, a methane equivalence ratio of 0·15 equals a methane flow of 5·9 cc/s or $3{\cdot}99\times10^{-6}$ kg/s. The heat of combustion for lean methane-air mixtures is 50 MJ/kg (JANAF tables, 1971) and so the heat loss from the uninsulated spouted bed is approximately 200 W. The rich stability limits, at 405 cc/s air, were 2·08 ø in the lagged bed and 1·64 ø in the unlagged bed; this represents methane flows of $6{\cdot}29\times10^{-6}$ and $4{\cdot}71\times10^{-6}$ kg/s respectively. From figure 25, chapter 3, the heats of combustion for methane equivalence ratios of 2·08 ø and 1·64 ø are 12·6 and 20·2 MJ/kg, and so the respective heat inputs are 792 W in the lagged bed and 951 W

GRAPH OF TOTAL GAS MIXTURE FLOWRATE VS EQUIVALENCE RATIO FOR METHANE COMBUSTION IN A 4 cm DIAMETER SPOUTED BED WITH 114g PARTICLES.

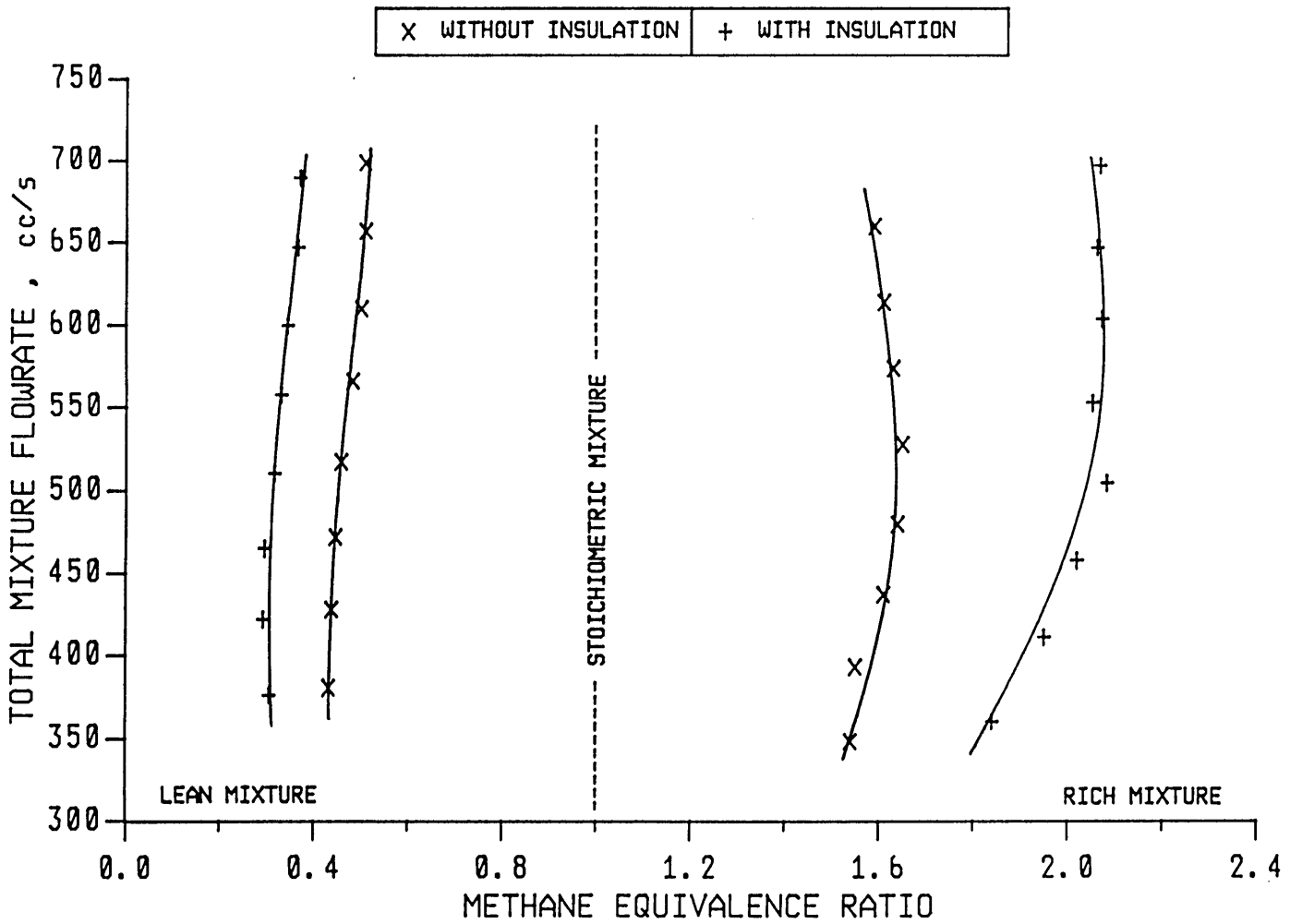

Figure 30

Plate 5 - Methane Combustion In The Spouted Bed

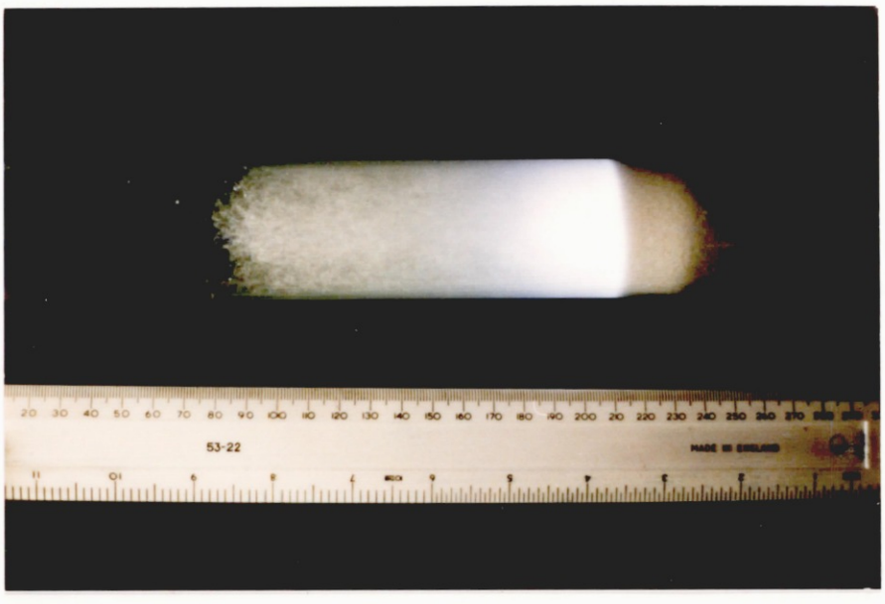

(a) Lean Combustion

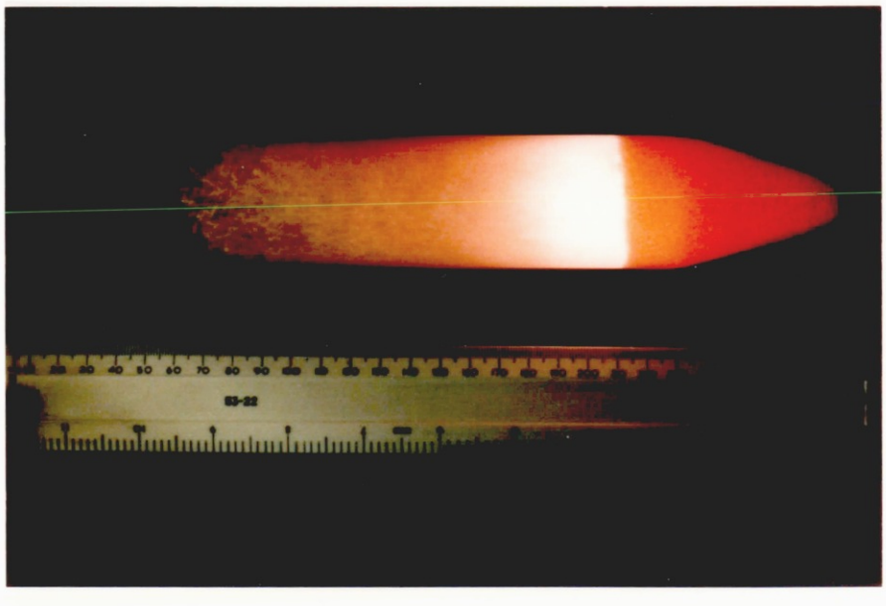

(b) Rich Combustion

in the unlagged bed. The heat loss from the uninsulated bed, at the rich limit is given by the difference, ie. 159 W.

Furthermore, if it is assumed that this heat is only lost from the annulus of the spouted bed, through the walls of the quartz vessel, and that the bed particle temperature is the same in both the lagged and the unlagged bed, the heat transfer coefficient of the bed for heat loss can be calculated. In these experiments the bed depth was about 9 cm which, with an internal cone angle of 30°, gives an outside surface area of 67·4 cm^2. The recorded bed temperatures were 665°C at the lean limit and 885°C at the rich limit and so, for a room temperature of 20°C, the calculated heat transfer coefficients are approximately 46 $W/m^2/K$ and 27 $W/m^2/K$ respectively.

The product gases from rich mixtures were analysed at equivalence ratios of 1·6, 1·7, 1·8, 1·9 and 2·0 with an air flow rate of 405 cc/s - this was the air flow that allowed the greatest extension to the rich limit. The results of the analyses are shown graphically in figure 31. As the equivalence ratio increased from 1·6 to 2·0 the CO and H_2 yields approached a maximum of about 13% and 12% respectively. At the same time the CO_2 yield dropped from 4% to 3%. The yields of C_2H_2 and unconverted CH_4 approximately mirrored each other rising from 0·5% to about 1%. Trace yields of C_2H_4 were also detected rising to about 0·2%. These trends are more or less as predicted by the work described in chapter 3 with the electrically heated burner, using an air flow rate of 410 cc/s. In that case too, CO and H_2 yields increased to a maximum of about 13% at an equivalence ratio of 2·0. The yields of CO_2, CH_4, C_2H_2 and C_2H_4 were also similar.

In the spouted bed, as the mixture was made richer so the bed temperature fell fom 1025°C at an equivalence ratio of 1·6 to 885°C at an equivalence ratio of 2·0. This is shown graphically in figure 32 and is due to the gradual decrease in the heat of combustion as the mixture becomes richer, as demonstrated in the electrically heated burner chapter (3).

Figure 31

GRAPH OF EXHAUST GAS COMPOSITION VS METHANE EQUIVALENCE RATIO FOR AN INSULATED SPOUTED BED WITH 485 cc/s AIR AND 114g PARTICLES.

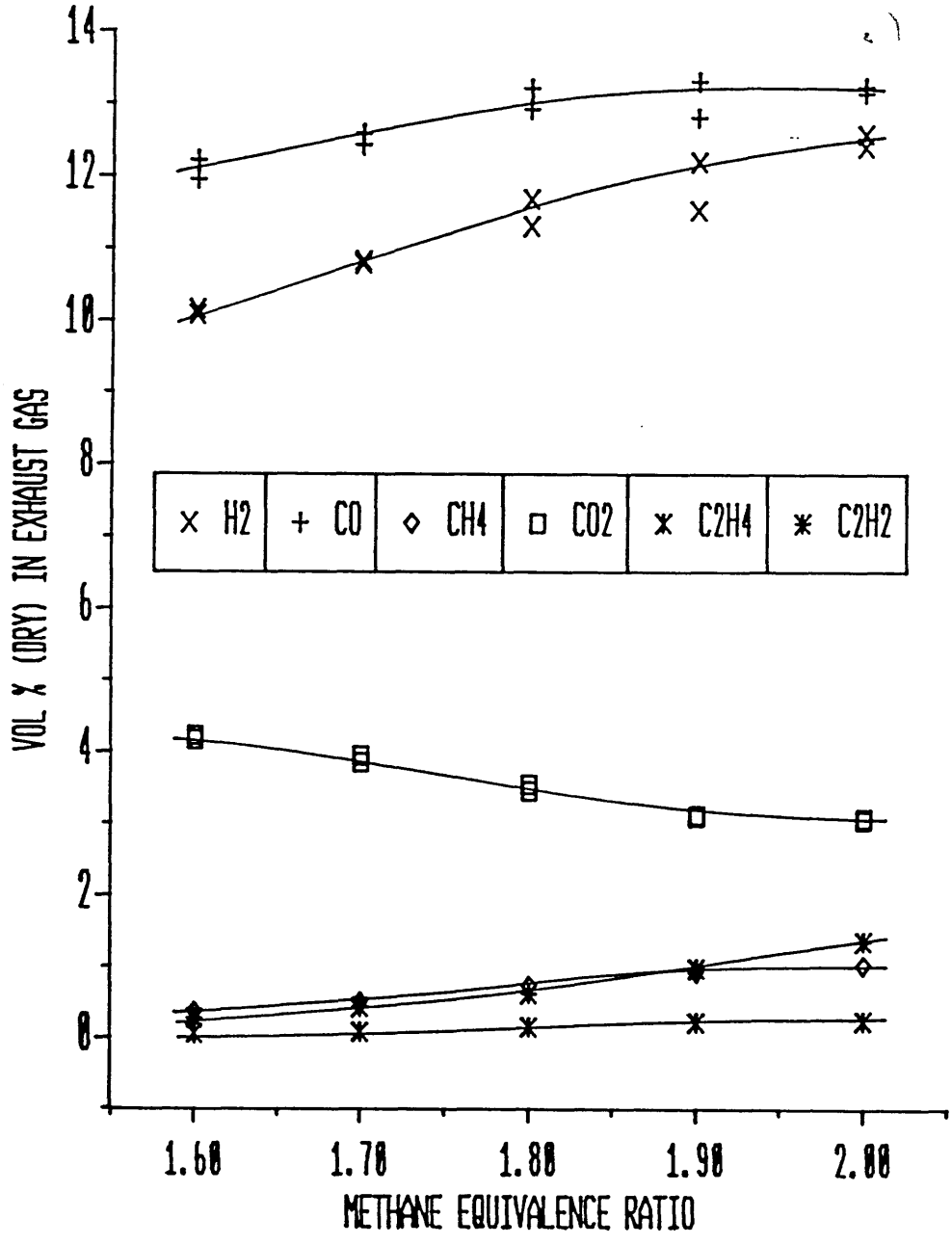

GRAPH OF BED TEMPERATURE VS METHANE EQUIVALENCE RATIO FOR A LAGGED SPOUTED BED WITH 114g PARTICLES AND 405 cc/s AIR.

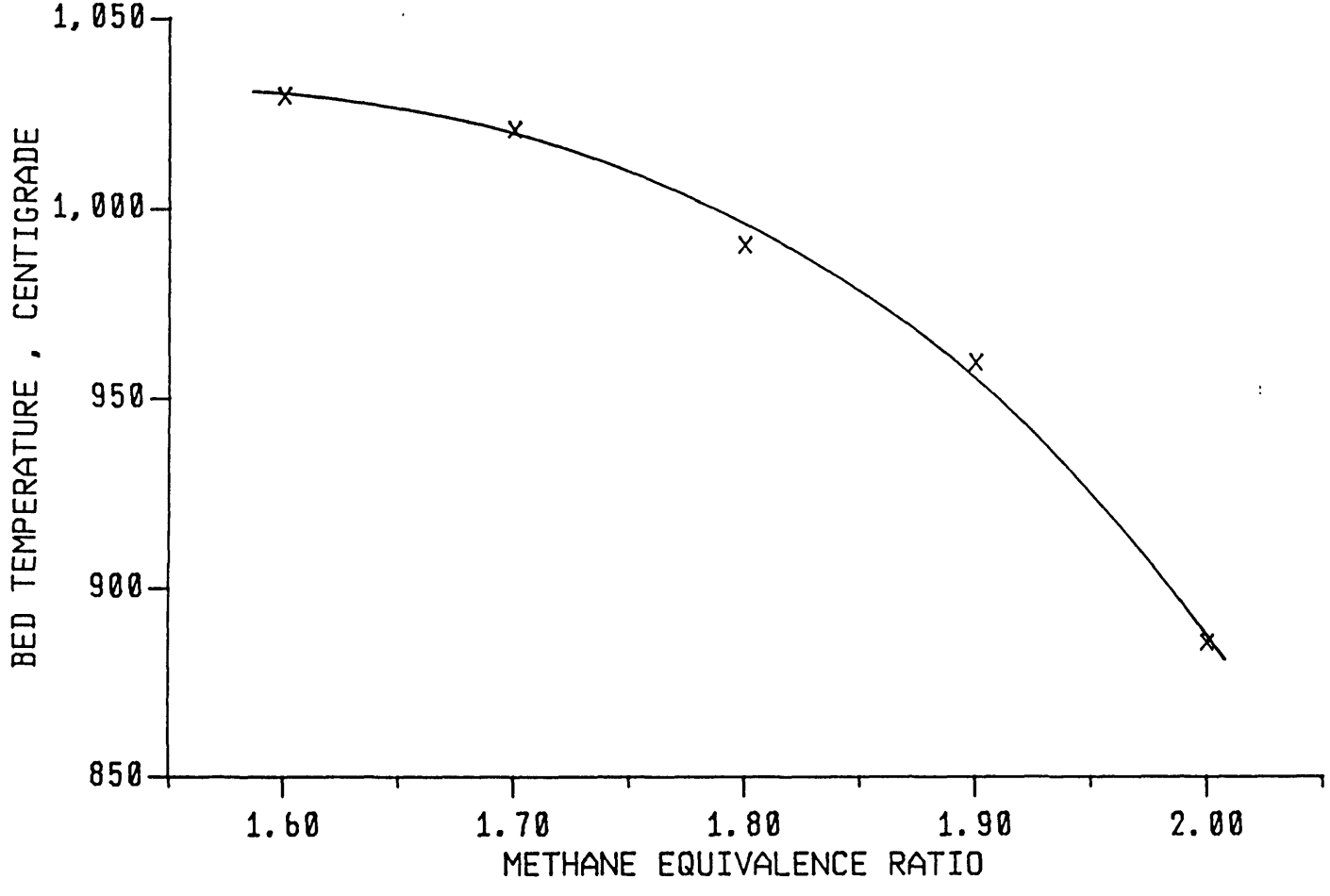

Figure 32

CHAPTER 5

THEORETICAL HEAT TRANSFER MODELS FOR THE SPOUTED BED

5.1 Aims

Simple models describing heat transfer in the spouted bed were formulated in order to help analyse data from the previous chapters and study the effect of varying the controlling parameters of the system. With a moving particle heat exchanger, the most important variable is the total surface area of particles being circulated, which depends upon ~~the heat capacity and~~ the mass circulation rate. The particle mass flow rate in the spouted bed, for a given gas flow rate, cannot easily be calculated theoretically. The mass flow of solids can be measured experimentally by timing single particles as they travel down in the annulus and then calculating their velocities. This, however, is not very accurate and only gives an average particle velocity which is not very suitable as the basis for a model. In the light of this, the ratio of the particle mass flow to gas mass flow was made a design variable for the purposes of the models. Thus the various other parameters, eg. temperatures, could be calculated for a series of particle to gas mass flow ratios from 0 to 30. Three such models were set up, one to calculate temperatures for a 3% methane in air mixture and two to predict the lean and rich stability limits for methane combustion in the spouted bed.

5.2 Lean Combustion Model

This model set out to predict the bed particle temperature, Tp_1, the fountain particle temperature, Tp_2, the gas preheat temperature, Tu, the gas flame temperature, Tf, and the combustion products gas temperature, Te, for an initial mixture of 3% methane in air at 293 K and atmospheric pressure. The model catered for alumina particles of size 0·4 to 1·4 mm and particle to gas mass flow ratios of 0 to 30.

5.2.1 Assumptions

In order to keep the model simple, several approximations were made:

a) The reactants were assumed to be gaseous and to obey the ideal gas laws.
b) The process was assumed to occur at constant pressure.
c) The products were assumed to be in thermal and chemical equilibrium.
d) Dissociation of the products was assumed to be negligible.
e) The system was assumed to be adiabatic.
f) All the gas was assumed to flow through the spout and combustion occurred above that.
g) Specific heat capacities were assumed to be constant and equal for products and reactants.

With an ultra lean combustion mixture, 3% methane, the temperatures are relatively low and hence product dissociation can justifiably be ignored. Also with a lean mixture the main constituent of both the reactants and products is air, thus using the heat capacity of air is a good approximation. Finally a spouted bed, well insulated with 4 cm of 'Kaowool' blanket, has very little heat loss, which can safely be neglected.

5.2.2 Theory

The spouted bed was considered to be a heat exchanger consisting of a cold limb (the spout), a hot limb (the fountain) and a flame zone. Heat transfer between gas and particles only took place in the two limbs with the gas also being heated in the thin flame zone. As mentioned earlier, heat lossses were neglected.

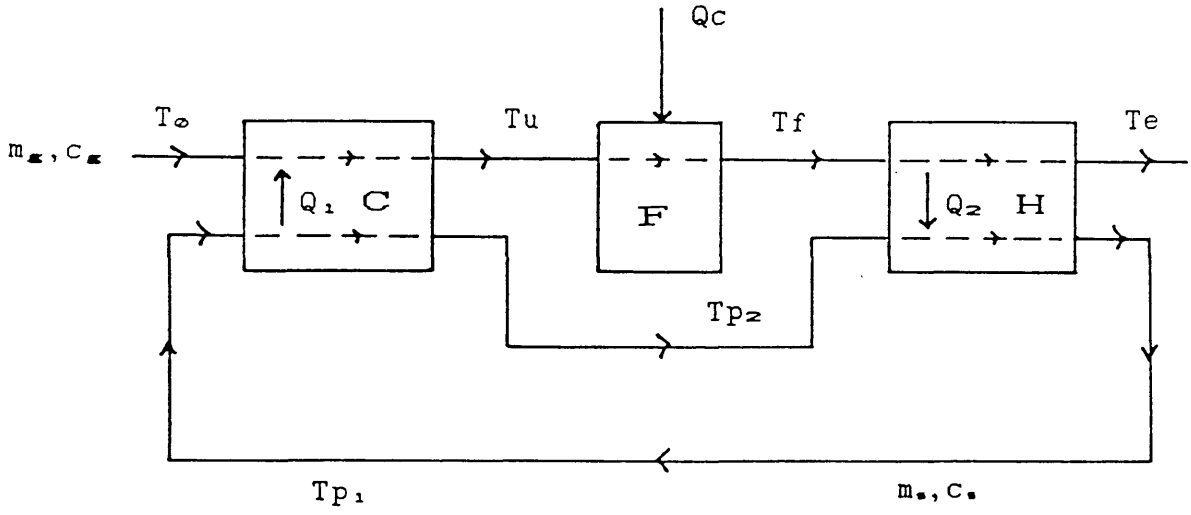

Figure 33 - The Spouted Bed Model

Where m_s is the mass flow of particles, m_g is the mass flow of gas, c_s is the particle heat capacity, c_g is the gas heat capacity and $Q_{2/1}$ are the heat transferred in the hot and cold limbs. The total heat input from combustion is shown by Qc, where

$$Qc = q_c . m_g . x_{CH4} . \rho_{CH4} / \rho_{mix}$$

with q_c being the specific heat of combustion of methane (J/kg), x_{CH4} being the mole fraction of methane and $\rho_{CH4/mix}$ being the density of methane/the methane air mixture (kg/m^3).

Defining a quantity, Hr, the temperature rise due to combustion,

$$Hr = (q_c/C_g).x_{CH4}.(\rho_{CH4}/\rho_{mix})$$

leads to,

$$Qc = Hr.m_g.c_g$$

The heat transferred in the hot and cold limbs of the heat exchanger can be considered by using an assumed common heat transfer coefficient and an arithmetically averaged temperature driving force.

$$Q_1 = h.A.[0{\cdot}5.(Tp_1 + Tp_2) - 0{\cdot}5.(Tu + T_\infty)]$$
$$Q_2 = h.A.[0{\cdot}5.(Te + Tf) - 0{\cdot}5.(Tp_1 + Tp_2)]$$

A series of energy balances over the various components of the system gives:

overall,

$$Te = T_\infty + Hr$$

flame zone,

$$Tu = Tf - Hr$$

cold limb,

$$Tp_1 - Tp_2 = (Tu - T_\infty)/[m_s.c_s/(m_g.c_g)]$$

Combining the heat transferred in the two limbs, which is equal ie. $Q_1 = Q_2$.

$$0{\cdot}5.h.A.[Tp_1+Tp_2-Tu-T_\infty] = 0{\cdot}5.h.A.[Te+Tf-Tp_1-Tp_2]$$

leads to,

$$(Tp_1 + Tp_2) = (Tf + Te + Tu + T_\infty)/2$$

If it is further assumed that Tf is a multiple, y, of the maximum flame temperature achievable without heat recirculation, then;

$$Tf = y.(Te - T_\infty) + T_\infty$$

The system of simultaneous equations can now be solved, given a value of y and the mass flow ratio $[m_s/m_g]$. This gives the following equations for Tf, Te, Tu, Tp_1 and Tp_2.

$$Tf = y.(Te - T_\infty) + T_\infty$$
$$Te = T_\infty + Hr$$
$$Tu = Tf - Hr$$
$$Tp_1 = (Tu-T_\infty)/(2.[m_s.c_s/(m_g.c_g)]) + (Tf+Te+Tu+T_\infty)/4$$
$$Tp_2 = Tp_1 - (Tu-T_\infty)/[m_s.c_s/(m_g.c_g)]$$

In order to establish a relationship between y and m_s/m_g, it was assumed that y was proportional to the surface area of particles being circulated, ie. -

$$y \propto Np.d_p^2$$

where : d_p = particle diameter

Np = particle number density, particles/m^3 gas

$$= \frac{6.m_s.\rho_g}{d_p^3.\rho_s.\pi.m_g}$$

Thus, it was assumed

$$y = 1 + K.Np.d_p^2/(1 + Np.d_p^2) \qquad ; K = \text{a constant}$$

and,

as $Np.d_p^2 \longrightarrow \infty$, $y \longrightarrow y_{max}$

as $Np.d_p^2 \longrightarrow 0$, $y \longrightarrow 1$

When $y = y_{max}$, $Tf = Tf_{max}$; thus to calculate the value of the constant K it is necessary to calculate Tf_{max}. The maximum flame temperature, Tf_{max}, is reached when the particles achieve thermal equilibrium with the gas.

ie. $Tp_2 = Tu$ and $Tp_1 = Te$

For this special case the previous equations can be solved independently of the factor y, to give,

$$Tf_{max} = T_\infty + \left[\frac{1 + 2.[m_s.c_s/(m_g.c_g)]}{1 + [m_s.c_s/(m_g.c_g)]} \right] . Hr$$

But also,

$$Tf_{max} = y_{max}.(Te - T_\infty) + T_\infty$$

Combining these gives,

$$y_{max} = 1 + \left[\frac{[m_s.c_s/(m_g.c_g)]}{1 + [m_s.c_s/(m_g.c_g)]} \right]$$

Which leads to,

$$K = \left[\frac{[m_s.c_s/(m_g.c_g)]}{1 + [m_s.c_s/(m_g.c_g)]} \right]$$

and thus,

$$y = 1 + \left[\frac{\left[\frac{[m_s.c_s/(m_g.c_g)]}{1 + [m_s.c_s/(m_g.c_g)]} \right] . Np.d_p^2}{1 + Np.d_p^2} \right]$$

With the factor y defined in terms of the particle to gas mass flow ratio, only this ratio and the particle diameter need to be set for the model to run - apart from the initial gas temperature and mixture strength.

5.2.3 Results And Discussion

Having formulated the simple model the equations were coded into fortran and programmed into a computer. The program varied the particle to gas mass flow ratio from 0 to 30 and the particle diameter from 0·4 to 1·2 mm. The results were sent by the computer to a graphics package which then plotted graphs of Tp_1, Tp_2, Tu and Tf against the above parameters. The values of T_o and Te were constant as T_o was set and Te was the exit temperature - external to the heat recirculation. T_o was set at 293 K and Te calculated as 969 K. All data for the program was extracted from JANAF tables (1971)and is identified in the program listing - see appendix A. Figures 34 to 37 show the graphs of Tp_1, Tp_2, Tu and Tf. As can be seen, as the particle size tends to zero or the mass flow ratio tends to infinity, the system approaches thermal equilibrium. At thermal equilibrium, Tp_1 = Te = 969 K; figure 34 shows the maximum value of Tp_1 to be about 960 K. Thus with a particle size of 0·4 mm and a mass flow ratio of 30 the system is virtually at thermal equilibrium. The general temperature profile for the system is shown in the sketch below; note that Tp_2 > Tu and that Te > Tp_1.

Figure 38

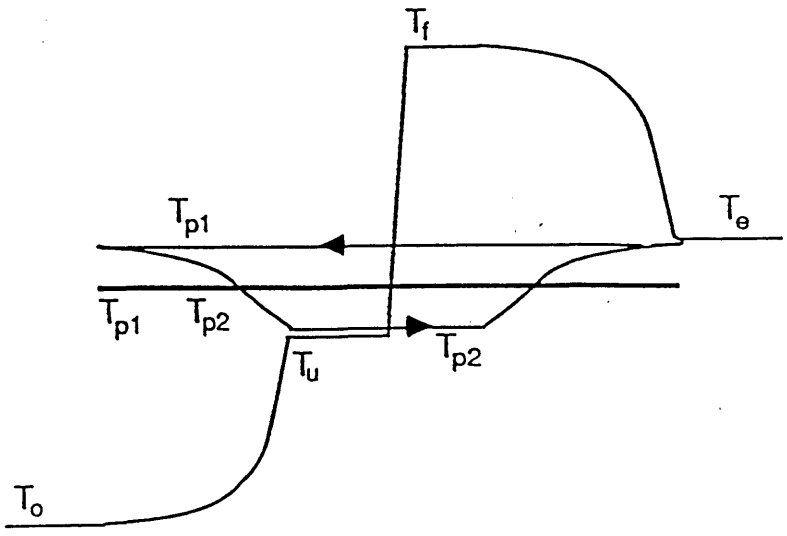

TP1 vs Particle Mass Flow / Gas Mass Flow For An Adiabatic System
Burning 3% Methane In Air And Using The Particle Sizes Shown.

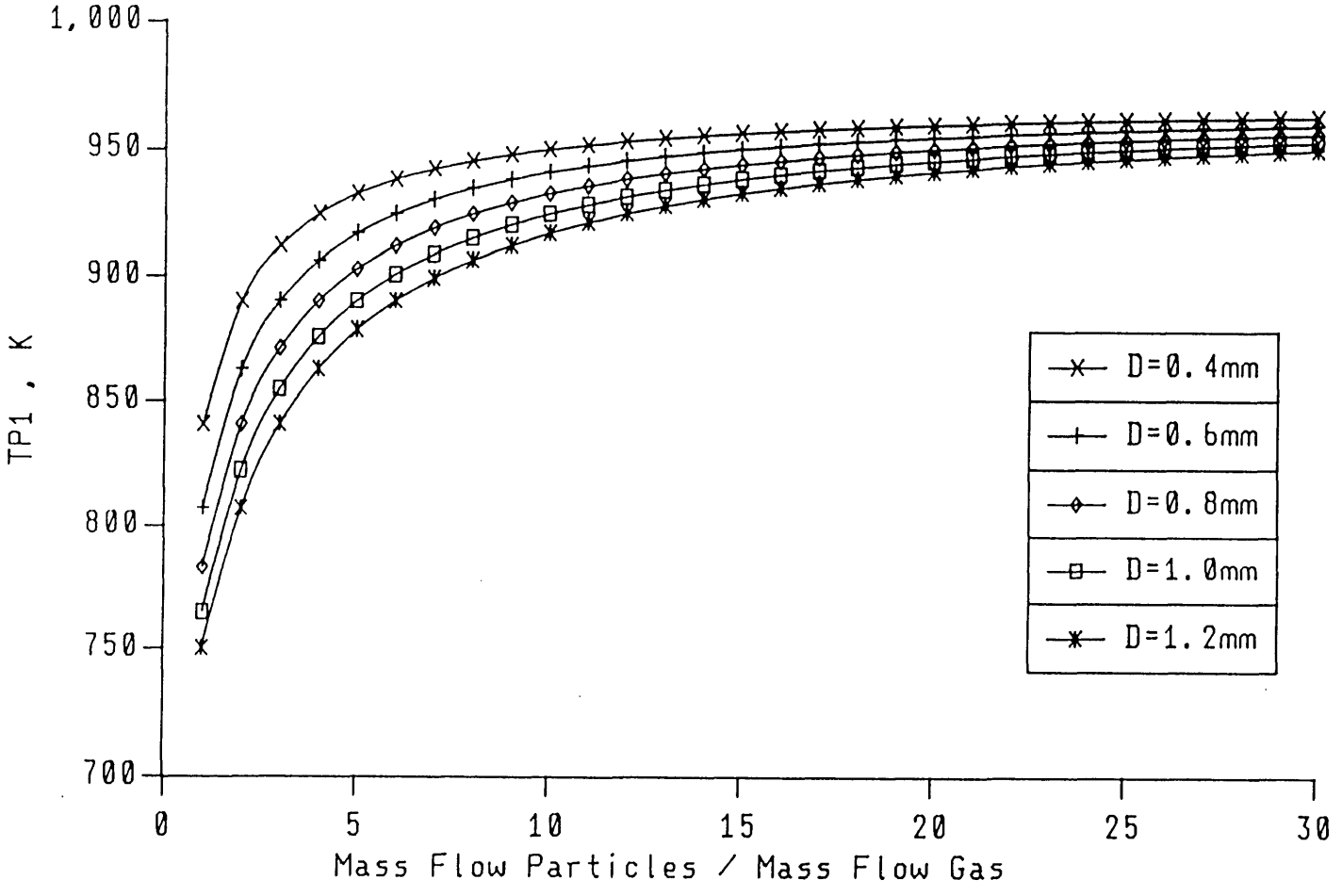

Figure 34

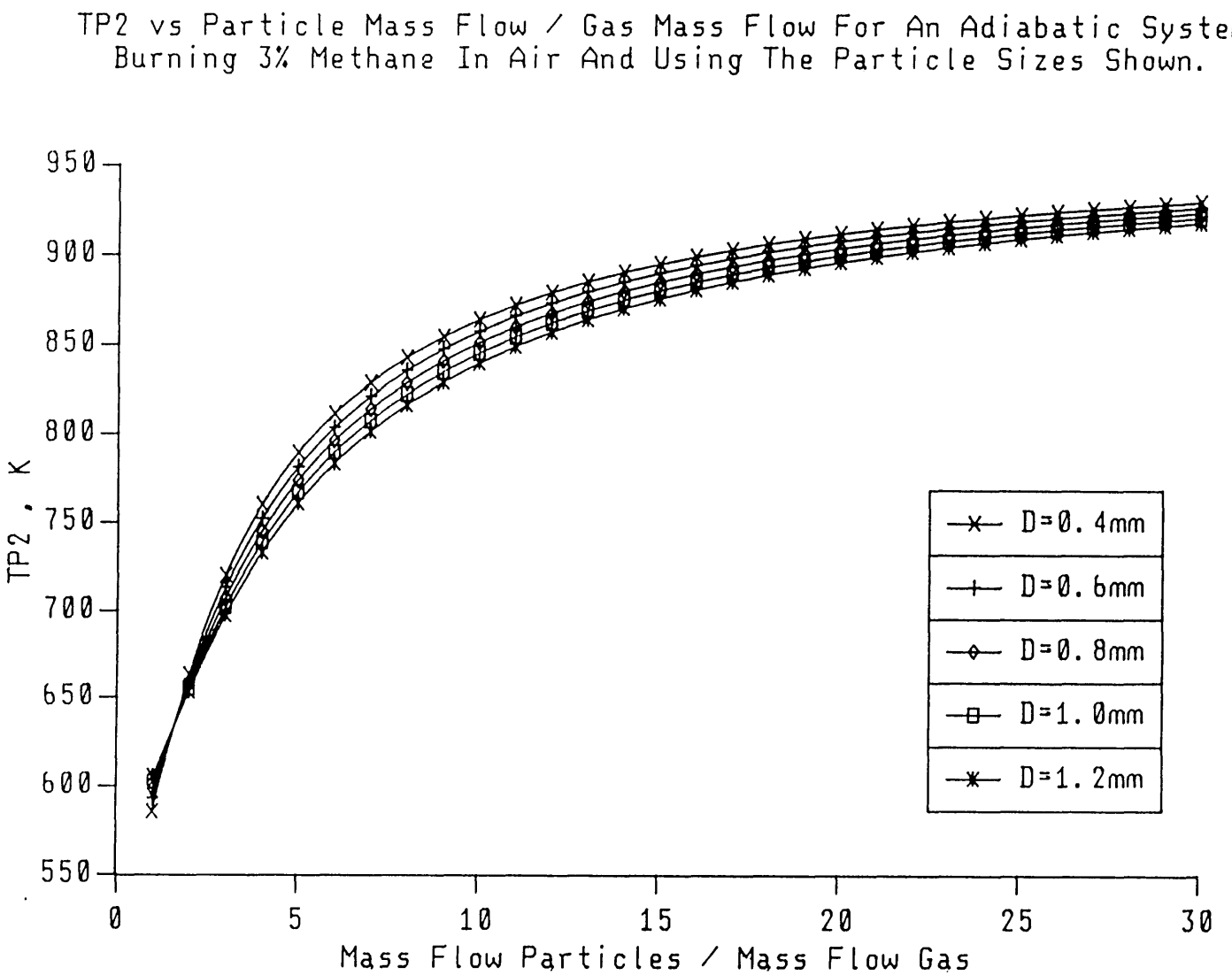
TP2 vs Particle Mass Flow / Gas Mass Flow For An Adiabatic System
Burning 3% Methane In Air And Using The Particle Sizes Shown.
950
900
850
800
750
700
650
600
550
TP2, K
0
5
10
15
20
25
30
Mass Flow Particles / Mass Flow Gas
D=0.4mm
D=0.6mm
D=0.8mm
D=1.0mm
D=1.2mm

Figure 35

TU vs Particle Mass Flow / Gas Mass Flow For An Adiabatic System
Burning 3% Methane In Air And Using The Particle Sizes Shown.

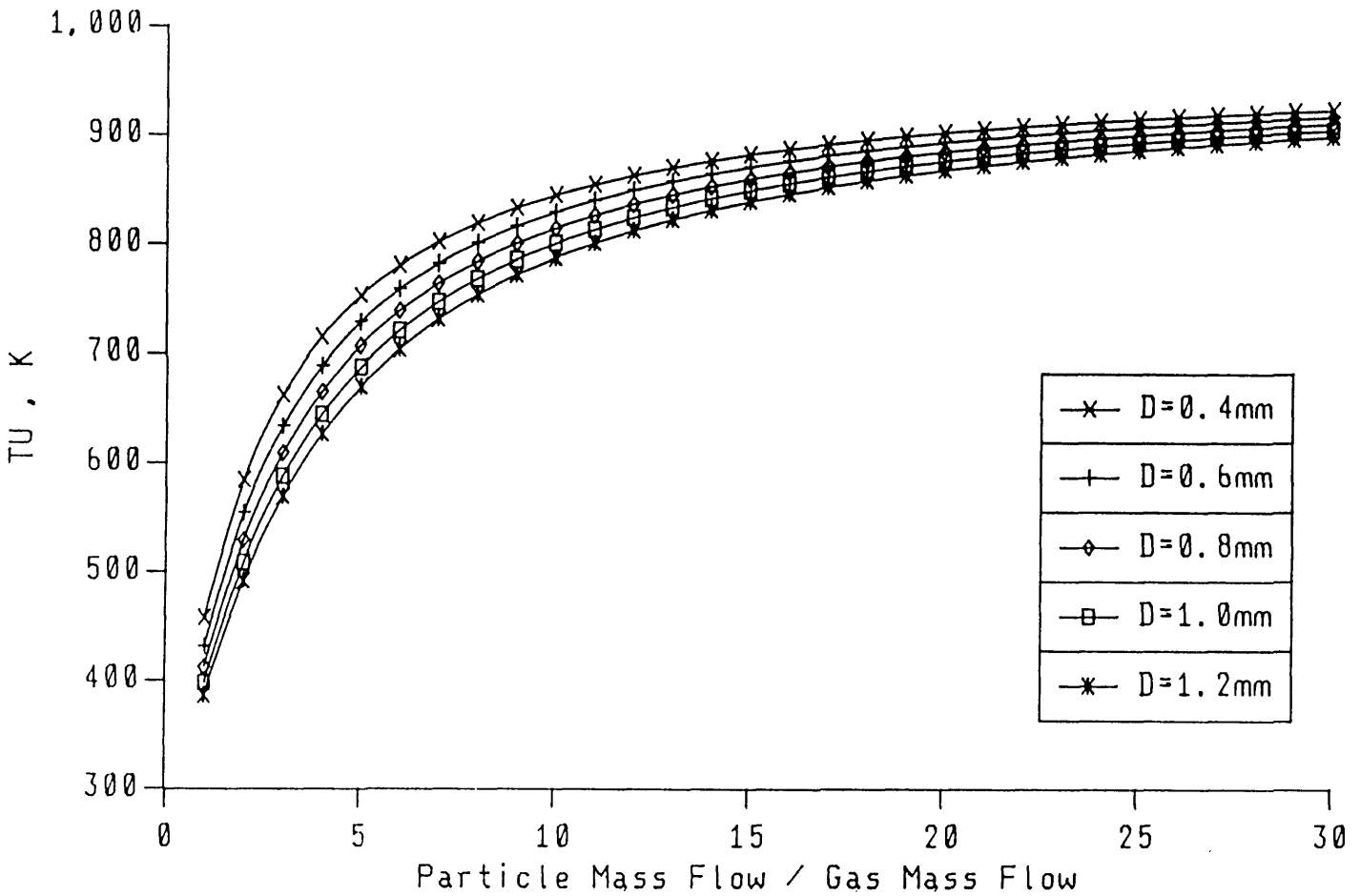

Figure 36

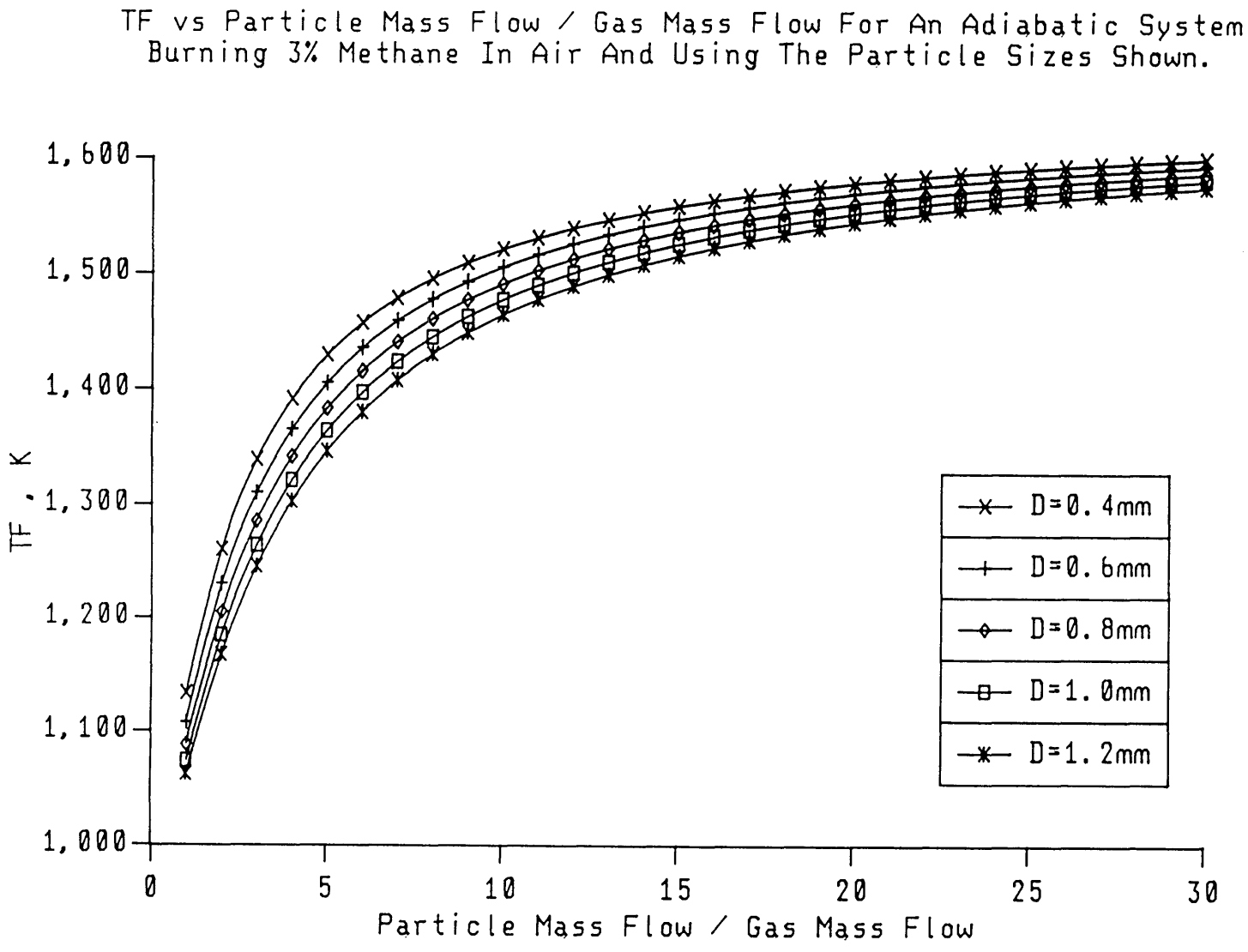
TF vs Particle Mass Flow / Gas Mass Flow For An Adiabatic System
Burning 3% Methane In Air And Using The Particle Sizes Shown.
TF , K
1,600
1,500
1,400
1,300
1,200
1,100
1,000
0
5
10
15
20
25
30
Particle Mass Flow / Gas Mass Flow
D=0.4mm
D=0.6mm
D=0.8mm
D=1.0mm
D=1.2mm

Figure 37

As the mass flow of particles tends to zero, the system reverts to the normal case without heat recirculation, as shown in the next sketch graph.

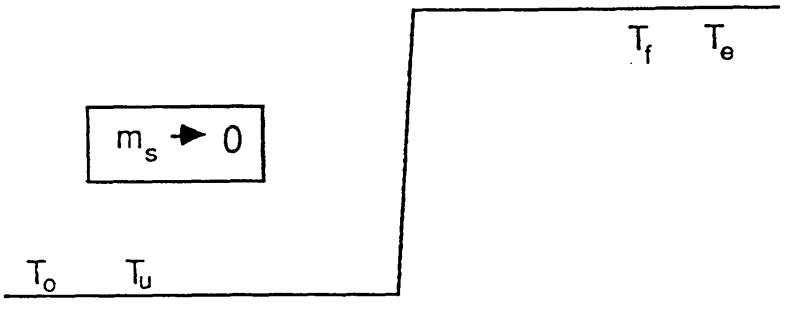

Figure 39

However, as shown by the graphs, when the mass flow tends to infinity the system attains thermal equilibrium and the temperature profile approaches that shown in the sketch below.

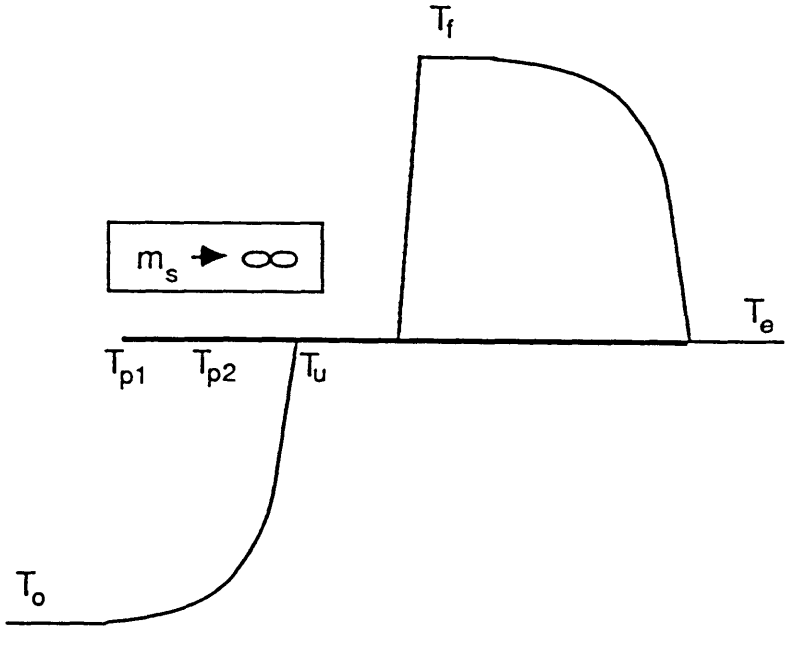

Figure 40

This is the case of perfect heat transfer when $Tp_1 = Tp_2 = Tu = Te$ and the factor $y = 2$, its maximum value. In reality, of course, this can never occur.

Jebrail (1987) reports that, with an air flow rate of 700 cc/s and a particle size of 0·85-1·00 mm, a non-combusting, isothermal, 4 cm diameter spouted bed has a maximum solids circulation rate of 12·5 g/s. This corresponds to a particle to gas mass flow ratio of approximately fifteen. From figures 34-37 this suggests that the predicted temperatures in such a spouted bed should be as below.

Bed temperature,	Tp_1	= 938 K
Fountain temperature,	Tp_2	= 880 K
Flame temperature,	Tf	= 1525 K
Preheat temperature,	Tu	= 849 K

During experiments described in the last chapter (4), bed temperatures were measured near the lean stability limit for methane combustion in the spouted bed. With a mixture of 3·27% methane in air, the measured bed temperature was 976 K. This is quite close to the predicted bed temperature for 3% methane of 938 K. The difference can probably be accounted for by the simplicity of the model, the inaccuracy of the particle mass flow rate measurments and the difference between the experimental and theoretical mixture strengths.

5.3 Lean Limit Prediction Model

This model set out to predict the lean stabilty limits for the combustion of methane in air, initially at 293 K and atmospheric pressure, in a spouted bed. The model tested the effect of varying the particle size from 0·4 to 1·2 mm and the particle to gas mass flow ratio from 0 to 30.

5.3.1 Assumptions

This model was derived from the previous one and so all the former assumptions apply here. However, an additional assumption of a constant final flame temperature at the lean stability limit was also incorporated into the model. As discussed previously (chapter 3) this concept is based upon experimental observations. It appears that for certain heat recirculating burner systems and fuels, where the combustion chamber is large enough not to quench and the flow velocity small enough not to affect the propagating mechanism, the lean stability limit behaves in a similar manner to the lean flammability limit in stationary gases - the spouted bed is an example of this. That is, the variation of the lean limit with initial temperature can be represented in terms of an approximately constant final flame temperature. This has been well documented for many years - Smith (1955), Zabetakis *et al.* (1959) and Gaydon and Wolfhard (1984). Lloyd and Weinberg (1975) found this constant final flame temperature to be 1403 K ± 39 K for ultra lean methane combustion in a spiral "Swiss-roll" burner. Hence this model sets the flame temperature to 1403 K for the purpose of predicting the lean stabilty limit for methane.

5.3.2 Theory

The theory for the present model is very similar to that of the previous one. The major difference, as described in the assumptions section, is that the flame temperature is assumed constant at 1403 K. The appropriate mixture strength can then be back calculated at the various particle sizes and mass flow ratios. The equations for this model are as summarised below.

$$Tf = 1403\ K$$

$$Np = \frac{6.m_s.\rho_g}{d_p^3.\rho_s.\pi.m_g}$$

$$y = 1 + \left[\frac{\left[\frac{[m_s.c_s/(m_g.c_g)]}{1 + [m_s.c_s/(m_g.c_g)]} \right] . Np.d_p^2}{1 + Np.d_p^2} \right]$$

$$Hr = (Tf - T_\infty)/y$$

$$x = \frac{Hr.c_g.\rho_{air}/\rho_{CH4}}{Hr.c_g.[(\rho_{air}/\rho_{CH4}) - 1] + q_c}$$

$$\phi = x.10{\cdot}52$$

Where : x = methane mole fraction
ϕ = methane equivalence ratio

5.3.3 Results And Discussion

The equations were again coded into fortran and programmed into a computer - the program listing is shown in appendix A, together with all the data which was extracted from JANAF tables (1971). The particle to gas mass flow ratio was varied from 0 to 30 and the particle size from 0·4 to 1·2 mm. The results were again sent by the computer to a graphics package which plotted the variation of the lean limit with the above parameters. The output graph is shown in figure 41. As the mass flow ratio approaches zero the system reverts to a normal flame and the lean stability limit becomes the normal lean flammability limit for methane - 5·3%, or an equivalence ratio of 0·558. As the particle to gas mass flow ratio tends to infinity, so the lean limit approaches an equivalence ratio of about 0·27. This agrees well with the work of Khoshnoodi and Weinberg (1978) who predicted that the leanest burnable mixture for a spouted bed with high recirculation and negligible heat losses was about half the

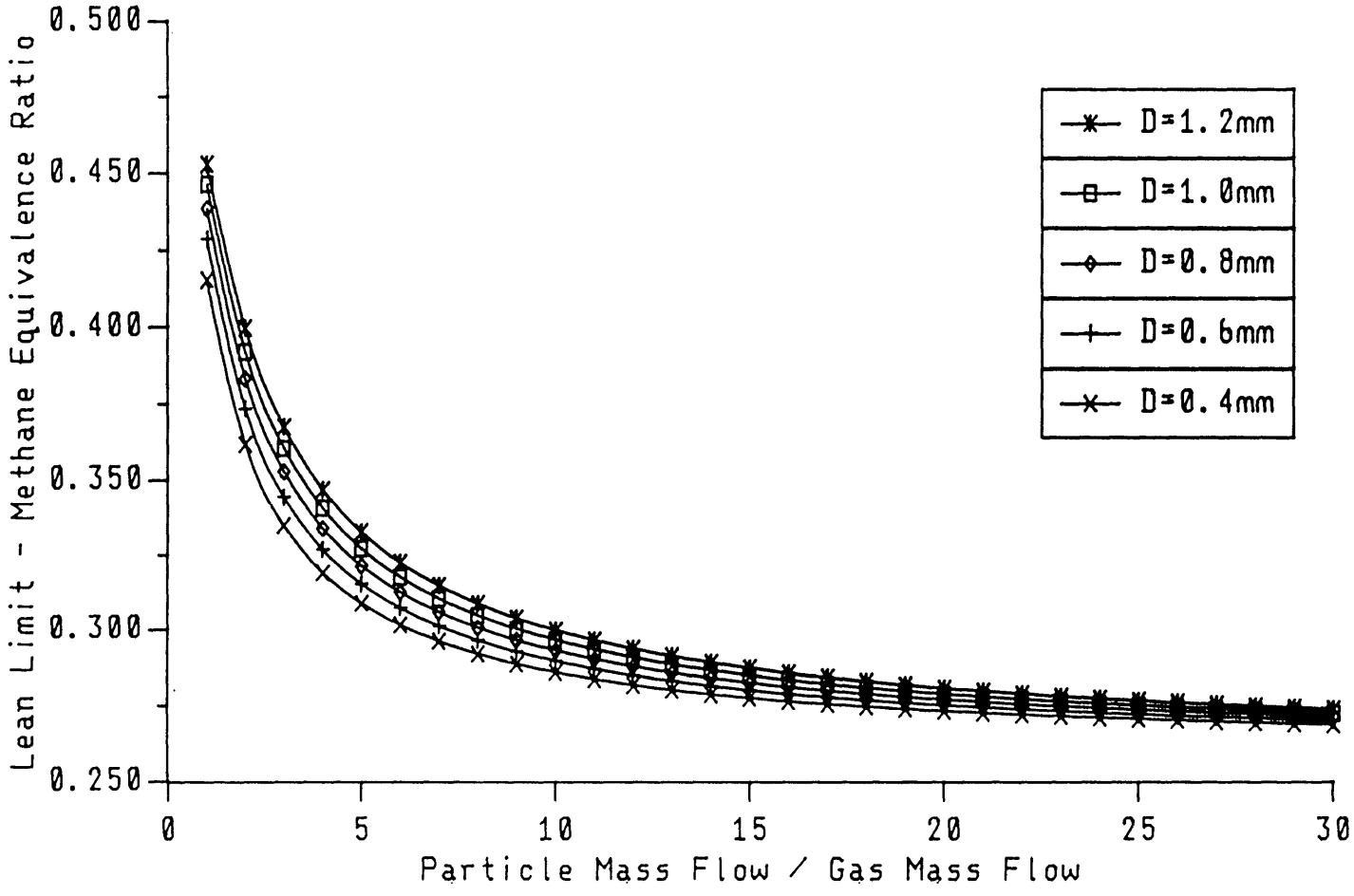
Lean Limit vs Particle Mass Flow / Gas Mass Flow For An Adiabatic System Burning Methane In Air And Assuming TF = 1403 K.
Lean Limit - Methane Equivalence Ratio
0.500
0.450
0.400
0.350
0.300
0.250
0
5
10
15
20
25
30
Particle Mass Flow / Gas Mass Flow
D=1.2mm
D=1.0mm
D=0.8mm
D=0.6mm
D=0.4mm

Figure 41

normal limit of flammability. However, their system was dependent upon the existence of thermal equilibrium between the particles and gas - the present model can also predict the lean limit away from thermal equilibrium. Assuming that the spouted bed has a particle to gas mass flow ratio of about fifteen (Jebrail, 1987), this model predicts that, with 1·0 mm sized particles, the lean stability limit for methane combustion in air has an equivalence ratio of 0·28. The results from chapter 4 for methane combustion in a lagged 4 cm diameter spouted bed showed the leanest burnable methane-air mixture to have an equivalence ratio of 0·292. Again the agreement of the model is quite good. Two factors could account for the slight difference, firstly that the experimental spouted bed is bound to suffer some heat loss - no matter how good the lagging is. Secondly that the assumed mass flow ratio may not actually be fifteen - a value of thirteen fits the data very well. This is quite possible as the method used by Jebrail, particle velocity measurements at the spouted bed wall, depended upon timing a single particle over a short distance by eye and was, therefore, only very approximate.

The model does suggest that the spouted bed operates very close to thermal equilibrium which seems unlikely in practice because of the very high velocities and short residence times of particles and gas in the spout. This apparent proximity to thermal equilibrium could be explained by the fact that all the gas does not flow up through the spout and that combustion does occur outside the spout. Mathur and Gishler (1955) showed that up to 30% of the gas flowing up the spout leaks into the annulus. This gas slowly percolates up through the descending phase and burns as a flat flame, on top of the annulus, surrounding the conical flame from the spout. This annular flat flame has been shown to be more stable than the spout flame (Arbib *et al.*, 1981) and thus has a higher preheat temperature. This is expected as the gas filtering up through the annulus not only has a lower flow velocity and a higher residence time but also contacts the particles countercurrently. Hence in the annulus particles and gas

approach thermal equilibrium. Heat transfer is further enhanced by the rotating vortex of particles in the fountain which probably acts to a small extent as a countercurrent heat exchanger. Thus although gas and particles in the spout are far from thermal equilibrium, the net effect of gas leaking into the annulus and rotating vortices in the fountain is to bring the system closer to thermal equilibrium.

In conclusion, then, although the approximations of the model seem somewhat naive, it is capable of predicting the lean limit for methane combustion in the spouted bed quite accurately.

5.4 Rich Limit Correlation Model

An attempt was made to correlate the rich stability limit for the combustion of methane in air, initially at 293 K and atmospheric pressure, in a spouted bed. The effect of varying the particle size from 0·4 to 1·2 mm and particle to gas mass flow ratio from 0 to 30 was theoretically tested by the model.

5.4.1 Assumptions

The approximations adopted for this model were the same as those used in the first model, except that the heat capacities of the reacants and products were no longer assumed to be equal - as this cannot be justified for rich combustion. Using the product analyses from the electrically heated burner (chapter 3), mean heat capacities for the products at 1600 K and reactants at 298 K were calculated for initial methane-air mixtures ranging from 14% to 21% methane. The variation in heat capacity was small for the reactants and not excessive for the products (5% and 10% respectively). Accordingly mean heat capacities were taken from an initial mixture of 20% methane in air for use in the model - as 20% methane was close to the expected rich limit for methane combustion in the spouted bed. This gave values of 1210 J/kg/K for the

reactants at 298 K and 1631 J/kg/K for the product gases at 1600 K.

The results from the electrically heated burner also showed that, for ultra rich combustion, the flame temperature is approximately constant, with a value of 1600 K for methane in air - see figure 24. On the basis of this a constant final flame temperature of 1600 K was also incorporated into the model.

5.4.2 Theory

Apart from the approximations described above the theory for this correlation model does not greatly differ from that for the lean limit prediction model. However, the relationship between mixture strength and flame temperature was empirically derived from the results of chapter 3. Again using the product analyses from the electrically heated burner, for initial mixtures of methane in air varying from 14% to 21% at two air flow rates, values of the temperature rise due to combustion, Hr, were calculated. In order to do this, mass balances were performed and the respective heats of combustion computed from the heats of formation of the products and reactants. Hr was then calculated from the equation.

$$Hr = q_c . X_{CH4} . \rho_{CH4} / (C_{g2} . \rho_{mix,in})$$

Hr was then plotted against the methane mole fraction and a straight line fitted to the points by linear regression - see figure 42. This gave an empirical correlation for the methane mole fraction in terms of the temperature rise due to combustion, Hr, as shown below.

$$X_{CH4} = 0{\cdot}328 - 1{\cdot}4 . 10^{-4} . (Hr)$$

When combined with the other equations below, this gave the rich limit. These equations were derived in a similar way to those for the lean limit but also included the additional assumptions necessary for rich combustion.

METHANE MOLE FRACTION VS TEMPERATURE RISE DUE TO COMBUSTION
AS DETERMINED FROM THE ELECTRICALLY HEATED BED.

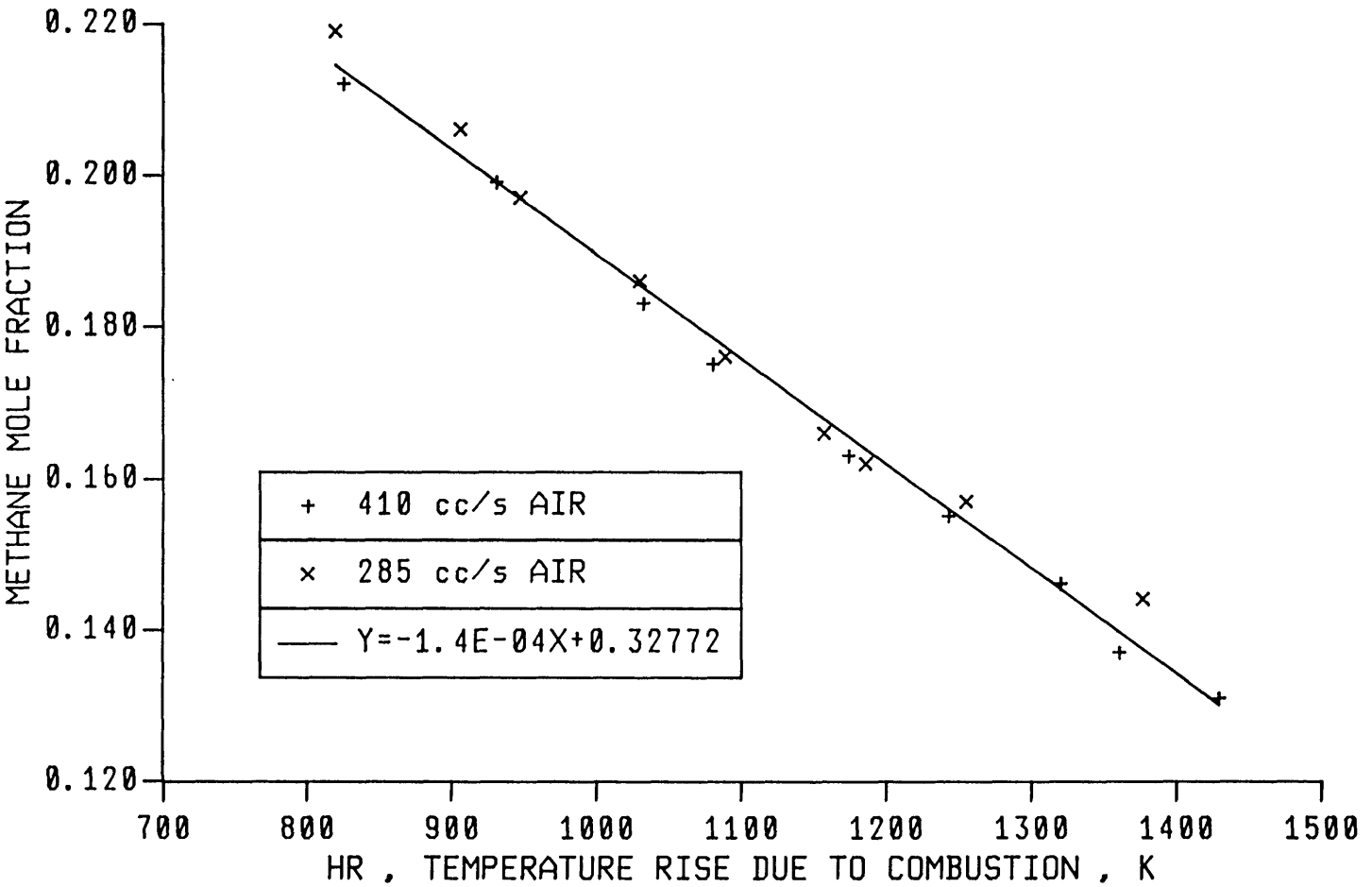

Figure 42

$$Tf = 1600\ K$$

$$Np = \frac{6.m_s.\rho_g}{d_p^3.\rho_s.\pi.m_g}$$

$$y = 1 + \left[\frac{\left[\frac{c_{g1}/c_{g2}}{1 + [m_g.c_{g1}/(m_s.c_s)]} \right] . Np.d_p^2}{1 + Np.d_p^2} \right]$$

$$Hr = [(Tf - T_\infty)/y] - [(c_{g1}/c_{g2}) - 1].T_\infty$$

Where : c_{g1} = specific heat capacity of reactants, J/kg/K
c_{g2} = specific heat capacity of products, J/kg/K

5.4.3 Results And Discussion

As with the previous models, the equations were coded into fortran and programmed into a computer - the program listing is given in appendix A. The particle to gas mass flow ratio was varied from 0 to 30 and the particle size from 0·4 to 1·2 mm. All data used was obtained from JANAF tables (1971) and is shown in the program listing. The output was again sent to a graphics package which plotted the variation of the rich limit with the above parameters. The output graph is shown in figure 43. As the mass flow ratio tends to zero so the system behaves like a normal flame without heat recirculation and the rich limit approaches the normal rich flammability limit for methane - 15% or an equivalence ratio of 1·578. As the mass flow ratio tends to infinity so the rich limit approaches an equivalence ratio of about 2·2. Again assuming a particle to gas mass flow ratio of fifteen for the spouted bed (Jebrail, 1987), the model predicts a rich limit of

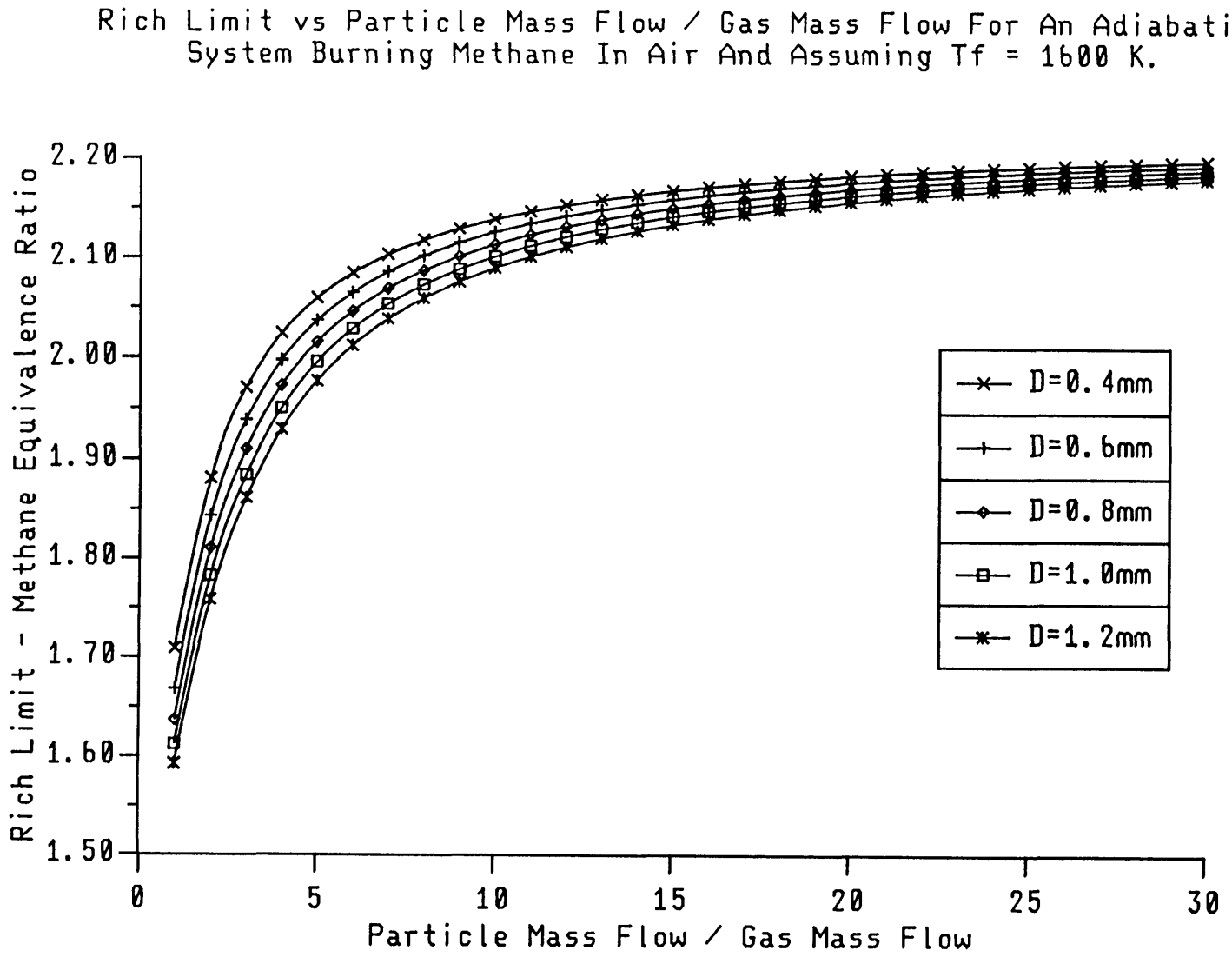
Rich Limit vs Particle Mass Flow / Gas Mass Flow For An Adiabatic System Burning Methane In Air And Assuming Tf = 1600 K.
Rich Limit - Methane Equivalence Ratio
2.20
2.10
2.00
1.90
1.80
1.70
1.60
1.50
0
5
10
15
20
25
30
Particle Mass Flow / Gas Mass Flow
D=0.4mm
D=0.6mm
D=0.8mm
D=1.0mm
D=1.2mm

Figure 43

equivalence ratio 2·1 with 1·0 mm sized particles. The results of the previous chapter (4) for methane combustion in a 4 cm diameter spouted bed showed that the richest burnable methane-air mixture, experimentally, had an equivalence ratio of 2·083. As with the lean model, the agreement is again, very good. Also, similar to the lean model, the system is closer to thermal equilibrium than real particle residence times would allow. However the same arguments, relating to gas percolation in the annulus and rotating particle vortices in the fountain, apply here as before.

In conclusion, a simple model predicts the rich stability limits for the combustion of methane in a spouted bed quite accurately. This, also, further supports the evidence for a constant final flame temperature at the rich limit.

CHAPTER 6

COAL COMBUSTION AND PARTIAL OXIDATION IN THE SPOUTED BED

6.1 Aims

The spouted bed has been shown to be of immense value in the field of gaseous combustion. It also possesses many features which well suit it for the combustion of solid fuels, especially coal. The recirculating particulate bed should allow coal particles a long residence time in a high temperature environment before being elutriated. In addition, this constant particle motion should break up any agglomerates and so reduce clinkering effects. Thus one aim of the work described in this chapter was to investigate the spouted bed's potential as a coal combustor.

As has been discussed earlier the spouted bed is very efficient at recirculating heat and can burn ultra rich mixtures of methane in air to produce significant yields of hydrogen and carbon monoxide. Thus another aim of the work in this chapter was to use the spouted bed's heat recirculating properties together with its ability to handle coal. The concept was to partially oxidise methane in the spouted bed, yielding hydrogen, and then to add coal for simultaneous gasification in this hydrogen atmosphere.

However before the main aims of this chapter, as described above, could be implemented, a method of introducing the coal into the spouted bed had to be developed. Accordingly, the first aim in this chapter was to design and construct a solids injection system for the spouted bed.

6.2 Experimental Apparatus

6.2.1 Gas Feeding System

The gas feeding equipment was identical to that used with the "Swiss-roll" burner. It consisted of a number of rotameters and mercury manometers measuring a supply of methane and air, at 2 bar (abs.) pressure, via a mixing vessel to the spouted bed. A schematic diagram of the system is shown in figure 44 together with the coal feeding system, which is described below. The spouted bed vessel and particles were also identical to those used in chapter 4; ie. a spouted bed of diameter 4 cm, an inlet nozzle of diameter 3 mm and alumina particles of size 0·85-1·00 mm.

6.2.2 Coal Feeding System

In designing a solids injection system, the first decision was whether to feed coal entrained in air to the base of the spouted bed or to feed it directly from the top of the burner (or in through the side) - due to the small scale of the burner the coal had to be in a pulverised form. Feeding from above the bed has the advantage that the coal is entrained into the annular descending phase allowing it a longer residence time and thus more preheat. However the coal can overheat at the feed point causing it to swell and become sticky - resulting in the blockage of the feeder tube. Bottom feeding has the advantage of the coal being entrained in cool air which stops it from swelling and prevents obstruction of the feed line. However, the coal is fed into a high velocity gas stream giving smaller coal particles a very short residence time - larger ones are recirculated with the inert spouted bed particulate material. Given that the bed temperature is of the order of 1000°C, it was estimated that the heating rates in the spout would be high enough to allow the devolatilisation and pyrolysis of even relatively small coal particles. Thus it was decided to opt for bottom feeding of the coal. This decision was confirmed by the

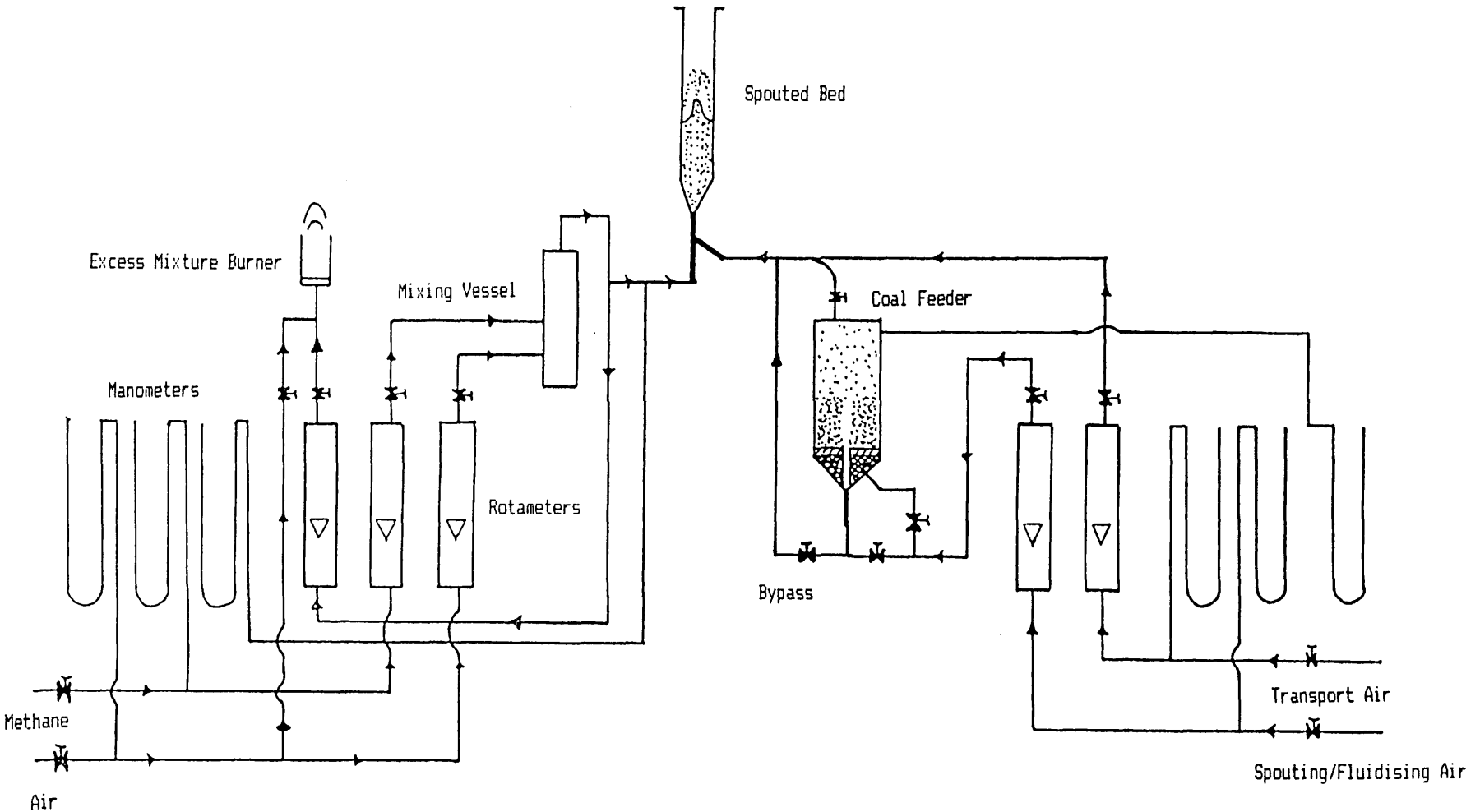

Figure 44 - Gaseous And Coal Feeding Systems

reportings of Foong *et al.* (1981), Zhao *et al.* (1987a) and Jarallah and Watkinson (1985) who all used bottom feeding to introduce coal into spouted beds. Foong *et al.* (1981) actually tried feeding coal to both the top and bottom of the bed and reported that bottom feeding, apart from giving better mixing, was easier to control - allowing higher feedrates which gave increased gas yields. A special nozzle has been designed to feed the pneumatically conveyed coal into the spouted bed together with the methane-air mixture from the gas feeding system. The nozzle is very similar to that shown in figure 28, being also made of quartz and having a tip diameter of 3 mm. However, it has two tubes feeding the nozzle - one for the coal and one for the methane-air mixture.

With regard to particle size, three cuts of pulverised coal were selected,

(a) - 152 + 104 μm

(b) - 425 + 250 μm

(c) - 600 + 425 μm

Relative to the inert spouted bed alumina particles (- 1000 + 800 μm) this gave proportions of approximately 0·1, 0·3 and 0·5 times the size. It was considered that below 100 μm the coal would be too small to feed and above 600 μm too large to feed - the spouted bed inlet nozzle being only 3 mm in diameter. As for coal type, a fairly standard British coal, Grimethorpe coal from Yorkshire, was chosen. This has a free swelling index of four and its analysis is as given below.

Moisture	1·0 wt%
Volatile Matter	38·3 wt%
Ash	4·3 wt%
Fixed Carbon	56·4 wt%
Sulphur	1·3 wt%
Total Carbon	71·2 wt%
Hydrogen	4·8 wt%
Nitrogen	1·5 wt%
Oxygen	8·5 wt%

6.2.3 The Coal Feeder

Having opted for a system pneumatically feeding pulverised coal to the bottom of the spouted bed, the next task was to design a coal feeder. It was calculated that the feeder would be required to supply coal for up to an hour at feedrates ranging from 20 g/h to 200 g/h. A study of the literature (eg. Wiberley and Phong-Anant, 1986) revealed that for steady feeding at both high and low feedrates a fluidised feeder was required. After many design modifications a feeder was finally constructed consisting of a spouted-fluidised bed of coal with an offtake from the lean phase above the bed. A schematic diagram is shown in figure 45. The hopper was made from interlocking perspex sections, 75 mm in diameter, and supported on an aluminium base. Fluidising air entering through the side wall of the cone was distributed by ballotini and a sintered bronze disc sealed in place across the vessel with silicon rubber. A small hole was drilled in the centre of the sintered disc and fitted with a perspex nozzle of 1mm orifice diameter; this connected with a tube from the apex of the cone supplying the spouting air. A glass 'quickfit' catch bottle beneath the spouting orifice was also attached by means of a 'T' piece, to collect any coal falling through when the spouting air was not flowing. A pressure tap installed in the hopper wall adjacent to the freeboard region monitored the pressure in the feeder. The device could be recharged when empty by means of a small brass funnel (provided with a valve) fixed into the lid of hopper.

By varying the flow rates of spouting and fluidising air, the coal suspension in the freeboard could be made more or less concentrated which in turn altered the coal feedrate. The exit stream from the feeder was diluted by a further air stream in order to transport the coal pneumatically to the spouted bed. A bypass was also included so that the spouting and fluidising air flows could be adjusted in preparation for feeding the coal without actually causing coal to exit from the feeder until

Figure 45 - Coal Feeder

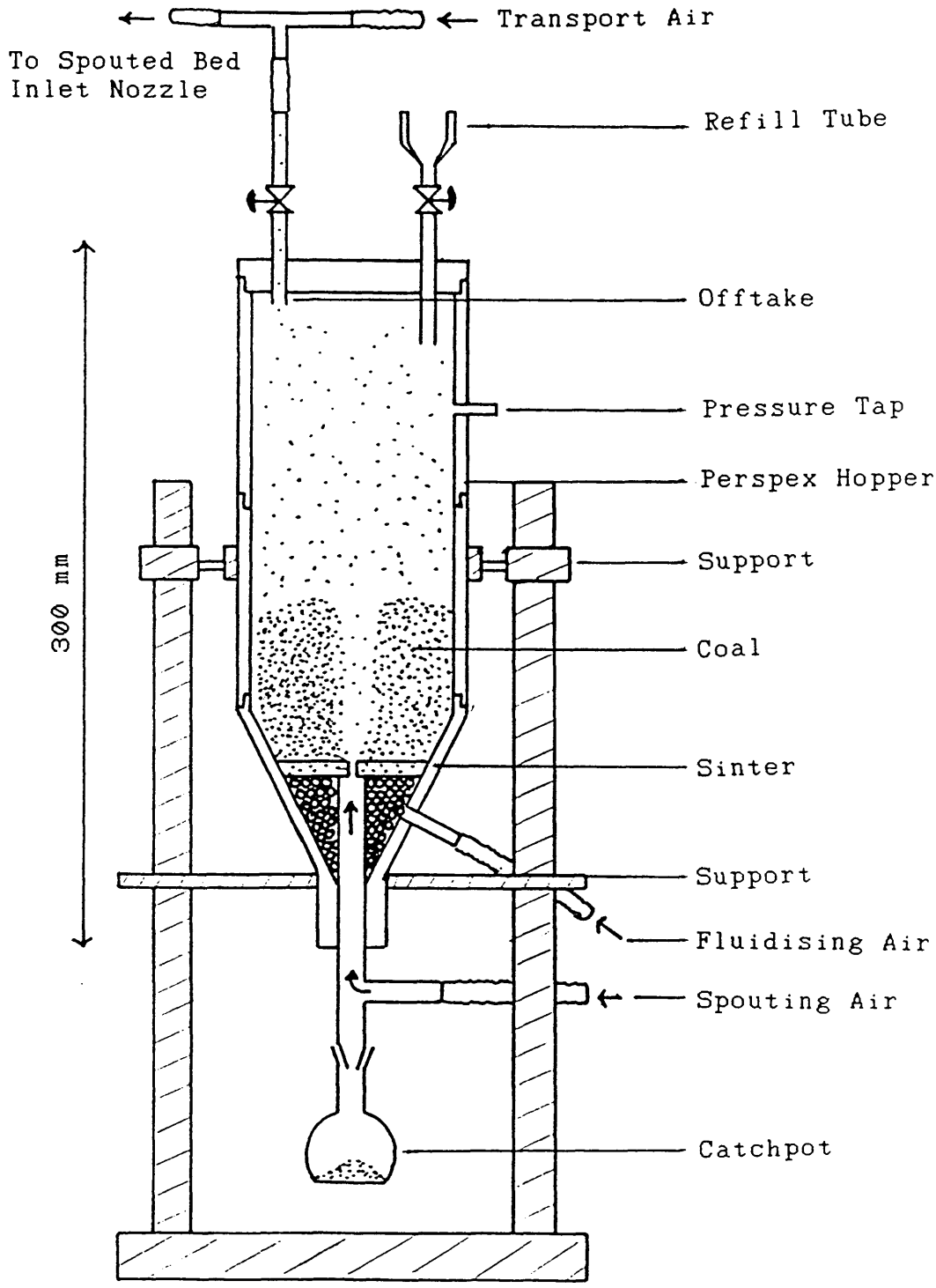

it was required. The spouting/fluidising and transport air flows were measured with the aid of two rotameters and mercury manometers at two bar (abs.) pressure. A schematic diagram of the whole coal feeding system together with the gas feeding system is shown in figure 44. To quantify the coal feedrate, the feeder was installed upon an electronic balance (Sartorius U4600P+) which was connected to a BBC microcomputer via an RS232 interface for the purpose of datalogging - this allowed the coal feedrate to be continuously monitored. To minimise vibrational effects upon the balance, all tubes supplying coal and air to and from the feeder were made of rubber. Three graphs of coal fed vs. time for various spouting air flow rates and the three coal size cuts are shown in figures 46, 47 and 48. As can be seen, the coal feedrate is quite steady at both high and low coal outputs.

6.2.4 Analytical Equipment

Gaseous products were analysed by gas chromatography, as described in chapter 2. Solid products were analysed by proximate analysis for volatile matter, moisture, ash and fixed carbon. All gas chromatography was carried out in the laboratory by the author whereas the proximate analyses were performed by technicians in the departmental analytical laboratory.

6.2.5 Sampling System

Gas samples were taken by means of a quartz sampling probe as described in chapter 3. A schematic diagram of the sampling system is shown in figure 18 - note however that instead of aspirating from a 'T' piece, as for the "Swiss-roll" burner, the system was connected to a quartz sampling probe. The design of the sampling probe is discussed in chapter 3 as it was identical to the one used there. This simple probe was found to operate quite satisfactorily in conjunction with the coal.

Solid combustion products were collected for analysis

GRAPH OF COAL FED VS TIME FOR THE FEEDER WITH 58.5 cc/s TRANSPORT AIR AND THE FLOWRATES SHOWN OF SPOUTING AIR.

COAL PARTICLE SIZE = 104 - 152 MICRONS

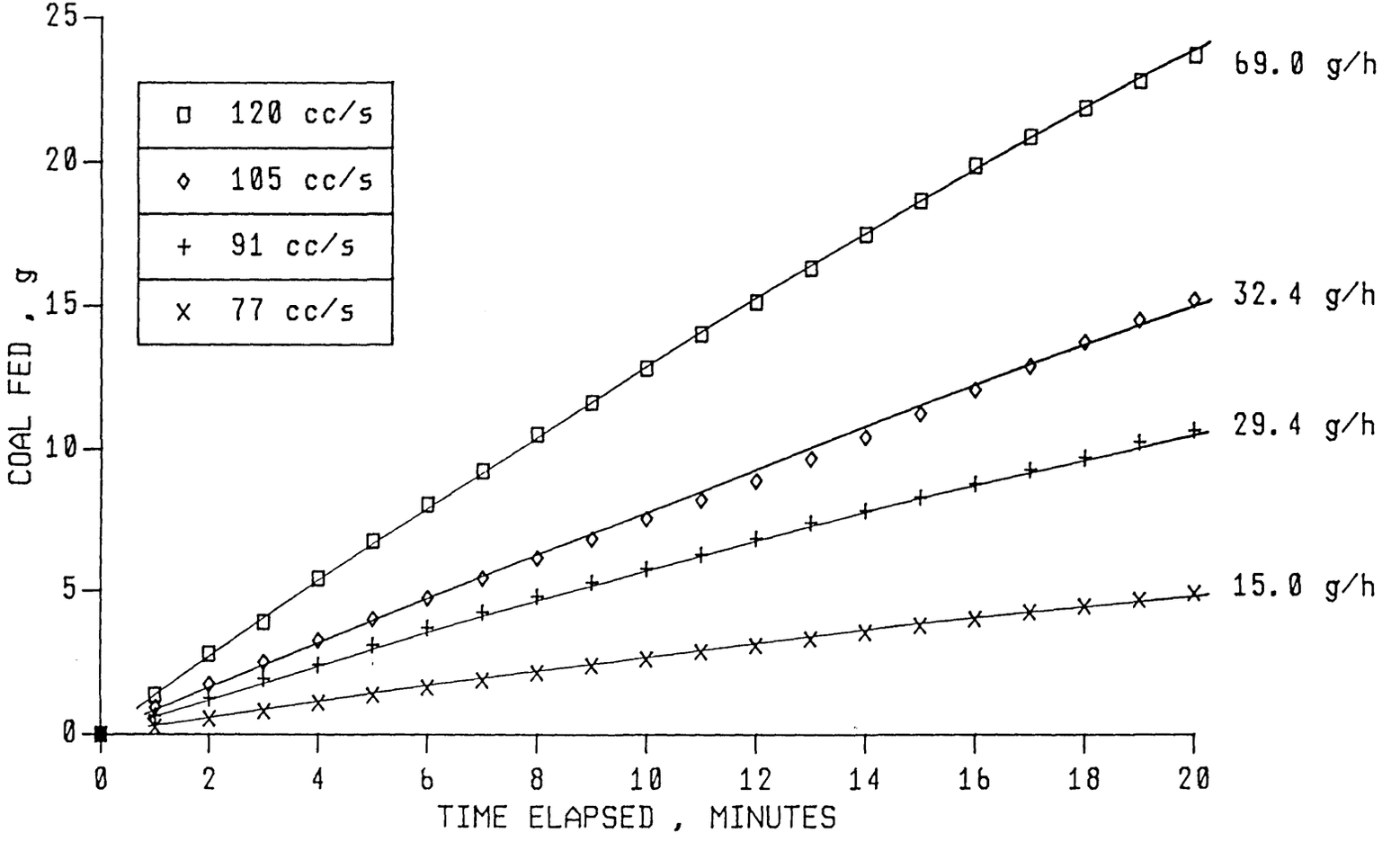

Figure 46

GRAPH OF COAL FED VS TIME FOR THE FEEDER WITH 58.5 cc/s TRANSPORT AIR AND THE FLOWRATES SHOWN OF SPOUTING AIR.

COAL PARTICLE SIZE = 250 - 422 MICRONS

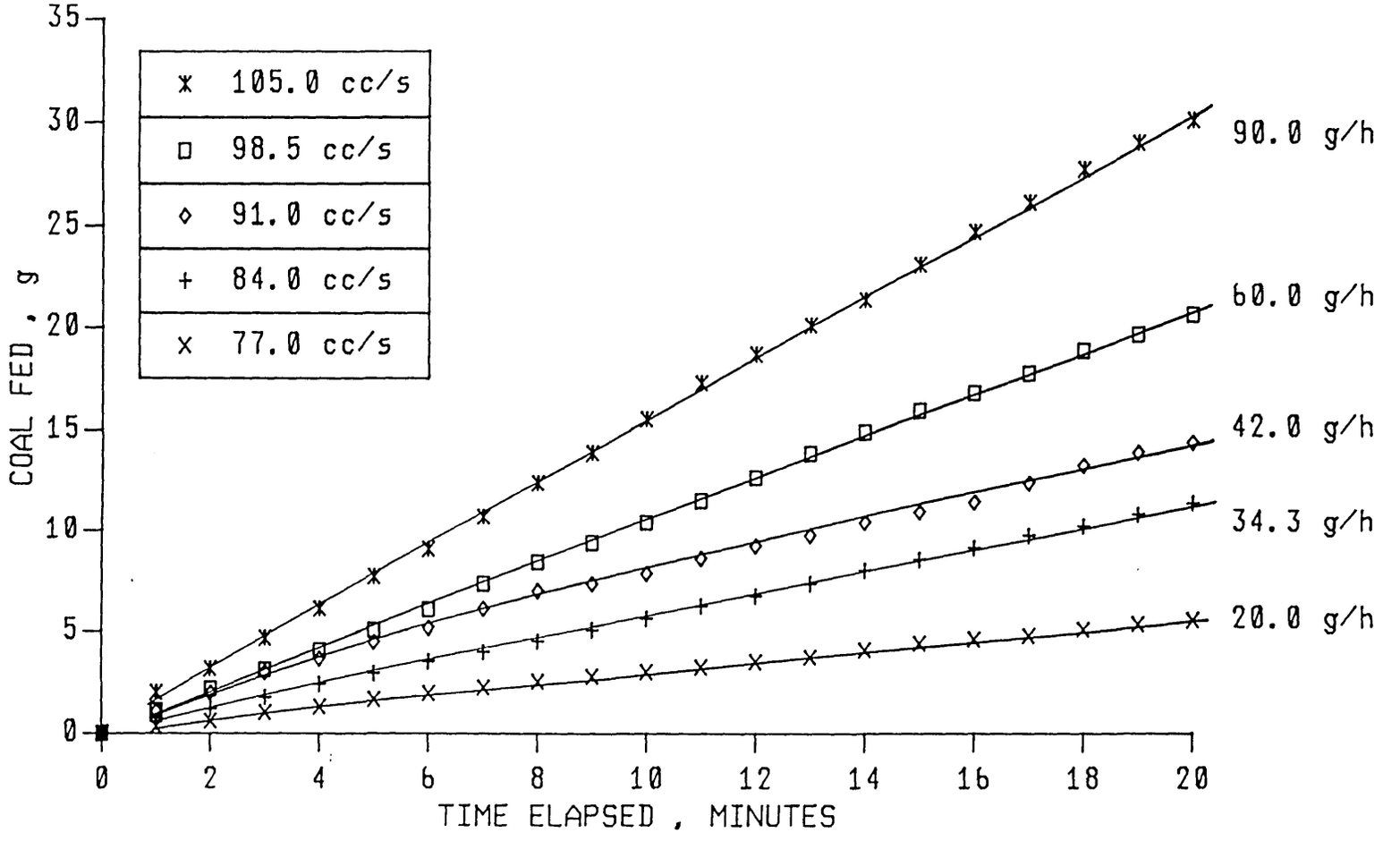

Figure 47

GRAPH OF COAL FED VS TIME FOR THE FEEDER WITH 58.5 cc/s TRANSPORT AIR AND THE FLOWRATES SHOWN OF SPOUTING AIR.

COAL PARTICLE SIZE = 425 - 600 MICRONS

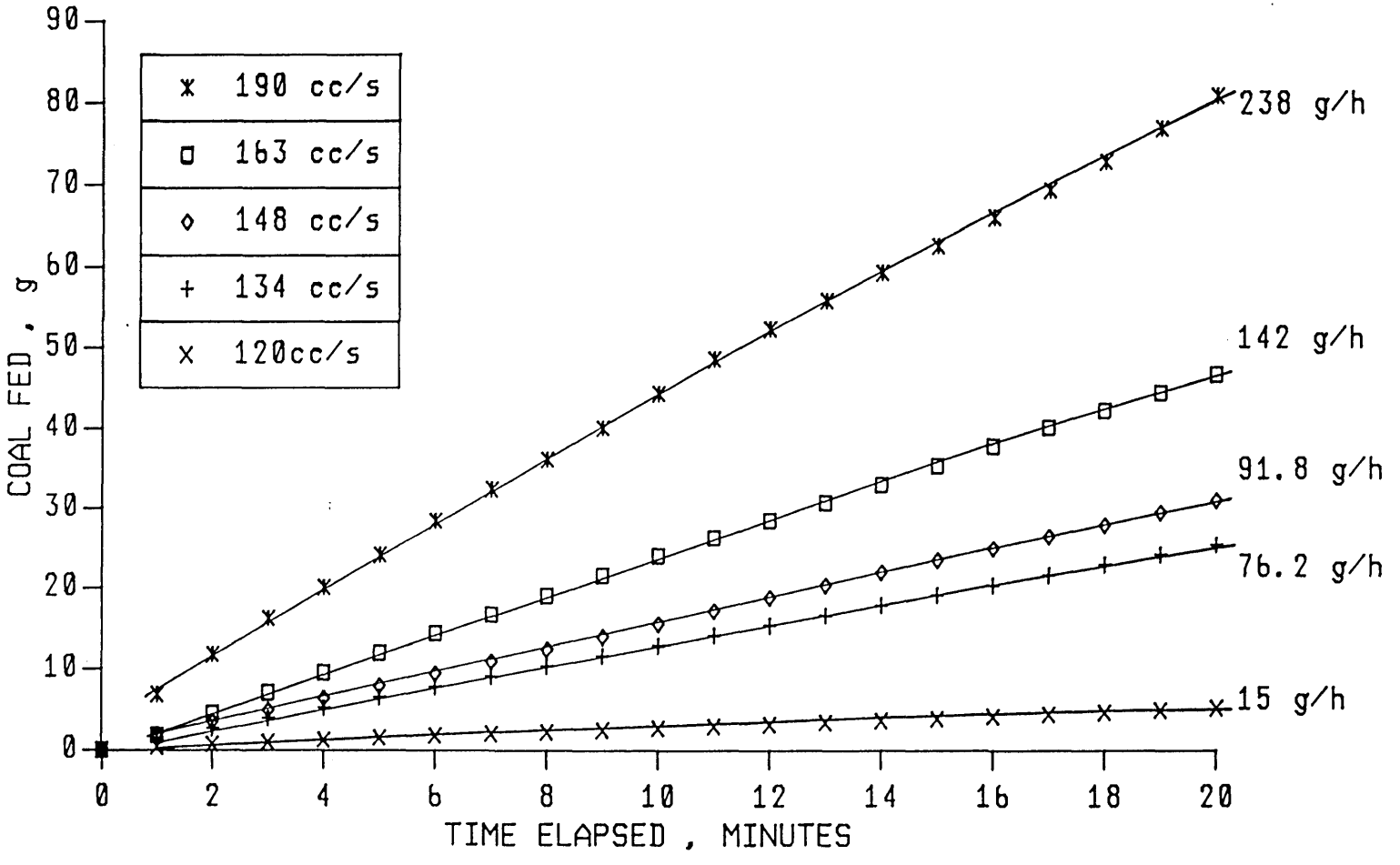

Figure 48

with the aid of a catchpot placed over the spouted bed. This consisted of a 10 cm diameter, flat bottomed, steel cylindrical vessel with a 4 cm diameter hole drilled in its base. When placed above the spouted bed, it acted so as to catch elutriated char particles. On hitting the sides of the container, the char particles were cooled by the cold metal walls. This method, although crude, gave a reasonable estimate of the average char composition for a particular run. Also, any soot or char deposited on the walls of the spouted bed vessel was collected after the run when the burner had cooled down.

6.3 Experimental Procedure

6.3.1 Start Up

First the desired coal feedrate, particle size and total air flow rate were selected. The appropriate spouting air flow could then be determined from the calibration graphs shown in figures 46, 47 and 48. This was adjusted to flow through the bypass line so that it could be diverted into the feeder by simply turning a valve. The spouted bed was ignited as for gaseous combustion with a 7% methane in air mixture and 114g alumina particles - this is fully described in chapter 4. Once the bed had warmed up, the air flow from the gas feeding system was set so as to make up the difference between the total air requirement and that flowing through the coal feeding system. Finally the methane flow was adjusted to give the desired methane equivalence ratio and the spouting air diverted through the coal feeder. A pilot light was also provided at the exit from the spouted bed to ignite any flammable combustion products, thus preventing their escape into the ventilation system.

6.3.2 Operation

Once the spouted bed had been successfully ignited and the coal feed switched on, the computer started to datalog the weight of the hopper every minute. The datalogging program was also set up to calculate the coal feedrate in g/h every minute. The time, total coal fed and current coal feedrate were displayed on the screen in tabular form, scrolling upwards as additional data was collected, and also stored on a floppy disk. Using this information, the spouting air flow rate to the coal feeder could be finely tuned to give the exact coal feedrate required. The feedrate generally remained constant for the duration of a run (up to one hour) and a graph of the coal fed vs. time could be plotted afterwards to determine an average value.

After the coal and methane flows had been set at their required values, the system was left to reach a steady state before the desired measurements were taken. The onset of steady state conditions was detected by a thermocouple, if the bed was insulated, or by changes in pressure drop across the bed, if not.

6.3.3 Shutdown

The first operation performed in shutting down the spouted bed whilst burning coal was to divert the spouting air from the feeder through the bypass line in order to cut off the coal supply to the burner. If the system was burning lean, the methane was shut off next, thus extinguishing the bed. However, if the system was burning rich, the total air flow was gradually reduced to zero to extinguish the flame and the methane flow then cut off.

6.4 Coal Combustion In The Spouted Bed

The spouted bed's potential as a coal combustor was evaluated in an experiment designed to burn coal unsupported in the bed, also using the optimised bed depth of 9 cm or 114g alumina particles.

6.4.1 Experimental Procedure

The first experiment was to determine whether the coal would burn unsupported in the spouted bed. This was carried out using the three cuts of Grimethorpe coal (104-152 μm, 250-425 μm and 425-600 μm) in both a lagged and an unlagged bed. The burner was ignited, as described before, with 114g alumina and a 7% methane in air mixture. The air flow rate was set to 374.5 cc/s which was high enough for good stable spouting but hopefully low enough to give the coal particles a reasonable residence time. Once the bed had warmed up, the methane flow was reduced to the lean stability limit - gradually as described in chapter 4. A low coal feedrate of about 20 g/h was then introduced to the bed and the methane flow further reduced to establish the new lean limit. This procedure was repeated, increasing the coal feedrate by about 20 g/h each time, until the methane flow could be reduced to zero or the coal feedrate exceeded 150 g/h. The bed was operated at each coal feedrate for approximately 20 minutes to allow the coal feed to stabilise and the system to reach steady state.

As the coal of size 425-600 μm proved to be the most successful, more work was carried out with this cut. After the bed had been insulated and ignited with methane, a coal feedrate of 120 g/h was supplied. This enabled the methane flow to be reduced to zero and the spouted bed to operate with coal as the only fuel. Maintaining the air flow rate constant, at 374.5 cc/s, the coal feed was increased in stages up about 300 g/h. At each stage, after about 20 minutes when a steady state had been achieved, a sample of the product gases was taken, using the quartz sampling probe, for later analysis. The probe did tend to block with char and soot from time to time, but this could easily be cleared by heating it with a gas torch to burn away the blockage. The average char compositions could also be determined by analysing the elutriated char by proximate analysis.

A similar experiment was also repeated to determine bed temperatures. The procedure was the same as above, except

that bed temperature readings were taken instead of product gas samples. Here the coal feedrate was varied from 150 g/h to 385 g/h.

6.4.2 Results And Discussion

With the coal of size 104-152 μm, the coal particles were observed to pass straight through the spout, burn in the flame and then be elutriated without being recirculated. This was observed in the unlagged bed, however the coal could not be burned without methane in either the lagged or unlagged bed. Increasing the coal size to 250-425 μm offered a slight improvement with a few coal particles visibly burning in the annulus of the spouted bed. Nevertheless the coal could still not be burned unsupported without methane. On further increasing the coal particle size to 425-600 μm a greater proportion of the coal was seen to be recirculated and burnt in the annulus. However a considerable amount of the coal was still seen to pass straight through, as a shower of incandescent particles. With the bed unlagged, the coal could still not be burned without a small amount of methane. However when the bed was insulated it could burn the coal usupported at feedrates above 120 g/h.

A graph of the effect of coal feedrate upon the leanest burnable methane mixture is shown in figure 49, using the above coal size of 425-600 μm and 374.5 cc/s air. As can be seen, at 100 g/h coal the methane flow is so small as not to be measurable and above 120 g/h coal, zero. Clearly, enough of the larger coal particles were recirculated in the bed to release sufficient heat to sustain combustion. Plate 6 shows four photographs of this form of coal burning, with a tiny amount of methane, as the bed was uninsulated for visual purposes. From the photographs it is clear that most of the coal is burning in the fountain region of the spouted bed, with some combustion also occurring in the upper layers of the annulus. The combustion in the fountain region appears to be mainly volatiles burning, especially in the cases where streaks of

Figure 49

GRAPH OF THE EFFECT OF COAL FEEDRATE ON THE LEANEST BURNABLE MIXTURE OF COAL, METHANE AND 374.5 cc/s AIR IN A LAGGED SPOUTED BED.

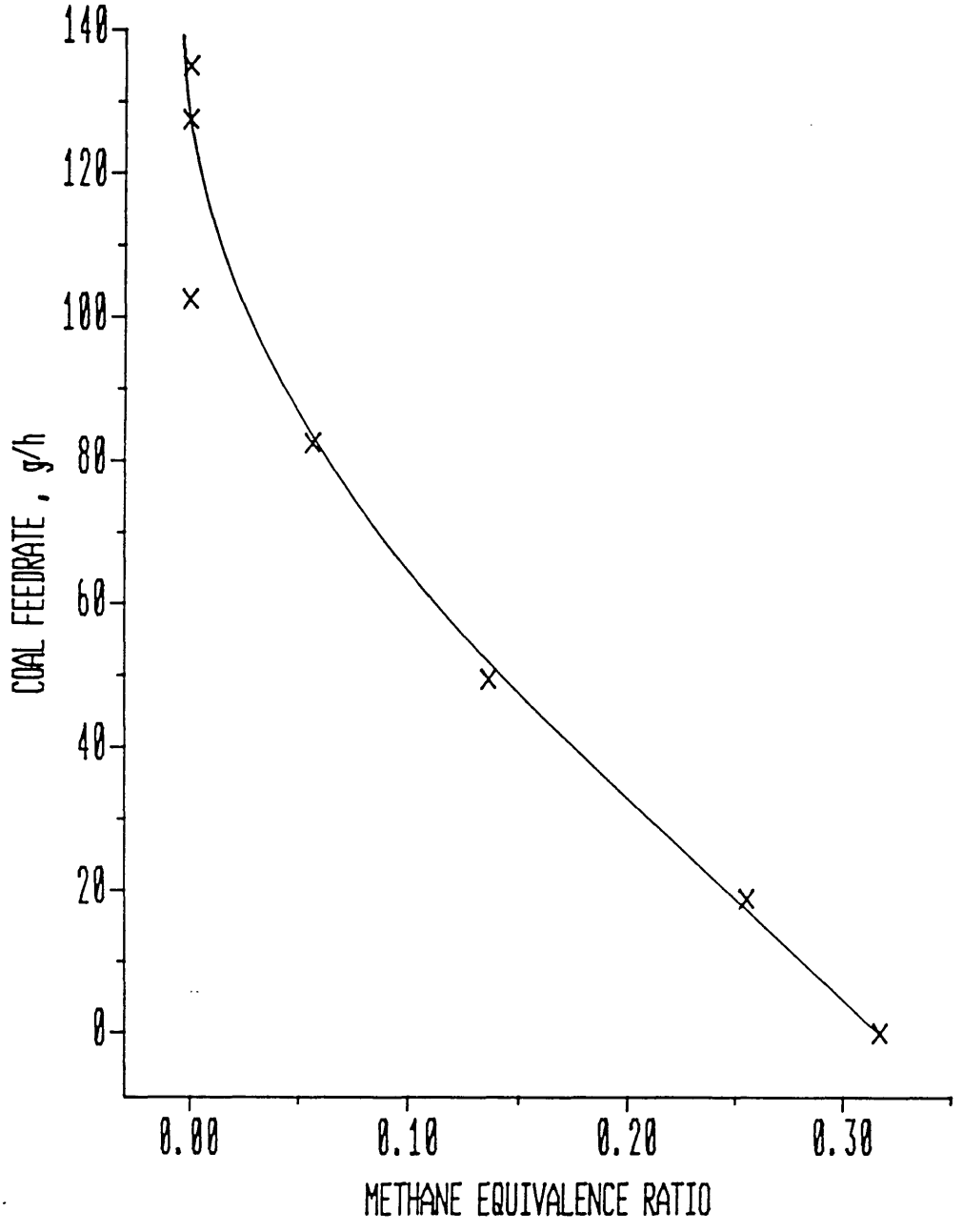

Plate 6 - Coal Combustion In

The Spouted Bed

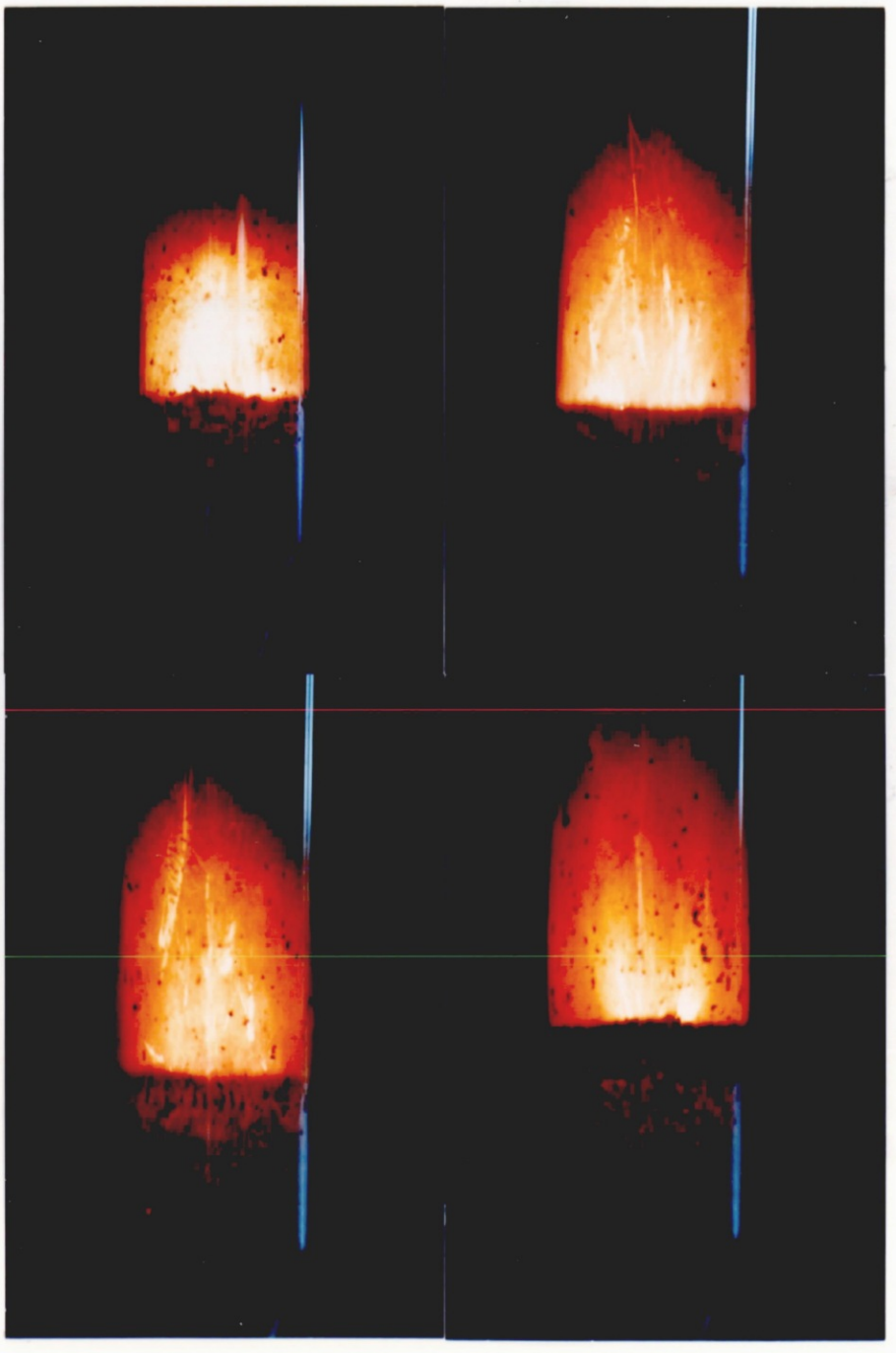

flame can be seen. Likewise the pockets of red in the annulus probably arise from volatiles, released during preheat in the spout, leaking into the annulus and burning in bubbles rising to the surface - like fluidised bed combustion. This agrees with the work of Zhao *et al.* (1987a) who reported that finer coal particles tended to burn in the fountain region of spouted-fluidised beds.

The product gas analyses from burning the 425-600 μm coal at feedrates from 130 g/h to 295 g/h in 374.5 cc/s air are shown in figure 50. CO and CO_2 yields rose with increasing coal feedrate to values of approximately 3% and 9% respectively, correspondingly the unconsumed O_2 level fell from about 11% to 6%. This was expected, as the carbon input to the bed increased, more of the fixed O_2 supply was consumed for conversion to carbon oxides. Also as the system became more fuel rich, at higher coal feedrates, so the oxidation of CO to CO_2 decreased and the CO_2/CO ratio was reduced. The yields of H_2 and CH_4 rose gradually with increasing coal feedrate from about 2% to 2.5% and 0% to 0·3% respectively. The coal contains approximately 5% H_2 by weight and thus as the coal feedrate increases so does the H_2 yield from the volatiles. The methane is formed from the reaction of some of this H_2 with the carbon in the coal particles.

$$C + 2\ H_2 \longrightarrow CH_4$$

This reaction occurs to a small extent in fuel-rich pockets of volatiles surrounding individual coal particles. Consequently, as the coal feedrate icreased so the quantity of methane produced by this reaction also increased. The fact that the ratio of H_2 to CH_4 in the product gas was of the order of ten (3% to 0.3%) suggests that approximately 10% of the H_2 in the volatiles reacted in this way.

The elutriated char from this experiment had a grey, spherical appearance and was of a size similar to the original coal (425-600 μm) - a photograph of the elutriated char is shown in plate 7(b_1). This is consistent with the coal having undergone devolatilisation with very little

Figure 50

GRAPH OF EXHAUST GAS COMPOSITION VS COAL FEEDRATE FOR A LAGGED SPOUTED BED BURNING COAL WITH 374.5 cc/s AIR.

COAL PARTICLE SIZE = 425-600 MICRONS

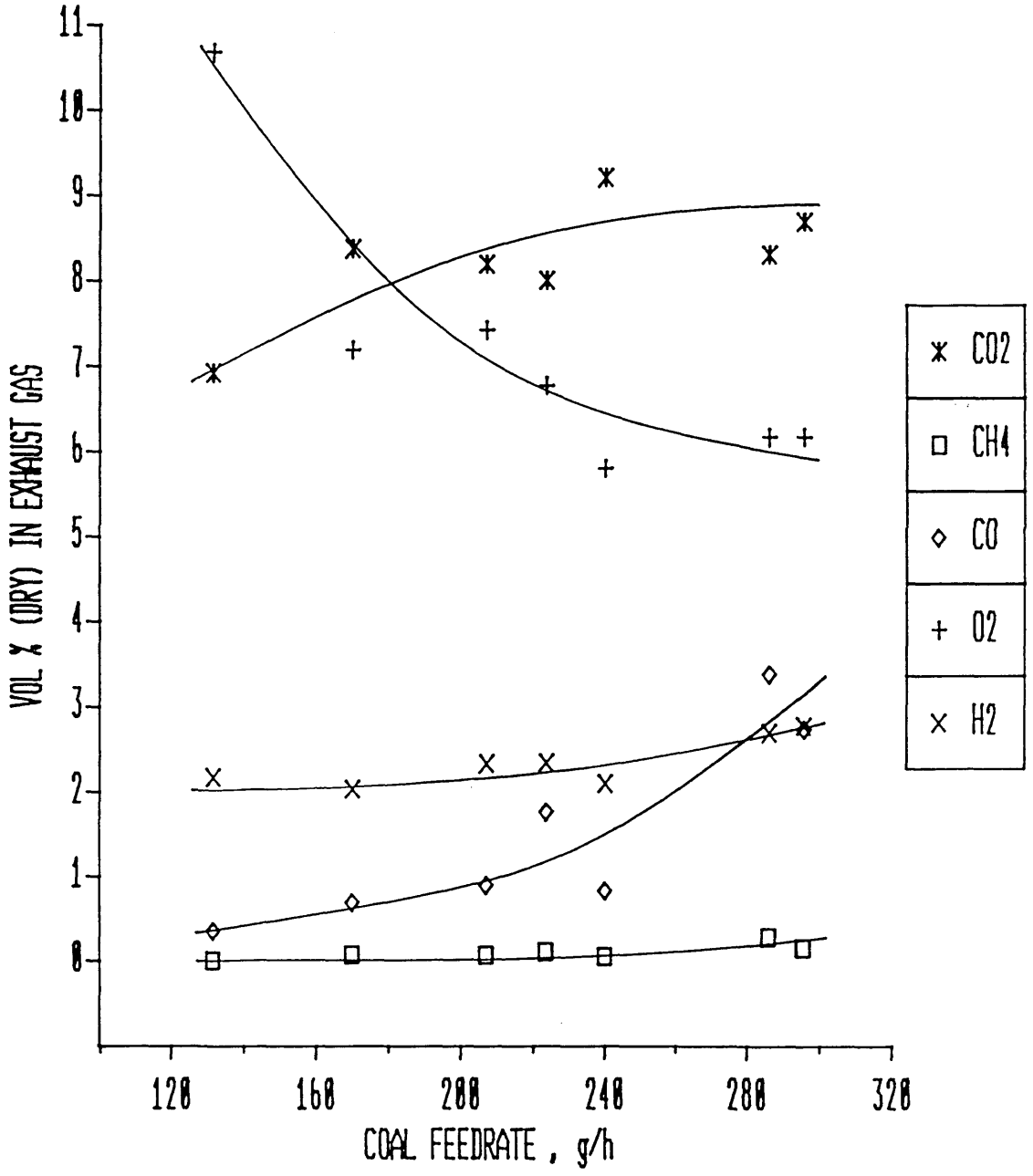

Plate 7 - Particles And Char After Coal Combustion

(a) Alumina Particles

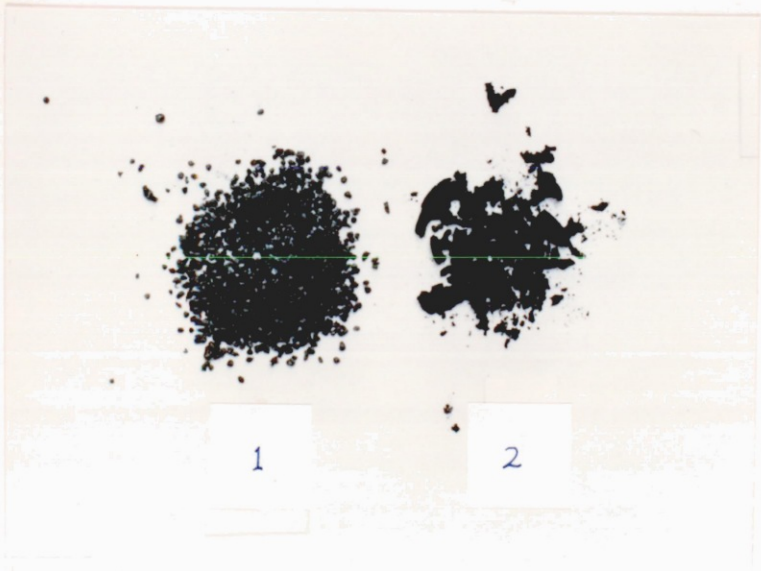

(b) Elutriated And Wall Char

fixed carbon burnout. Horton *et al.* (1977) report that during the early phases of pyrolysis, while the volatiles are still evolving, coal particles become plastic, lose their angularity and become more spherical in shape. Also that the size of the particles does not change greatly with neither a large swelling nor shrinking occurring. The results of the proximate analysis on the char are shown below.

Moisture	1·7 wt%
Volatile Matter	2·9 wt%
Ash	9·0 wt%
Fixed Carbon	86·4 wt%

Using the ash as a tracer enables the fixed carbon burnout and the loss of volatiles to be calculated. This calculation suggests that 96·4% of the volatiles have been evolved but that only 26·8% of the fixed carbon has been burned. This confirms the observations made about the char particles themselves and is discussed again later.

Small quantities of soot were formed during the coal combustion which collected on the wall of the quartz spouted bed vessel. This deposition occurred near to the top of the burner, above the insulation, where the wall was relatively cool. The soot had a very dark blue-black colour and was of a very soft, flocculent nature appearing to be 'fluffy'. A photograph of the soot is shown in plate 7($b_{\geq}$). The layer of deposited carbon was in the form of a thick shaggy carpet resembling an overgrown uncut lawn. The soot could have been formed in one or both of two ways:

Pyrolytic products generated near to the centre of the relatively large coal particle diffuse to the surface of the particle in order to escape. During this migration these products may crack, condense or polymerise with some carbon formation occurring. Soot is also produced from volatile hydrocarbons forming fuel-rich pockets surrounding the coal particles. Generally soot formation occurs when the carbon to oxygen ratio exceeds unity (Smoot and Pratt, 1979). The above is consistent with lampblack formation, a

product of restricted combustion made from hydrocarbons and used for pigments - its use dates back to ancient Egypt. Mantell (1968) describes lampblack as consisting of "feathery particles deposited together in groups resembling elongated tadpoles". He does also warn that all carbon deposits from the decomposition of hydrocarbon oils and gases are not lampblack - a heavy dense allotropic form of carbon is sometimes produced. This however is not consistent with the carbon deposits formed in the present work.

Other possibilities for the deposit would be acetylene black or carbon black. Unlike lampblack, carbon black is not amorphous but has a mainly crystalline structure which again does not fit with the carbon formed here. Acetylene black is also very dense and unlikely to be present here because of the total absence of acetylene in the product gases. Furthermore acetylene black is very hard to ignite (Schwob, 1979) due to its graphitic character - it gives a negative result when subjected to conventional flammability tests. Thus if the deposit were acetylene black it would also have formed on the high temperature, insulated, surfaces of the spouted bed vessel. In the light of all this the evidence suggests that the most likely characterisation of the soot formed here is as lampblack.

On examination after the run, the walls of the reactor vessel were tinted with an orange-brown pigment. The alumina particles, initially white, were also coated with a deposit of this colour. A photograph of the alumina particles after and before coal combustion is shown in plate 7(a). This discolouration is attributed to tar formation and deposits from the ash of the coal.

The results derived from recording the bed temperatures at various coal feedrates are shown in figure 51. The bed temperature rose from 996°C at 150 g/h coal to a maximum of 1124°C at 343 g/h coal before dropping to 1061°C at 385 g/h coal - using 374.5 cc/s air. Clearly the stoichiometric coal feedrate, at this air flow, is that which gave the highest bed temperature. On the basis of this, the stoichiometric coal feedrate with 374.5 cc/s air in this

GRAPH OF BED TEMPERATURE VS COAL FEEDRATE FOR A LAGGED SPOUTED BED BURNING COAL, SIZE 425-600 MICRONS, WITH 374.5 cc/s AIR.

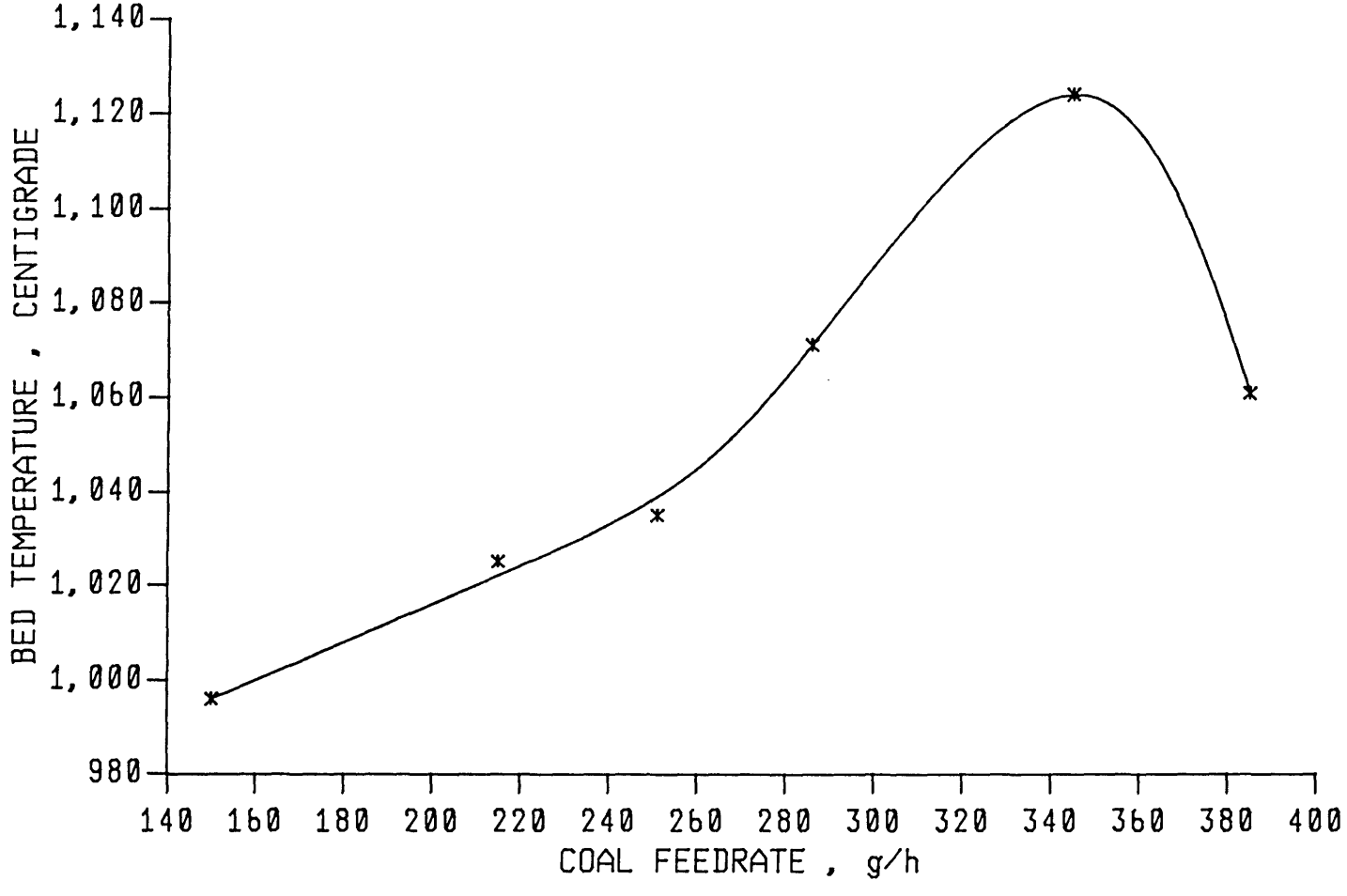

Figure 51

particular burner is 343 g/h coal. The theoretical air requirement for a coal can be calculated from its composition (by weight) from a formula (Babcock and Wilcox, 1972).

$$\text{kg air/kg fuel} = 11{\cdot}53.C + 34{\cdot}34.(H_2 - O_2/8) + 4{\cdot}29.S$$

This suggests that with 374.5 cc/s air, the theoretical stoichiometric coal requirement is 171 g/h; if only the volatiles were burnt this figure would rise to 525 g/h. This implies that the residence time of the coal particles in the spouted bed is such that only the volatiles and a small proportion of the fixed carbon are burned.

This formula can be rearranged to calculate the actual coal burnout from an experimentally determined coal-air stoichiometry. A coal feedrate of 343 g/h requires 374.5 cc/s air, so the actual air requirement is 4.815 kg air per kg fuel. If this is entered into the formula it gives,

$$4.815 = 11{\cdot}53.C + 34{\cdot}34.(0{\cdot}0476 - 0{\cdot}085/8) + 4{\cdot}29.0{\cdot}013$$

$$\text{so, } C = 0{\cdot}303$$

If it is assumed that all the carbon in the volatiles burns together with some of the fixed carbon, then the fixed carbon burnout can be calculated. The carbon content of the volatiles can be calculated from ,

$$\begin{aligned} C_{volatiles} &= C_{total} - C_{fixed} \\ &= 0{\cdot}7219 - 0{\cdot}564 \\ &= 0{\cdot}158 \end{aligned}$$

Therefore the amount of fixed carbon burned is,

$$0{\cdot}303 - 0{\cdot}158 = 0{\cdot}145$$

Thus the percentage burnout of fixed carbon is,

$$0{\cdot}145/0{\cdot}564 \approx 26\% \quad \text{(by weight)}$$

and similarly the total carbon burnout is,

$$0{\cdot}303/0{\cdot}7219 \approx 42\% \quad \text{(by weight)}$$

This agrees well with the result from a proximate analysis of the elutriated char from the previous experiment which suggested that the fixed carbon burnout was only 27% by weight.

Thus with only a quarter of the fixed carbon being burned the system is far from efficient. The reason for this lies partially with the nature of the experiment - the complete spouted bed system is very small and hence only allows the coal particles very short residence times. Also, because of the coal feeding system, the spouted bed inlet nozzle (of diameter 3 mm) restricts the coal particle size to below about 600 μm. The result of this is that, in the fountain, the free fall velocity of the coal particles is much less than that of the spouted bed particles and hence the former are elutriated without being recirculated in the bed. In a larger scale spouted bed these problems would not arise as firstly, the bed would be much deeper giving even small coal particles longer residence times and secondly, much larger coal particles could be used which would recirculate in the bed. These higher residence times would, accordingly lead to greater coal conversions. An attempt to improve coal conversion in small spouted beds is described later in this chapter.

6.5 The Reaction Of Coal With Methane In The Spouted Bed

Coal of size 425-600 μm was added to rich mixtures of methane and air for simultaneous gasification. First the rich locus of stability was determined for mixtures of methane, coal and air. Subsequently the effect on product gas composition of varying the coal and methane feedrates was studied.

6.5.1 Experimental Procedure

The first part of the study was to find the rich stability limits for different mixtures of methane, coal and air. This was carried out using the Grimethorpe coal of size 425-600 μm, 114g alumina particles and 374.5 cc/s air in both a lagged and an unlagged spouted bed. The rich limit was defined as the mixture where the flame lifted up from the bed surface, above the fountain region, without returning. It was determined visually in the unlagged bed and with the aid of a thermocouple in the lagged bed. The spouted bed was ignited in the normal way with a 7% methane in air mixture. After the bed had warmed up, the airflow was reduced to 374.5 cc/s and the methane flow gradually increased until the rich limit of stability without coal was reached. This was carried out in small increments, waiting for about five minutes before each increase in methane feedrate in order to allow the flame to stabilise - to guard against recording an artificially high rich limit. Once this rich limit had been found, the methane flow was reduced to the normal rich limit (15% methane) and the coal flow adjusted to about 20 g/h. The rich limit was again determined by gradually increasing the methane feedrate, as before, until the flame lifted from the bed. This procedure was repeated five times, increasing the coal feedrate by 20-30 g/h each time up to a maximum of about 120 g/h.

The second experiment used the same air flow rate, particles and coal as the first but was only performed in a lagged bed. After the bed had been ignited and allowed to warm up, the air flow was reduced to 374.5 cc/s and the methane flow adjusted to an equivalence ratio of 1·436 (13·7%). Using the quartz sampling probe, a duplicate sample of the product gases was taken when the system had reached the steady state and the bed temperature was noted. The sample was collected with the probe centrally positioned approximately 5 cm upstream of the burner exit. This procedure was repeated four times with duplicate samples being taken at coal feedrates of 30 g/h, 83 g/h,

106 g/h and 142 g/h. At each coal feedrate the system was left for up to 20 minutes before a sample was taken to allow the coal feedrate to stabilise and the steady state to be reached.

The third experiment was basically a repeat of the second, except that the coal feedrate was fixed and the methane equivalence ratio varied. The insulated spouted bed was ignited as before and a methane equivalence ratio of 1·25 (11·9% methane) set with 374.5 cc/s air. A coal feedrate of 99 g/h was then introduced into the bed and, after waiting 20 minutes for steady state conditions, a duplicate sample of the exhaust gas was taken for later analysis. The sampling probe was positioned as for the previous experiment and the bed temperature was also recorded. This was repeated four times with duplicate samples being taken at methane equivalence ratios of 1·326, 1·400, 1·474 and 1·546.

6.5.2 Results And Discussion

In the unlagged spouted bed the coal was observed to burn in a very similar way to that described earlier in this chapter. A small proportion of the coal was seen to burn in the annulus with the rest burning in the fountain of the spouted bed. The rich loci of stability in both a lagged and an unlagged bed are shown in figure 52. This is a graph of the richest burnable methane equivalence ratio at various coal feedrates in 374.5 cc/s air for both insulated and non-insulated conditions. The curves are approximately parallel with a separation of about 0·37 ø. As would be expected, increasing the coal feedrate made the mixture richer and thus reduced the maximum burnable methane concentration. Both curves also start off with a shallow gradient at low coal feedrates which then becomes much steeper above about 20 g/h coal. This suggests that, at low coal feedrates, the degree of coal burnout was high but that, at large coal feedrates, a high proportion of the coal passed through the flame with only the voaltiles being combusted. This hypothesis is supported by the temperature

Figure 52

GRAPH OF THE EFFECT OF COAL FEEDRATE ON THE RICHEST BURNABLE MIXTURE OF COAL, METHANE AND 374.5 cc/s AIR IN A SPOUTED BED.

COAL PARTICLE SIZE = 425-600 MICRONS

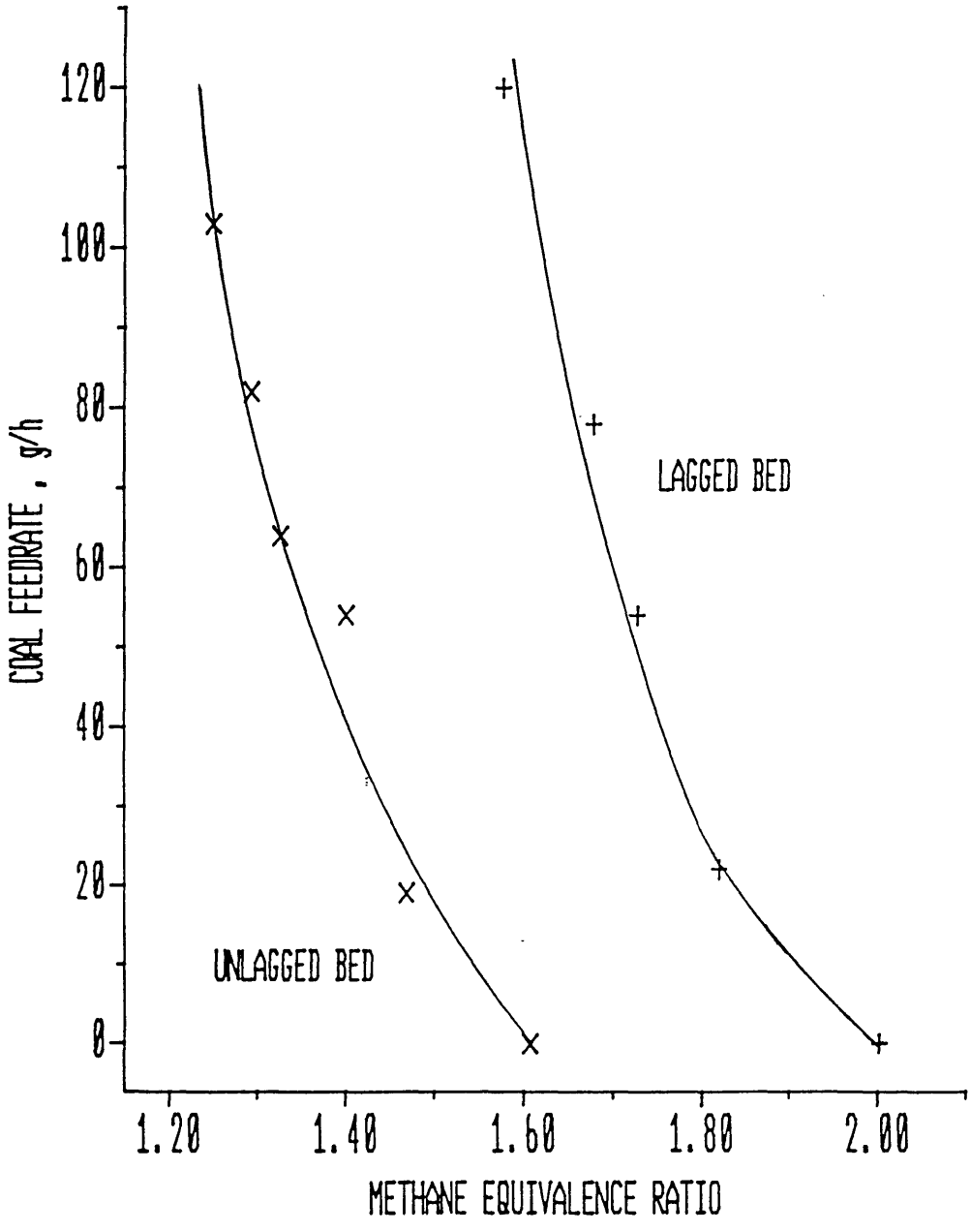

measurements of the previous section.

Figure 53 shows a graph of the effect on product gas composition of increasing the coal feedrate at a fixed methane equivalence ratio of 1·436. Yields of CO, H_2 and CO_2 all increased to a maximum at a coal feedrate of about 85 g/h before decreasing towards their original values at about 140 g/h of coal. Yields of CO rose from 8% to 10·5% and then fell to 9·5%, yields of H_2 rose from 6% to 7·5% before falling to 6% and yields of CO_2 rose marginally from 4% to 4·5% before returning to 4%. The level of CH_4 in the product gases steadily rose from 0·7% to 1·5% whilst the levels of C_2H_4 and C_2H_2 increased to constant values of 0·15% and 0·5% rspectively above 20 g/h coal. The initial rise in the CO, H_2 and CO_2 yields was as expected, due to the increased carbon and hydrogen input into the bed from the coal. The fall in the yields of these products was probably due to soot formation which occurred as the mixture became richer. A thin layer of very black, feathery soot was deposited near the exit from the burner above the insulation. This was very similar to that found during coal combustion without methane and for the same reasons was deduced to have been lampblack. The evidence for this is further enhanced by the fact that the acetylene levels, as shown in figure 53, did not fall as the mixture became richer - had they done so, the soot could have been acetylene black. Lampblack can contain up to 1·76% by weight of hydrogen (Mantell, 1968) and this would explain the simultaneous fall off of carbon oxide and hydrogen yields. The fact that the CH_4 yield continued to rise does not contradict this hypothesis as the soot is formed from the gas phase whereas the CH_4 can be formed by a reaction with the coal particle itself. Hydrogen from the volatiles can react with the fixed carbon of the coal particle in the reaction.

$$C + 2\ H_2 \longrightarrow CH_4$$

Alternatively the CH_4 could have been the result of the increased coal feedrate reducing the conversion of the

Figure 53

GRAPH OF EXHAUST GAS COMPOSITION VS COAL FEEDRATE FOR A LAGGED SPOUTED BED WITH 374.5 cc/s AIR AND A CH4 EQUIVALENCE RATIO OF 1.436.

COAL PARTICLE SIZE = 425-600 MICRONS

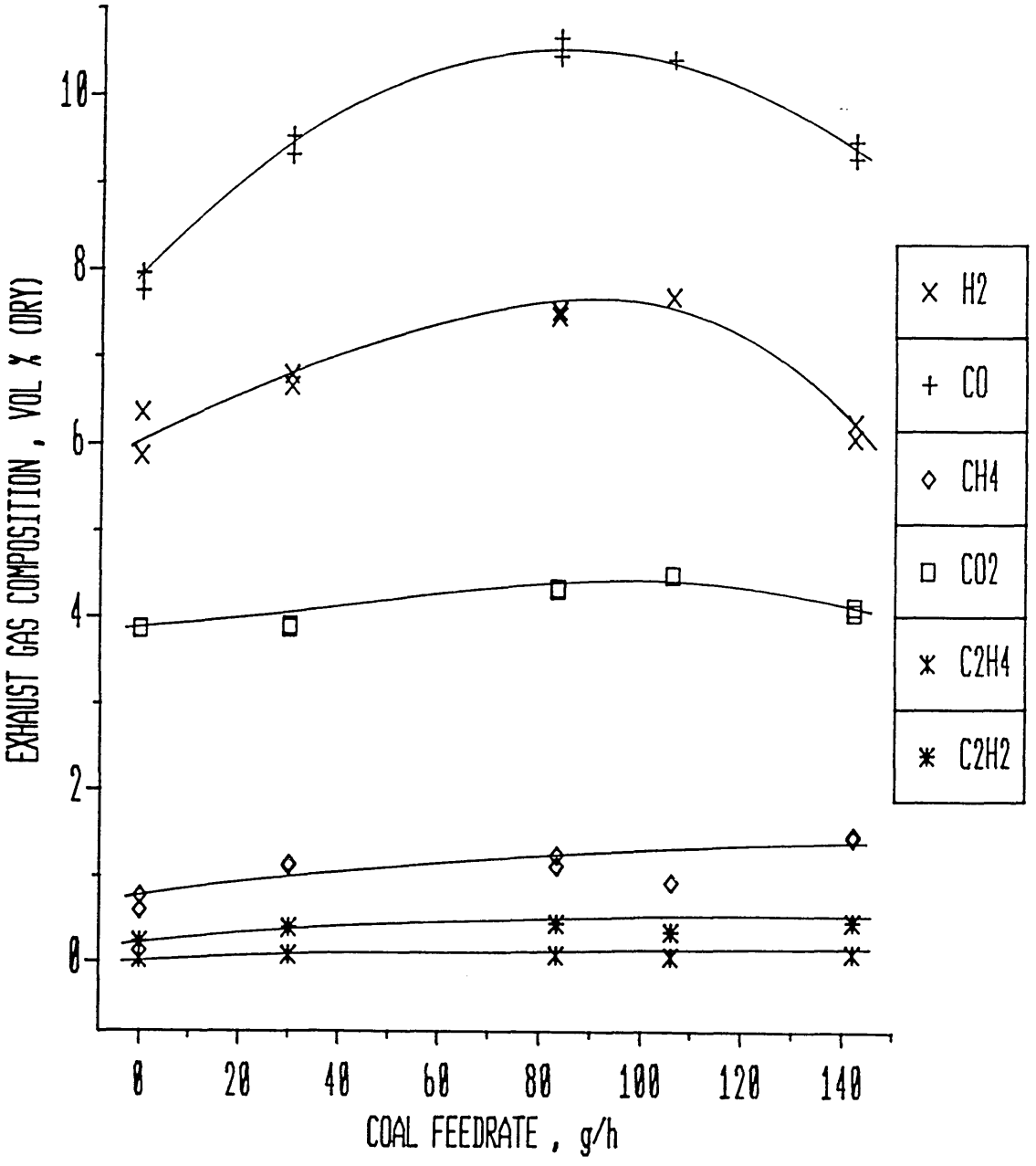

methane initially fed to the reactor. The latter is found to occur in methane-air systems as the mixture becomes richer. Figure 54 shows the variation of bed temperature with coal feedrate for the above experiment. As would be expected, the bed temperature fell steadily as the mixture became richer.

Figure 55 shows a graph of the effect on product gas composition of increasing the methane equivalence ratio at a fixed coal feedrate of 99 g/h. The yields of CO and H_2 rose from 6% and 5% to maxima of 7% and 6·5% at a methane equivalence ratio of approximately 1·35 and then fell off rapidly to 4% and 3% respectively. The production of CO_2 fell from 4·5% to 3·5% and that of CH_4 rose from 0·3% to a constant level of 0·7% above a methane equivalence ratio of 1·4. The yields of C_2H_4 were low and constant at about 0·05% and the yields of C_2H_2 rose from 0·15% to a maximum of 0·3% at a methane equivalence ratio of 1·4 before decreasing to 0·2%. The initial rises in CO and H_2, the fall in CO_2 and the rise in CH_4 yields are all consistent with increasing the methane equivalence ratio - in a system burning only CH_4 and air this would be expected as the mixture became richer. However the fall in the C_2H_2 yield and certainly the drastic drops in CO and H_2 yields are unexpected. This can only be explained by tar and soot formation.

After the experiment, when the reactor tube was removed from the insulation, three layers of deposit were observed on the walls of the quartz vessel - a photograph of this is shown in plate 8(b). As with the other coal burning experiments, a thick layer of black 'fluffy' soot was found at the top of the reactor tube. Below this the tube was stained with a coating of orange-brown tar which continued to about half way down the tube where it merged with the tail end of another deposit. This silvery grey coating of the vessel occurred just above the flame zone in the hottest part of the reactor and continued for about 4 cm. The deposit was of a grey metallic colour and consisted of a thin laminar wafer which was also coated, on the inside, with a very fine dense black powdery soot. The grey laminar

GRAPH OF BED TEMPERATURE VS COAL FEEDRATE FOR A LAGGED SPOUTED BED WITH 374.5 cc/s AIR AND A CH4 EQUIVALENCE RATIO OF 1.436.

COAL PARTICLE SIZE = 425-600 MICRONS

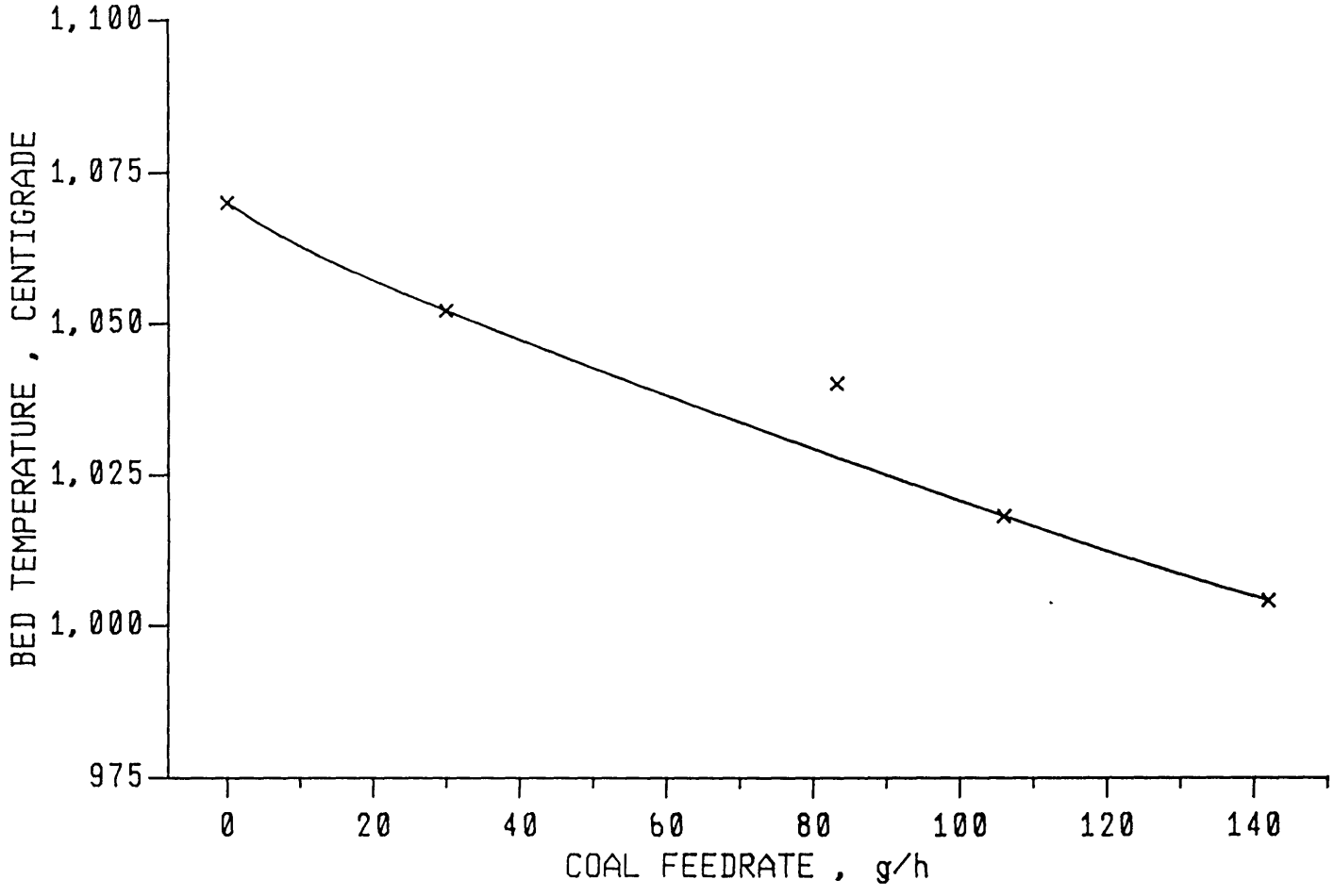

Figure 54

Figure 55

GRAPH OF EXHAUST GAS COMPOSITION VS METHANE EQUIVALENCE RATIO FOR A LAGGED SPOUTED BED WITH 374.5 cc/s AIR AND 99.2 g/h COAL.

COAL PARTICLE SIZE = 425-600 MICRONS

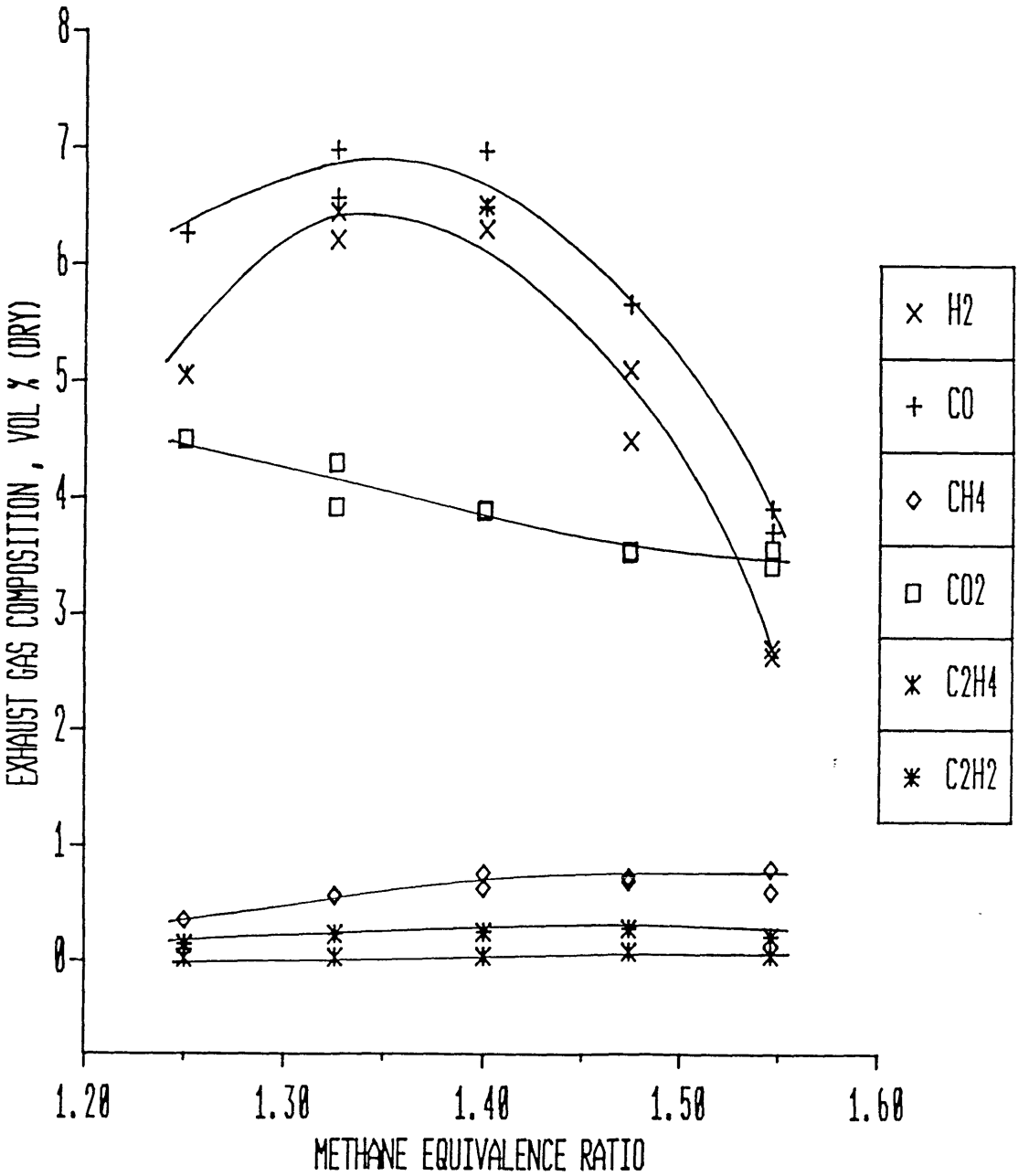

layer had a hard brittle structure being easily removed from the reactor vessel in small jagged pieces - see plate 8(a). The pieces had a sonorous sound when struck, like a metal, and the black coating could be readily brushed off.

The thick layer of 'fluffy' soot at the top of the tube was probably lampblack as before, produced as the mixture became richer. This together with the tar formation may explain the drop in H_2 yield and some of the reduction in CO. The silvery deposit was most likely pyrolytic graphite, a high density polycrystalline carbon of a more or less graphitic nature and formed at high temperatures. It exhibits the lustre of metal, rings when struck and is a good electrical conductor. It was first made in 1880 by the thermal decomposition of hydrocarbons upon a hot surface (Sawyer, 1880) and was later found to be a by-product from water-gas plants in the USA and Canada. It was originally used for the manufacture of carbon brushes because of its hardness and sharp edges but is now finding applications in relation to specialist carbon products, particularly in connection with space vehicles. If it is further subjected to temperatures of up to 3000°C more crystal growth occurs to produce the most nearly perfect graphite available from a crystallographic point of view (Hutcheon, 1970). This pyrolytic graphite formation could account for a considerable amount of carbon removal from the product gases. The thin coating of powdery soot found on the inside surface of the pyrolytic graphite could well have been acetylene black - this is one of the few blacks that could withstand the high temperatures in that region. This would explain the small decrease in acetylene yield from the product gases as the methane equivalence ratio was increased. Alternatively it could have been a high density polycrystalline carbon black which had not been converted to pyrolytic graphite due to the fall in temperature as the reactant mixture became richer. This seems more likely as the acetylene yield was very low even at its maximum value. Figure 56 shows the fall in bed temperature as the methane equivalence ratio was increased.

The elutriated char particles in these two experiments

Plate 8 - Pyrolytic Graphite Formation In The Spouted Bed

(a) Fragments Of Pyrolytic Graphite

(b) Deposits On The Spouted Bed Walls After Coal Combustion

were very similar to those obtained from burning coal alone in the spouted bed. Again, this suggests a low carbon conversion. The proximate analyses for the chars are shown below.

	Char from varying coal	Char from varying CH_4
Moisture	1·5 wt%	1·2 wt%
Volatile Matter	3·3 wt%	3·5 wt%
Ash	12·0 wt%	10·9 wt%
Fixed Carbon	83·2 wt%	84·4 wt%

Using the ash as a tracer to calculate the conversion gives the result that in the experiment with a varying coal feedrate 96·9% of the volatiles were evolved and 47% of the fixed carbon was burned. Similarly for the experiment varying the methane equivalence ratio, 96·4% of the volatiles were evolved and 41% of the fixed carbon was burned. Hence the carbon burnout was better than for the combustion of coal alone in the spouted bed but still very low - for the same reasons. The conversion was probably higher because of the lower coal feedrates used here.

GRAPH OF BED TEMPERATURE VS CH4 EQUIVALENCE RATIO FOR A LAGGED SPOUTED BED WITH 374.5 cc/s AIR AND A COAL FEEDRATE OF 99.2 g/h.

COAL PARTICLE SIZE = 425-600 MICRONS

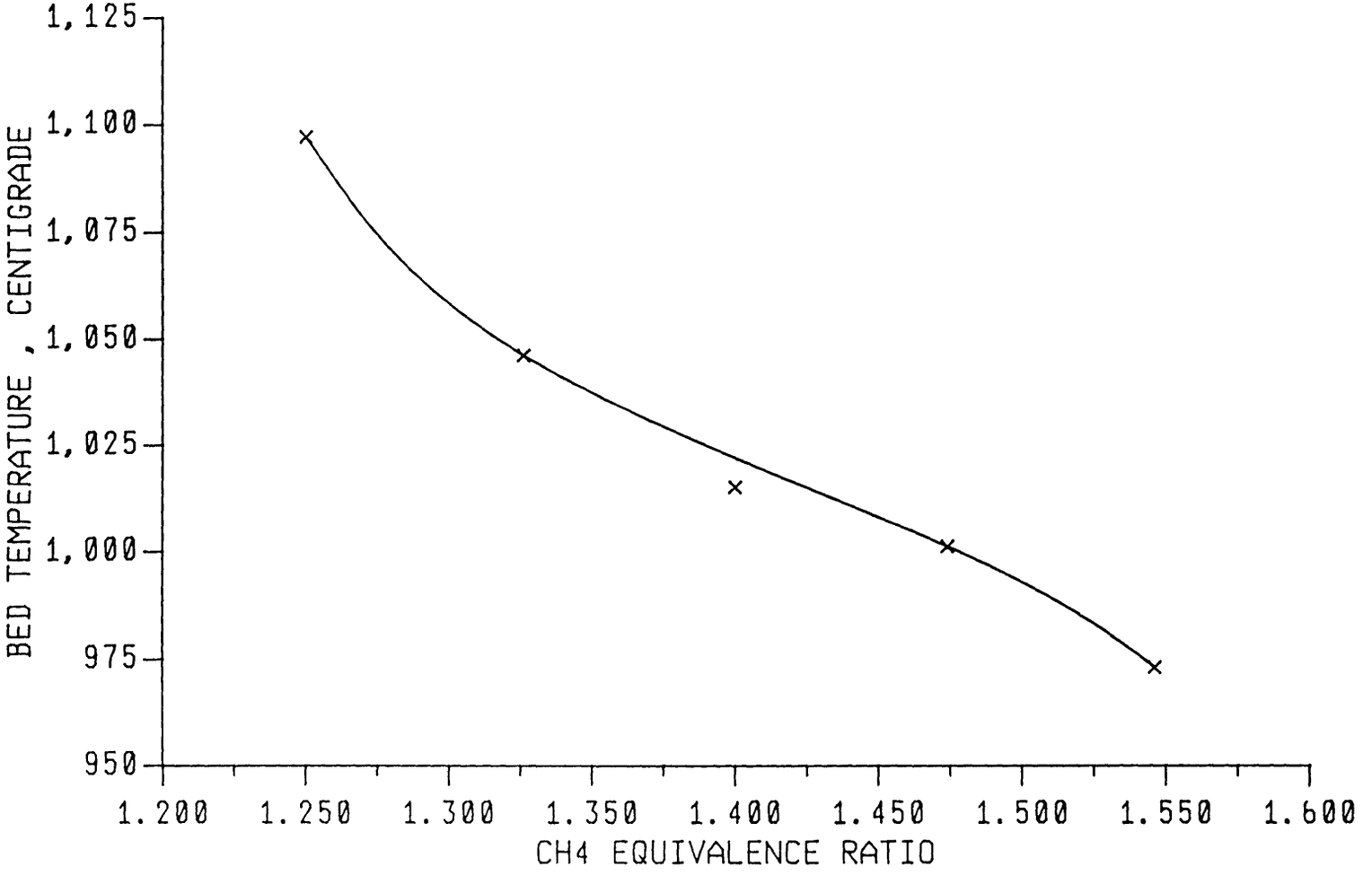

Figure 56

6.6 The Use Of A Secondary Fluidised Bed To Improve Coal Conversion

A coarse stainless steel gauze was lowered into the fountain region of the spouted bed in order to produce a secondary fluidised bed above the spout. It was hoped that this would prevent coal particles from being elutriated and so improve the coal conversion.

6.6.1 Experimental Procedure

Firstly a 3·5 cm diameter disc was cut out from a sheet of 8 mesh stainless steel gauze. This was attached to a piece of steel wire so that it could be lowered into the spouted bed vessel from above. The unlagged spouted bed was then ignited as before, with a 7% methane in air mixture and 114 g alumina particles, and the gauze lowered into the fountain region, with a view to producing a secondary fluidised bed. It was found that the air flow rate to the spouted bed had to be increased from the previous value of 374·5 cc/s to 466·5 cc/s, to form a fluidised bed of a reasonable depth (ie. about 2 cm). At this higher air flow rate, the best fluidised bed was produced with the gauze positioned about 4 cm above the bed surface. (Gauzes of finer mesh sizes were also tried, but these proved to be unsatisfactory for the purpose of forming fluidised beds). Having established the optimum gauze size and position in the fountain for producing a secondary fluidised bed, the spouted bed was re-ignited with the 'Kaowool' insulating jacket in place and two experiments were performed with an air flow rate of 466·5 cc/s. Firstly, a coal feedrate of 168 g/h was fed to the spouted bed and the methane flow set to zero whilst the steel gauze was in place, 4 cm above the bed suface. The spouted bed was operated in this mode for 30 minutes and the elutriated char was collected for later

analysis. In the second experiment the methane flow was set to 72 cc/s (ø = 1·4), the coal feedrate to 108 g/h and the steel gauze was initially removed. When the system had reached a steady state, a duplicate sample of the exhaust gas was taken for later analysis. This procedure was repeated with the steel gauze suspended at heights of 1 cm, 4 cm and 7 cm above the bed surface - waiting for the system to reach a steady state before taking each sample. Again the char elutriated during the course of the experiment was also collected for later analysis.

6.6.2 Results And Discussion

With the stainless steel gauze suspended in the fountain of the spouted bed, a secondary fluidised bed of depth about 1·5-2·0 cm was produced. When coal was fed into the system with this gauze in place, the coal particles were seen to burn below the fluidised bed although a fair proportion of them burned above and were prematurely elutriated.

The elutriated char collected during the combustion of 168 g/h coal was of a similar appearance to that described in the previous sections of this chapter. A proximate analysis was carried out on the char which gave the reslults below.

Moisture:	0·3 wt%
Volatile Matter:	3·4 wt%
Ash:	17·4 wt%
Fixed Carbon:	78·4 wt%

Using the ash as a tracer allows the fixed carbon burnout to be calculated as 66·6% and the percentage of volatile matter burned as 97·7%. This is a great improvement over the previous fixed carbon burnout of 27% for coal combustion and thus much more of the heat released from the coal is being utilised by the bed. During the course of the

experiment the bed temperature remained approximately constant at 995°C.

The analyses of the exhaust gas with the gauze in the different positions above the bed and 108 g/h coal with 72 cc/s methane are shown in figure 57. The effect of suspending the gauze 1 cm above the bed surface was to increase the yields of CO, H_2 and CO_2 from 5·3% to 9%, 4·3% to 7% and 1·5% to 3·3% respectively. On lifting the mesh to 4 cm above the bed the yields of H_2 and CO_2 remained approximately constant whilst the CO yield increased slightly to 9·5%. Raising the height of the gauze further to 7 cm above the bed caused the yields of the above gases to decrease. The yields of CH_4 and C_2H_2 followed the same patterns as above, but to a lesser extent. The recorded bed temperature increased from 1041°C without the mesh to 1085°C with the mesh at a height of 4 cm above the bed and then fell to 1055°C with the gauze at a height of 7 cm. Clearly the rise in the yields of carbon oxides, for a fixed coal input, shows that more of the fixed carbon in the coal is being converted. Also, the higher H_2 yield suggests that as more of the coal is burned, the system becomes more fuel rich and partial oxidation reactions become more important.

A proximate analysis of the elutriated char is shown below.

Moisture	1·1 wt%
Volatile Matter	4·5 wt%
Ash	17·4 wt%
Fixed Carbon	77·0 wt%

Again, using the method of ash tracing, the fixed carbon burnout can be calculated as 66·2% and the fraction of the volatiles burned as 97·1%. This provides further evidence for the hypothesis that coal burns much more efficiently in the spouted bed with the aid of a secondary fluidised bed. Also, as mentioned before, because the fluidised bed is positioned in the fountain region, the heat released

Figure 57

THE EFFECT OF LOWERING A STEEL GAUZE INTO THE SPOUTED BED WITH 100 g/h COAL, 466.5 cc/s AIR AND A CH4 EQUIVALENCE RATIO OF 1.4.

COAL PARTICLE SIZE = 425-600 MICRONS

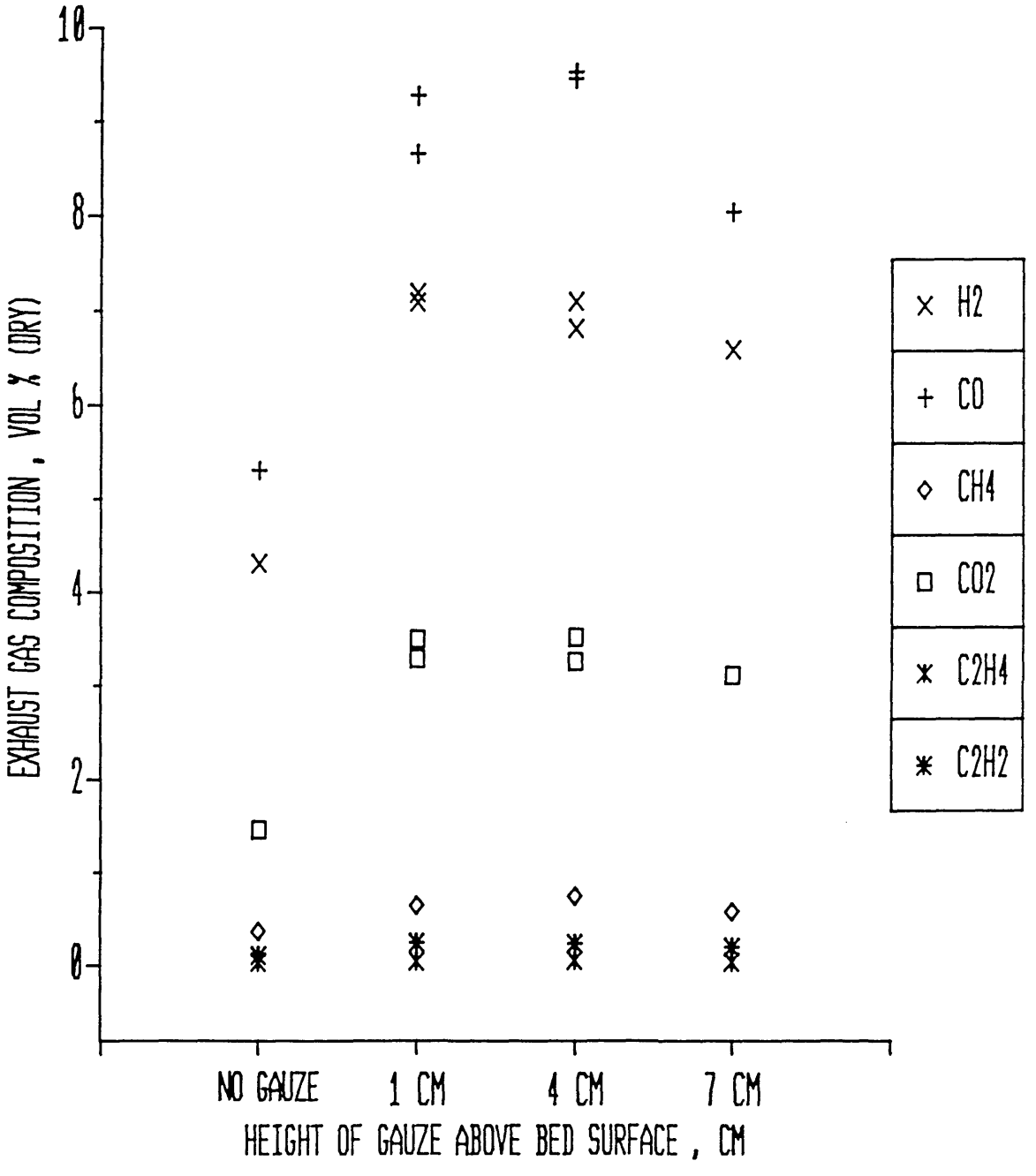

from the coal is recirculated into the bed by means of the spouting alumina particles.

Thus, a method has been found which overcomes, to a considerable extent, the problems associated with burning fine coal particles in a small spouted bed burner.

CHAPTER 7

SUMMARY AND CONCLUSIONS

This thesis contains a study of combustion systems in which the reactants are preheated by the recirculation of heat from the exhaust gases. This was achieved by studying two such systems directly, the "Swiss-roll" and the spouted bed, and also by using a burner which preheated the reactants electrically, in order to imitate a heat recirculating burner. The effect of this preheat was to enable leaner or richer fuel-air mixtures to be burned than would otherwise have been possible. Burning lean was used to study the effectiveness of a particular heat exchanger as a combustor with respect to the various parameters controlling it. Rich combustion was used to process both gaseous and solid fuels to more valuable products, and enabled the fraction of the fuel used for heat release to be minimised. These concluding paragraphs are intended to link the work together and suggest future applications.

The "Swiss-roll" burner is very efficient as a heat exchanger and could easily burn up to 25% methane in air without any evidence of soot formation. Despite a low methane conversion (59%) it did manage to produce reasonable levels of synthesis gas (5·7% H_2 and 9·4% CO). However the "Swiss-roll" burner's greatest problem was its susceptibility to the high thermal stresses of operation in excess of 1000°C. Because of the different relative coefficients of thermal expansion of its constituent construction materials, it developed cracks in its casing as it heated up and cooled down before and after operation. The burner was consequently unusable after only a few runs. Thus although the laboratory model of a "Swiss-roll" burner used here is a completely impractical combustion device, this work does show that such a stationary (ie with no moving parts) heat exchanger could function very well as a

heat recirculating burner if the operational problems could be overcome. Accordingly, if such an efficient heat exchanger was found to be necessary for a particular combustion application, more work would be required with regard to developing a spiral burner of, perhaps, a total ceramic construction which could withstand the thermal stresses.

The electrically heated burner was designed to simulate heat recirculating burners with varying degrees of preheat so as to investigate the unique relationships between composition, flow and temperature independently, in the latter burners generally. This work revealed that the rich limit of stability for methane, similar to the lean limit, was also an approximately linear function of the preheat temperature. By calculating the final flame temperature from the known preheat temperature and the product gas compositions it was established that this parameter had a constant value of approximately 1600 K at the rich stability limit. The lean stability limit for methane was found to have a constant final flame temperature of 1403 K (Lloyd and Weinberg, 1975) and so this result, together with the previous linear dependence, suggests some similarity between the rich and lean stability limits. However, the main result of this part of the study was the finding that the highest yields of synthesis gas were obtained from methane-air mixtures in the region of 20% methane. This discounts the previously held idea that the richest mixtures lead to maximum synthesis gas production. It also renders burners such as the "Swiss-roll", which achieve very high levels of preheat, unnecessary for attaining maximum yields of synthesis gas.

So with regard to future work, the use of a much simpler heat recirculating burner should be investigated for the production of synthesis gas and higher hydrocarbons. A very suitable, simple, heat recirculating burner would be a single pass annular countercurrent heat exchanger such as that used by Hardesty and Weinberg (1974). The electrically heated burner was also found to be very useful for testing potential catalysts for rich combustion.

Various metals were tested and although none of them had a very great effect on the combustion products the electrically heated burner could be used again for this purpose in the future.

The objective of the experimental work on the lean combustion of methane in the spouted bed, described in chapter 4, was to investigate the relationship between the bed depth and the degree of heat recirculation. This was achieved by assuming that the bed depth which allowed the most heat recirculation would also enable the leanest methane-air mixture to be burned. The results from this chapter revealed an optimum bed depth for heat recirculation of 9 cm in a 4 cm diameter spouted bed or 114g alumina particles. In a heat exchanger such as the spouted bed, heat is transferred by the moving particles and thus the degree of heat recirculation depends upon the mass circulation rate of the particles. Clearly, at bed depths above or below 9 cm the mass flow rate of solids is reduced for this particular system. There is, in addition, the effect that as the bed becomes deeper so the gas-particle contact times are increased and the system moves closer to thermal equilibrium; however in very deep beds this is over compensated for by the reduced mass circulation rate.

The simple heat transfer models for gaseous combustion in a well insulated spouted bed were derived in order to investigate the parameters controlling the spouted bed system. Three such models were set up, one to calculate gas and particle temperatures for a 3% methane in air mixture and two to predict the lean and rich stability limits for methane combustion in air. The first model predicted that as the mass flow rate of particles increases or as the particle diameter decreases so the system approaches thermal equilibrium, where the gas temperatures equal the particle temperatures in the various parts of the heat exchanger. Also, using a crude measurement of the mass circulation rate of particles in the spouted bed, the predicted bed temperature from the model was found to be in close agreement with that found experimentally in the work

of chapter 4. The models predicting the lean and rich stability limits for methane combustion in the spouted bed were also found to be in very close agreement with the experimental results from chapter 4. However these models did suggest that the spouted bed was operating closer to thermal equilibrium than would seem likely in practice - because of the very high velocities and short residence times in the spout. The most probable explanation for this is that about 30% of the gas in the spout leaks into the annulus and slowly percolates, countercurrently, to the surface where it burns as a flat flame. This gas almost certainly reaches thermal equilibrium with the particles in the annulus and thus raises the efficiency of the system. Furthermore, heat transfer is probably further enhanced in the rotating vortex of particles in the fountain. So, although these models are very crude, they do predict the rich and lean stability limits for methane combustion in the spouted bed quite well. With regard to future work the models could be refined to take account of heat losses and the dissociation of the product gases. In fact, using the heat loss calculations of chapter 4, based upon the lean and rich limits with and without insulation, the models could be extended to cover gaseous combustion in unlagged spouted beds.

Using Grimethorpe coal particles of size 425-600 μm in a lagged spouted bed, the coal could easily be burned unsupported at feedrates in excess of 120 g/h with very few operational problems. Temperature measurements and a proximate analysis of the elutriated char revealed that only about 25% of the fixed carbon in the coal was being burned. Thus although the spouted bed seemed to burn the coal very cleanly, it was far from efficient. The reason for this is probably related to the feed system and the small scale of the experiment. In a larger scale spouted bed the coal particles would have a longer residence time because of the deeper bed and if necessary, or if desired, much larger coal particles could be used which would recirculate in the bed. An interesting soot deposit was also formed which probably consisted of lampblack.

In other experiments coal was introduced into a rich methane flame for simultaneous gasification. At low coal feedrates this increased the yields of synthesis gas but at high feedrates, yields were reduced due to the formation of various carbonaceous deposits on the reactor tube. These deposits were lampblack at the exit from the burner, as before, an orange-brown tar and a silvery wafer type deposit in the flame zone which was probably pyrolytic graphite. Proximate analyses of the elutriated char in these experiments showed that the fixed carbon burnout had increased to about 45%, which was an improvement but is still low.

In order to burn coal more efficiently in a small scale spouted bed, a development was tested whereby a coarse stainless steel gauze disc, of a similar diameter to the spouted bed vessel, was lowered into the fountain region. This resulted in the formation of a secondary, shallow slugging, fluidised bed above the spouted bed. When coal, of size 425-600 μm, was introduced into this modified spouted bed, much of the coal was seen to burn below the fluidised bed and was thus prevented from being elutriated too quickly. In this way the devolatilised char particles are forced to burn in the fountain region of the spouted bed and, therefore, transfer their combustion heat back to the bed. Proximate analyses of the char elutriated whilst operating the spouted bed in this mode revealed that the fixed carbon burnout had increased to about 67%, for the combustion of coal both alone and together with methane. Also, when burning coal in a rich methane flame, the effect of the secondary fluidised bed was to increase the yields of synthesis gas by approximately 70%. Thus a method for overcoming the problems associated with burning fine coal particles in a small spouted bed has been found. Any future work should be directed at optimising the position and fineness of the steel gauze, ie. to investigate how the depth of the secondary fluidised bed could be varied to extract the maximum amount of heat from the coal and recirculate it to the spouted bed.

REFERENCES

ARBIB, H.A. and LEVY, A. (1982)
"Combustion of low heating value fuels and wastes in the spouted bed." Can. J. Chem. Eng. v.60, 1982, pp. 528-531.

ARBIB, H.A., SAWYER, R.F. and WEINBERG, F.J. (1981)
"The combustion characteristics of spouted beds."
18th Symposium (International) on Combustion, The Combustion Institute, 1981, pp. 233-241.

BABCOCK and WILCOX (1972)
Chapter 6 - " Principles of combustion."
In: "Steam, Its Generation And Use.", New York 1972.

BARTLEET, T.G. and RIMBOTTI, P. (1982)
3rd Year Undergraduate Research Report, Department of Chemical Engineering and Chemical Technology, Imperial College, London.

BARTOK, W. and SONG, Y.H. (1982)
"Rate controlling reactions in fixed nitrogen conversion to N_2." 19th Symposium (International) on Combustion, The Combustion Institute, 1982, pp. 1291-1299.

BARTON, R.K., RIGBY, G.R. and RATCLIFFE, J.S. (1968)
"The use of a spouted bed for low temperature carbonisation of coal." Institution of Engrs., Australia, Mech. and Chem. Eng. Trans., May 1968, pp. 105-112.

BRITISH STANDARD 1756:Pt.1:1971 (1971)
"Methods for the sampling and analysis of flue gases."
"Part 1, methods of sampling."
British Standards Institution Gr 7.

BROPHY, J.H. and TELFORD, C.D. (1985)
"Process for producing synthesis gas by partial combustion of hydrocarbons."
International patent class C01B3/44.
International publication number WO 85/05094.
Innternational publication date 21/11/1985.

BURGOYNE, J.H. and HIRSH, H. (1954)
"The combustion of methane at high temperatures."
Proc. R. Soc. v.A227, 1954, pp. 73-93.

BUTT, A.R., BOWER, C.J., GREEN, P.C., PATERSON, N.P. and GALE, J.J. (1987)
"Coal fired appliances for process heating." I. Chem. E. Symposium Series No. 105, 1987, pp. 377-412.

COLE, W.E. and ESSENHIGH, R.H. (1973)
Proc. 3rd Int. Conf. on Fluidised Combustion, Dec. 1973.

FOONG, S.K., CHENG, G. and WATKINSON, A.P. (1981)
"Spouted bed gasification of Western Canadian coals."
Can. J. Chem. Eng. v.59, 1981, pp. 625-630.

FOONG, S.K., LIM, C.J. and WATKINSON, A.P. (1980)
"Coal gasification in a spouted bed."
Can. J. Chem. Eng. v.58, 1980, pp. 84-91.

GAYDON, A.G. and WOLFHARD, H.G. (1984)
"Flames.", Chapman and Hall Ltd., London, 1984.

HAJI-SULAIMAN, Z., LIM, C.J. and WATKINSON, A.P. (1986)
"Gas composition and temperature profiles in a spouted bed coal gasifier." Can. J. Chem. Eng. v.64, 1986, pp. 125-132.

HARDESTY, D.R. and WEINBERG, F.J. (1974)
"Burners producing large excess enthalpies."
Combustion Science and Technology v.8, 1974, pp. 201-214.

HORTON, M.D., GOODSON, F.P. and SMOOT, L.D. (1977)
"Characteristics of flat, laminar coal dust flames."
Comb. and Flame v.23, 1977, pp. 187-195.

HUSTAD, J.E. and SONJU, O.E. (1988)
"Experimental studies of lower flammability limits of gases and mixtures of gases at elevated temperatures."
Comb. and Flame v.71, 1988, pp. 283-294.

HUTCHEON, J.M. (1970)
"Manufacturing technology of baked and graphitised carbon bodies." In: "Modern Aspects Of Graphite Technology."
Ed. L.C.F. Blackman. Academic Press London, New York 1970.

INGLE, A.N. and SARKAR, S. (1976)
"Gasification of coal in spouted bed."
Indian J. Technol. v.14, 1976, pp. 515-517.

JANAF THERMOCHEMICAL TABLES (1971)
2nd Edition, June 1971.
Nat. Stand. Ref. Data Ser., Nat. Bur. Stand. (US), 37.
D.R. Stull and H. Prophet - project directors.

JARALLAH, A. and WATKINSON, A.P. (1985)
"Pyrolysis of Western Canadian coals in a spouted bed."
Can. J. Chem. Eng. v.63, 1985, pp. 227-236.

JEBRAIL, F.F. (1987)
"Combustion and partial oxidation of hydrocarbon fuels in a spouted bed burner." Ph.D. Thesis, Imperial College, University of London, 1987.

JONES, A.R., LLOYD, S.A. and WEINBERG, F.J. (1978)
"Combustion in heat exchangers."
Proc. R. Soc. Lond. v.A360, 1978, pp. 97-115.

KHOSHNOODI, M. and WEINBERG, F.J. (1978)
"Combustion in spouted beds."
Comb. and Flame v.33, 1978, pp. 11-21.

KOTANI, Y. and TAKENO, T. (1982)
"An experimental study on stability and combustion characteristics of an excess enthalpy flame."
19th Symposium (International) on Combustion, The Combustion Institute, 1982, pp. 1503-1509.

KUMPINSKY, E. and AMUNDSON, N.R. (1984)
"Reactor model assessment for the combustion of char in spouted beds of sand."
Ind. Eng. Chem. Process. Des. Dev. v.23, 1984, pp. 784-794.

LEVENSPIEL, O. (1966)
"Chemical Reaction Engineering"
2nd Ed., Wiley, New York, 1966.

LEWIS, B. and VON ELBE, G. (1961)
"Combustion, Flames and Explosions of Gases"
Academic Press, New York 1961.

LLOYD, S.A. and WEINBERG, F.J. (1974)
"A burner for mixtures of very low heat content."
Nature v.251, 1974, pp. 47-49.

LLOYD, S.A. and WEINBERG, F.J. (1975)
"Limits to energy release and utilisation from chemical fuels." Nature v.257, 1975, pp. 367-370.

LLOYD, S.A. and WEINBERG, F.J. (1976)
"A recirculating fluidised bed combustor for extended flow ranges." Comb. and Flame v.27, 1976, pp. 391-394.

MALEK, M.A. and LU, B.C.Y. (1965)
"Pressure drop and spoutable bed height in spouted beds."
Ind. Eng. Chem. Process. Des. Dev. v.4, 1965, p. 123.

MANTEL, C.L. (1968)
"Carbon and Graphite Handbook."
Interscience, New York, London, Sydney, Toronto, 1968.

MATHUR, K.B. and EPSTEIN, N. (1974a)
"Developments in spouted bed technology."
Can. J. Chem. Eng. v.52, 1974, p.129

MATHUR, K.B. and EPSTEIN, N. (1974b)
"Spouted Beds." Academic Press, New York, 1974.

MATHUR, K.B. and GISHLER, P.E. (1955)
"A technique for contacting gases with coarse solid particles." A. I. Ch. E. J. v.1, 1955, p. 157.

McNAB, G.S. (1972)
"Prediction of spout diameter."
Brit. Chem. Eng. Proc. Tech. v.17, 1972, p. 532.

MUKHLENOV, I.P. and GORSCHTEIN, A.E. (1964)
"Hydraulic resistance of the suspended layer in grateless conical sets."
Zh. Prikl. Khim. (Leningrad) v.37, 1964, p. 609.

MUKHLENOV, I.P. and GORSCHTEIN, A.E. (1965)
"Investigation of a spouting bed."
Khim. Prom. (Moscow) v.41, 1965, p. 443.

MURCAR, W.G. and BODEN, J.C. (1984)
"Heat recovery from solvent incineration."
In: "Solvent Problems In Industry." Ed. G.Kakabadse.
Elsevier Applied Science Publishers Ltd., 1984

OHTAKE, K., SAWYER, R.F. and HART, J.R. (1984)
"Combustion and flow in a two dimensional spouted bed."
20th Symposium (International) on Combustion, The Combustion Institute, 1984, pp 1427-1433.

QUINLAN, B.E. and RATCLIFFE, J.S. (1971)
"A design equation for the low temperature carbonisation of coal under spouted bed conditions." Institution of Engrs., Australia, Mech. and Chem. Eng. Trans., May 1971, pp. 1-5.

RATCLIFFE, J.S. and RIGBY, G.R. (1969)
"Low temperature carbonisation of coal in a spouted bed; prediction of exit char volatile matter."
Institution of Engrs., Australia,
Mech. and Chem. Eng. Trans., May 1969, pp 1-6.

RAY, T.B. and SARKAR, S. (1976)
"Kinetics of coal pyrolysis in spouted beds."
Indian Chemical Engineer v.18, No. 2, 1976, pp. 11-19.

ROXBEE COX, H. (1951)
Proc. Instn. Mech. Engrs. v.164, 1951, pp. 407-424.

SAWYER, W.E. (1880)
U.S. Patent 229,335 1880.

SCHWOB, Y. (1979)
"Acetylene black: manufacture, properties and applications."
In: "Chemistry and Physics of Carbon" v.15, pp. 109-228.
Eds. P.L. Walker Jr. and P.A. Thrower
Marcel Dekker Inc., New York and Basel, 1979.

SMITH, I.E. (1955)
Ph.D Thesis, Imperial College, University of London, 1955.

SMOOT, L.D. and PRATT, D.T. (Eds.) (1979)
"Pulverised Coal Combustion And Gasification."
Plenum Press, New york, London, 1979.

TEO, K.C. and WATKINSON, A.P. (1986)
"Rapid pyrolysis of Canadian coals in a miniature spouted bed reactor." Fuel v.65, 1986, pp. 949-959.

WARNATZ, J. (1984)
"Chemistry of high temperature combustion of alkanes up to octane." 20th Symposium (International) on Combustion,
The Combustion Institute, 1984, pp. 845-856.

WATKINSON, A.P., CHENG, G. and PRAKASH, C.B. (1983)
"Comparison of coal gasification in fluidised and spouted beds." Can. J. Chem. Eng. v.61, 1983, pp. 468-474.

WEINBERG, F.J. (1971)
"Combustion temperatures: the future?"
Nature v.233, Sept. 1971, pp. 239-241.

WEINBERG, F.J. (1975)
"The first half million years of combustion research and todays burning problems."
Prog. Energy Comb. Sci. v.1, 1975, pp. 17-31.

WEINBERG, F.J. (1982)
"Lean times for old flames."
Physics Bulletin v.33, 1982, pp. 124-128.

WEINBERG, F.J. (Ed.) (1986)
"Advanced Combustion Methods."
Academic Press Inc., New York 1986.

WEINBERG, F.J., BARTLEET, T.G., CARLETON, F.B., RIMBOTTI, P., BROPHY, J.H. and MANNING, R.P. (1988)
"Partial oxidation of fuel rich mixtures in a spouted bed combustor." Comb. and Flame v.72, 1988, pp. 235-239.

WIBBERLEY, L.J. and PHONG-ANANT, D. (1986)
"A simple laboratory feeder for fine particles."
Comb. Sci. and Technol. v.49, 1986, pp 93-97.

ZABETAKIS, M.G., LAMBIRIS, S. and SCOTT, G.S. (1959)
"Flame temperatures of limit mixtures."
7th Symposium (International) on Combustion, The Combustion Institute, 1959, pp. 484-487.

ZHAO, J., LIM, C.J. and GRACE, J.R. (1987a)
"Flow regimes and combustion behaviour in coal burning spouted and spout-fluid beds."
Chem. Eng. Sci. v.42, no. 12, 1987, pp. 2865-2875.

ZHAO, J., LIM, C.J. and GRACE, J.R. (1987b)
"Coal burnout times in spouted and spout-fluid beds."
Chem. Eng. Res. Des. v.65, Sept. 1987, pp. 426-429.

APPENDIX A

This appendix contains program listings for the three computer models described in chapter 5.

APPENDIX A1

Lean Combustion Model

FILE: TEMPA1 FORTRAN A1 VM/SP CONVERSATIONAL MONITOR

```
      DIMENSION HH(200,200)
C
C-----HEAT OF COMBUSTION FOR METHANE, J/KG, AND VOL% IN AIR
C
      QQR=50E6
      X=0.03
C
C-----SET INITIAL TEMPERATURES , K
C
      T0=293
      TU=0
      TF=0
      TE=0
      TP1=0
      TP2=0
C
C-----SET SPECIFIC HEAT CAPACITIES , J/KG/K
C
      CS=0.8E3
      CG=1.246E3
C
C-----SET SOLID AND GAS DENSITIES
C
      RHOS=3600
      RHOAIR=1.225
      RHOCH4=0.679
      RHOMIX= X*RHOCH4+(1-X)*RHOAIR
C
C-----SET OTHER CONSTANTS AND VARIABLES
C
      PI=3.14159
      L=1
C-------------------------
      WRITE(10,*)'CH4 % (VOL) =',X*100,'%'
C
C-----CALCULATE TEMP RISE DUE TO COMBUSTION, HR
C
      HR=QQR*X*RHOCH4/(RHOMIX*CG)
      WRITE(10,*)'HR=',HR,'K'
C
C-----CALCULATE EXIT TEMP TE
C
      TE=T0+HR
      WRITE(10,*)'T0=',T0,'TE=',TE
C
C-----START LOOP TO VARY SOLID / GAS MASS FLOW RATIO , Z
C
      DO 100 K=1,30
      Z=K*1.0
      WRITE(10,300)
      WRITE(10,310)
      WRITE(10,325)
C
C-----START LOOP TO VARY PARTICLE DIAMETER FROM 0.4 TO 1.2 MM
C
```

FILE: TEMPA1 FORTRAN A1 VM/SP CONVERSATIONAL MONITOR

```
      DO 50 J=1,5
      DS=0.2*J+0.2
      DSS=DS*1E-3
C
C-----CALCULATE PARTICLE NUMBER DENSITY , PARTICLES/CUBIC METRE
C
      XN=1*DSS**3*RHOS*PI/(6*RHOAIR)
      XN=Z/XN
C
C-----CALCULATE FACTOR Y WHICH GOVERNS TF/TE
C
      ZZ=Z*CS/CG
      YY=XN*DSS**2
      Y=1+(ZZ/(1+ZZ))*(YY/(1+YY))
C
C-----CALCULATE TU (UNBURNED TEMP) AND TF (FLAME TEMP)
C
      TF=Y*HR+T0
      TU=TF-HR
C
C-----CALCULATE TP1 AND TP2 THE PARTICLE TEMPS
C
      TP1=(TU-T0)/(2*ZZ)+(TE+TF+TU+T0)/4
      TP2=TP1-(TU-T0)/ZZ
C
C-----CALCULATE THE THERMAL EQUILIBRIUN FACTOR, F
C
      F=(TU-T0)/(TP2-T0)
C
C-----CONVERT PARTICLE NUMBER DENSITY TO PARTICLES/CC
C
      XNN=XN/1E6
C
C-----WRITE OUT RESULTS IN FULL
C
      WRITE(10,310)
      WRITE(10,330) TP1,TP2,DS,Z,TU,TF,XNN,F
C
C-----LOAD RESULTS INTO ARRAY
C
      HH(L,1)=TP1
      HH(L,2)=TP2
      HH(L,3)=TU
      HH(L,4)=TF
      HH(L,5)=F
      HH(L,6)=Z
      L=L+1
 50   CONTINUE
      WRITE(10,310)
      WRITE(10,300)
 100  CONTINUE
C
C-----FORMAT STATEMENTS
C
 300  FORMAT (1X,79('*'))
```

FILE: TEMPA1 FORTRAN A1 VM/SP CONVERSATIONAL MONITOR

```
 310  FORMAT (1X,'*',77X,'*')
 325  FORMAT (1X,'*',1X,'TP1,K',5X,'TP2,K',5X,'DS,MM',5X,'MS/MG',5X,
     &'TU,K',6X,'TF,K',6X,' NP ',6X,'  F  ',1X,'*')
 330  FORMAT (1X,'*',1X,F7.2,3X,F7.2,3X,F7.2,3X,F7.2,3X,F7.2,3X,F7.2,
     &3X,F7.2,3X,F5.2,1X,'*')
C
C-----WRITE OUT RESULTS FROM ARRAY SUCH THAT THEY CAN BE READ BY
C-----A GRAPHICS PACKAGE
C
      DO 380 M=1,5
      WRITE(10+M,400)
      WRITE(10+M,420)
      DO 350 L=1,146,5
      WRITE(10+M,410) HH(L,6),HH(L,M),HH(L+1,M),HH(L+2,M),HH(L+3,M)
     &,HH(L+4,M)
 350  CONTINUE
 380  CONTINUE
C
C-----FORMAT STATEMENTS FOR GRAPHICS PACKAGE
C
 400  FORMAT (13X,'1',9X,'2',9X,'3',9X,'4',9X,'5')
 410  FORMAT (1X,F6.2,3X,F7.2,3X,F7.2,3X,F7.2,3X,F7.2,3X,F7.2)
 420  FORMAT (10X,'D=0.4MM',3X,'D=0.6MM',3X,'D=0.8MM',3X,'D=1.0MM',
     &3X,'D=1.2MM')
C
C-----SUMMARY OF OUTPUT FILES
C
C-----FILE FT10F001 = FULL OUTPUT
C-----FILE FT11F001 = TP1
C-----FILE FT12F001 = TP2
C-----FILE FT13F001 = TU
C-----FILE FT14F001 = TF
C-----FILE FT15F001 = F
C
      END
```

APPENDIX A2

Lean Limit Prediction Model

FILE: LIM2E1 FORTRAN A1 VM/SP CONVERSATIONAL MONITOR

```
      DIMENSION HH(200,200)
C
C-----HEAT OF COMBUSTION FOR METHANE , J/KG
C
      QQR=50E6
C
C-----SET INITIAL TEMPERATURES AND ASSUMED VALUE OF TF , K
C
      T0=293
      TU=0
      TF=1403
      TE=0
      TP1=0
      TP2=0
C
C-----SET SPECIFIC HEAT CAPACITIES , J/KG/K
C
      CS=0.8E3
      CG=1.246E3
C
C-----SET SOLID AND GAS DENSITIES , KG/CUBIC M
C
      RHOS=3600
      RHOAIR=1.225
      RHOCH4=0.679
C
C-----SET OTHER CONSTANTS AND VARIABLES
C
      PI=3.14159
      Z=0
      F=0
      L=1
C
C-----START LOOP TO VARY SOLID / GAS MASS FLOW RATIO , Z
C
      DO 100 K=1,30
      Z=K*1.0
C
C-----START LOOP TO VARY PARTICLE DIAMETER FROM 0.4 TO 1.2 MM
C
      DO 50 J=1,5
      DS=0.2*J+0.2
      DSS=DS*1E-3
C
C-----CALCULATE PARTICLE NUMBER DENSITY , PARTICLES/CUBIC M
C
      XN=1*DSS**3*RHOS*PI/(6*RHOAIR)
      XN=Z/XN
C
C-----CALCULATE FACTOR Y WHICH GOVERNS TF/TE
C
```

```
      ZZ=Z*CS/CG
      YY=XN*DSS**2
      Y=1+(ZZ/(1+ZZ))*(YY/(1+YY))
C
C-----CALCULATE HR , THE TEMPERATURE RISE DUE TO COMBUSTION
C
      HR=(TF-T0)/Y
C
C-----CALCULATE THE LEAN LIMIT : X THE % OF CH4 OR EQU THE
C-----EQUIVALENCE RATIO
C
      X=HR*CG*RHOAIR/RHOCH4
      X=X/(HR*CG*(RHOAIR/RHOCH4-1)+QQR)
      EQU=X*10.52
C
C-----LOAD RESULTS INTO AN ARRAY
C
      HH(L,1)=EQU
      HH(L,2)=Z
      HH(L,3)=(X*100)
      L=L+1
 50   CONTINUE
 100  CONTINUE
C
C-----WRITE OUT RESULTS FROM ARRAY SUCH THAT THEY CAN BE READ
C-----BY A GRAPHICS PACKAGE
C
      WRITE(11,400)
      WRITE(11,420)
      DO 350 L=1,146,5
      WRITE(11,405) HH(L,2),HH(L,1),HH(L+1,1),HH(L+2,1),HH(L+3,1)
     &,HH(L+4,1)
 350  CONTINUE
      WRITE(12,400)
      WRITE(12,420)
      DO 360 L=1,146,5
      WRITE(12,410) HH(L,2),HH(L,3),HH(L+1,3),HH(L+2,3),HH(L+3,3)
     &,HH(L+4,3)
 360  CONTINUE
C
C-----FORMAT STATEMENTS FOR GRAPHICS PACKAGE
C
 400  FORMAT (13X,'1',9X,'2',9X,'3',9X,'4',9X,'5')
 410  FORMAT (1X,F6.2,3X,F7.2,3X,F7.2,3X,F7.2,3X,F7.2,3X,F7.2)
 405  FORMAT (1X,F6.2,3X,F7.4,3X,F7.4,3X,F7.4,3X,F7.4,3X,F7.4)
 420  FORMAT (10X,'D=0.4MM',3X,'D=0.6MM',3X,'D=0.8MM',3X,'D=1.0MM',
     &3X,'D=1.2MM')
C
C-----SUMMARY OF OUTPUT FILES
C
C-----FILE FT11F001 = EQU RAT VS Z
C-----FILE FT12F001 = X VS Z
C
      END
```

APPENDIX A3

Rich Limit Correlation Model

```
      DIMENSION HH(200,200)

C
C-----SET INITIAL TEMPERATURES AND ASSUMED VALUE OF TF , K
C
      T0=293
      TU=0
      TF=1600
      TE=0
      TP1=0
      TP2=0
C
C-----SET SPECIFIC HEAT CAPACITIES , J/KG/K
C
      CS=0.8E3
      CG1=1210
      CG2=1631
      C=CG1/CG2
C
C-----SET SOLID AND GAS DENSITIES , KG/CUBIC M
C
      RHOS=3600
      RHOAIR=1.225
      RHOCH4=0.679
C
C-----SET OTHER CONSTANTS AND VARIABLES
C
      PI=3.14159
      Z=0
      F=0
      L=1
C
C-----START LOOP TO VARY SOLID / GAS MASS FLOW RATIO , Z
C
      DO 100 K=1,30
      Z=K*1.0
      R=CG1/(CS*Z)
C
C-----START LOOP TO VARY PARTICLE DIAMETER FROM 0.4 TO 1.2 MM
C
      DO 50 J=1,5
      DS=0.2*J+0.2
      DSS=DS*1E-3
C
C-----CALCULATE PARTICLE NUMBER DENSITY , PARTICLES/CUBIC M
C
      XN=1*DSS**3*RHOS*PI/(6*RHOAIR)
      XN=Z/XN
C
C-----CALCULATE FACTOR Y WHICH GOVERNS TP/TE
C
      YY=XN*DSS**2
      Y=1+(C/(1+R))*(YY/(1+YY))
```

FILE: LIM2ER FORTRAN A1 VM/SP CONVERSATIONAL MONITOR

```
C
C-----CALCULATE HR , THE TEMPERATURE RISE DUE TO COMBUSTION
C
      HR=((TF-T0)/Y)-(C-1)*T0
C
C-----CALCULATE THE LEAN LIMIT : X THE % OF CH4 OR EQU THE
C-----EQUIVALENCE RATIO
C
      X=0.32772-(1.4E-4*HR)
      EQU=X*10.52
C
C-----LOAD RESULTS INTO AN ARRAY
C
      HH(L,1)=EQU
      HH(L,2)=Z
      HH(L,3)=(X*100)
      L=L+1
 50   CONTINUE
 100  CONTINUE
C
C-----WRITE OUT RESULTS FROM ARRAY SUCH THAT THEY CAN BE READ
C-----BY A GRAPHICS PACKAGE
C
      WRITE(11,400)
      WRITE(11,420)
      DO 350 L=1,146,5
      WRITE(11,405) HH(L,2),HH(L,1),HH(L+1,1),HH(L+2,1),HH(L+3,1)
     &,HH(L+4,1)
 350  CONTINUE
      WRITE(12,400)
      WRITE(12,420)
      DO 360 L=1,146,5
      WRITE(12,410) HH(L,2),HH(L,3),HH(L+1,3),HH(L+2,3),HH(L+3,3)
     &,HH(L+4,3)
 360  CONTINUE
C
C-----FORMAT STATEMENTS FOR GRAPHICS PACKAGE
C
 400  FORMAT (13X,'1',9X,'2',9X,'3',9X,'4',9X,'5')
 410  FORMAT (1X,F6.2,3X,F7.2,3X,F7.2,3X,F7.2,3X,F7.2,3X,F7.2)
 405  FORMAT (1X,F6.2,3X,F7.4,3X,F7.4,3X,F7.4,3X,F7.4,3X,F7.4)
 420  FORMAT (10X,'D=0.4MM',3X,'D=0.6MM',3X,'D=0.8MM',3X,'D=1.0MM',
     &3X,'D=1.2MM')
C
C-----SUMMARY OF OUTPUT FILES
C
C-----FILE FT11F001 = EQU RAT VS Z
C-----FILE FT12F001 = X VS Z
C
      END
```